Fakultät für Medizin

Institut für Klinische Chemie und Pathobiochemie

The C-type lectin receptor Clec12A positively regulates type I interferon response

Kai Li

Vollständiger Abdruck der von der Fakultät für Medizin der Technischen Universität München zur Erlangung des akademischen Grades eines

Doctor of Philosophy (Ph.D.)

genehmigten Dissertation.

Vorsitzende/r: Prof. Dr. Roland Schmid

Betreuer/in: Prof. Dr. Jürgen Ruland

Prüfer der Dissertation:

1. Prof. Dr. Olaf Groß

2. Prof. Dr. Mathias Heikenwälder

Die Dissertation wurde am 18.12.2017 bei der Fakultät für Medizin der Technischen Universität München eingereicht und durch die Fakultät für Medizin am 28.02.2018 angenommen.

Abbreviations

3pRNA	5’-triphosphate double strand RNA
AA	amino acid
AIM2	absent in melanoma 2
ALT	alanine aminotransferase
AST	aspartate aminotransferase
BCA	bicinchoninic acid assay
BCL10	B-cell chronic lymphocytic leukemia/lymphoma 10
BMDC	bone marrow derived dendritic cell
CARD	caspase activation and recruitment domain
cDC	classical dendritic cell
cGAMP	cyclic GMP-AMP
cGAS	cyclic GMP–AMP synthase
CLR	C-type lectin receptor
CTLD	C-type lectin-like domain
DAMP	danger-associated molecular pattern
DC	dendritic cell
DCAL-2	dendritic cell-associated lectin 2
DCIR	dendritic cell immunoreceptor
ELISA	enzyme-linked immunosorbent assay
FACS	fluorescent-activated cell sorting
FBS	fetal bovine serum
FDR	false discovery rate
FPKM	fragments per kilobase of transcript per million mapped reads
g	gravity
g	gram
GAS	gamma-activated sequence
GM-CSF	granulocyte-macrophage colony-stimulating factor
GSEA	gene set enrichment analysis
Gy	Gray
HIN-200	hematopoietic IFN-inducible nuclear proteins with a 200-AA repeat
HMGB1	high mobility group box 1
HRP	horseradish peroxidase
IFIT	interferon induced protein with tetratricopeptide repreat
IFITM	IFN-inducible transmembrane protein
IFN-I	type I interferon
IFNAR	interferon-α receptor
IKK	inhibitor of nuclear factor kappa-B kinase
IL	interleukin
ILC	Innate lymphoid cell
IRAK	IL-1R-associated kinase
IRF	interferon regulatory factor
ISG	interferon-stimulated gene
ISGF3	interferon-stimulated gene factor 3
ISRE	interferon-stimulated response element

ITAM	immunoreceptor tyrosine-based activation motif
ITIM	immunoreceptor tyrosine-based inhibitory motif
JAK	Janus kinase
l	liter
LCMV	lymphocytic chriomeningitis virus
LDH	lactate dehydrogenase
LPS	lipopolysaccharide
LRR	leucine rich repeat
M	molar
MAL	MYD88-adaptor-like protein
MALT1	Mucosa-associated lymphoid tissue lymphoma translocation protein 1
MAVS	mitochondrial antiviral signalling protein
MDA5	melanoma differentiation-associated protein 5
MHC	major histocompatibility complex
MICL	myeloid inhibitory C-type lectin receptor
MMP	metalloprotinase
MSU	monosodium urate (crystal)
MVA	modified vaccinia virus Ankara
MYD88	myeloid-differentiation primary response protein 88
NET	neutrophil extracellular trap
NF-κb	nuclear factor kappa-light-chain-enhancer of activated B cells
NKC	Natural killer receptor gene complex
NLR	NOD-like receptor
NLRC	NACHT, LRR and CARD-containing protein
NLRP	NACHT, LRR and PYD-containing protein
NOD	nucleotide-binding and oligomerization
NP	nucleoprotein
OVA	ovalbumin
p	phosphorylated
PAMP	pathogen-associated molecular pattern
PBS	phosphate buffered saline
pDC	plasmacytoid dendritic cell
PFU	plaque forming unit
polyIC	polyinosinic-polycytidylic acid
PRD	positive regulatory domain
PRR	pattern recognition receptor
PYD	pyrin domain
PYHIN	pyrin and HIN200 domain-containing protein
QPCR	quantitative real-time PCR
R5	RPMI supplemented with 5% FBS
RIG-I	retinoic acid inducible gene I
RIN	RNA integrity number
RIP	receptor interacting serine/threonine-protein kinase
RLR	RIG-I like receptor
ROS	respiratory oxygen species
SEM	standard error of the mean
SFK	Src family kinase

SH2	Src-homology 2 domain
SHIP	Src homology 2 domain containing inositol phosphatase
SHP	Src homology 2 domain containing protein tyrosine phosphatase
SSC	side scatter
STAT	signal transducer and transactivator
STING	stimulator of interferon genes
SYK	spleen tyrosine kinase
TBK1	TANK-binding kinase 1
TBST	tris-buffered saline with Tween 20
$TCID_{50}$	50% tissue culture infective dose
TIR	Toll/interleukin-1 receptor homology domain
TLR	Toll-like receptor
TNF	tumor necrosis factor
TRAF	TNF receptor-associated factor 6
TRAM	TRIF-related adaptor molecule
TRIF	TIR-domain-containing adaptor-inducing interferon-β
TYK2	non-receptor tyrosine-protein kinase
V	Voltage

Abstract

Innate immune receptors rely on the detection of diverse immunological cues and intensive crosstalk to generate a context-dependent response. Clec12A, a C-type lectin receptor, has been shown to sense dead cells and the danger-associated molecular pattern uric acid crystals, and subsequently inhibit inflammation induced by cell activating signals. However, whether Clec12A plays additional roles in innate immunity is unknown. In this thesis, we show that Clec12A also modulates the induction of type I interferons (IFN-I), an essential aspect of the anti-infection immune response. Combining RNA-seq and subsequent gene set enrichment analysis, as well as biochemical studies, we prove that Clec12A is required for optimal transcription of interferon-stimulated genes and regulates events that precede the IFN-I receptor engagement with autocrine or paracrine IFN-I. Specifically, Clec12A activates Src family kinases, which then act on TBK1 to amplify RIG-I activated type I interferon production. Consistently, we observed that the lack of Clec12A *in vivo* led to impaired IFN-I production during both acute and chronic lymphocytic choriomeningitis virus (LCMV) infections. Notably, while exacerbating susceptibility to acute LCMV infection, Clec12A deficiency increased resistance to chronic LCMV infection—a pattern that fits with the known function of IFN-I in acute or chronic virus infection settings, respectively. Taken together, our work defines a novel positive regulatory function of Clec12A in IFN-I response both *in vitro* and *in vivo*.

Zusammenfassung

Rezeptoren des angeborenen Immunsystems detektieren diverse immunologische Reize und interagieren intensiv mit vielen Signalwegen, um eine kontextabhängige Antwort zu generieren. Der C-Typ Lektinrezeptor Clec12A erkennt tote Zellen und Harnsäurekristalle, welche eine mit Gefahr assoziierte molekulare Struktur darstellen. Daraufhin inhibiert Clec12A zellaktivierende Signale und daraus resultierende Entzündungen. Ob Clec12A darüber hinausreichende Funktionen in der angeborenen Immunität übernimmt, ist derzeit nicht bekannt. In dieser Arbeit zeigen wir, dass Clec12A die Induktion von Typ I Interferonen (IFN-I) moduliert, die ein essenzieller Aspekt der Immunantwort gegen Infektionen ist. Anhand von RNA-Sequenzierung, anschließender Gen-Anreicherungsanalyse sowie biochemischer Studien zeigen wir, dass Clec12A für die optimale Transkription von Interferon-stimulierten Genen notwendig ist. Wir zeigen außerdem, dass Clec12A Ereignisse beeinflusst, die der IFN-I-Rezeptoraktivierung durch autokrines oder parakrines IFN-I vorausgehen: Clec12A aktiviert Src Kinasen, welche wiederum auf TBK1 wirken, um die RIG-I-induzierte IFN-I Produktion zu verstärken. Im Einklang mit diesen Daten beobachteten wir, dass das Fehlen von Clec12A *in vivo* zu einer Beeinträchtigung der IFN-I Produktion führt – sowohl bei akuter als auch bei chronischer Infektion mit dem lymphozytischen Choriomeningitis Virus (LCMV). Bemerkenswerterweise sind Clec12A-defiziente Mäuse anfälliger für eine akute, jedoch resistenter gegen eine chronische LCMV-Infektion. Dies spiegelt die Rolle von IFN-I in akuten und chronischen Virusinfektionen wider. Zusammengefasst definiert unsere Arbeit eine neue regulatorische Funktion von Clec12A in der IFN-I Antwort sowohl *in vitro* als auch *in vivo*.

TABLE OF CONTENTS

ABBREVIATIONS 1

ABSTRACT 4

ZUSAMMENFASSUNG 5

1. INTRODUCTION 8

1.1. Innate immunity 8
1.1.1. The innate immune cells 9
1.1.2. Pattern recognition receptors 12

1.2. Type I interferon 22
1.2.1. Type I interferon signaling 22
1.2.2. The production of type I interferon 24
1.2.3. The functions of type I interferon 26

1.3. Clec12A 29

1.4. Purpose of the study 31

2. MATERIAL AND METHODS 32

2.1. Cell culture 32
2.1.1. Bone marrow derived dendritic cell culture 32
2.1.2. Cell treatment and stimulation 32

2.2. Molecular biology 33
2.2.1. MSU crystal preparation 33
2.2.2. RNA extraction 34
2.2.3. Real time quantitative PCR 34
2.2.4. RNA-seq and gene set enrichment analysis 35
2.2.5. Immunoblotting 36
2.2.6. Cytokine and LDH Measurement 38
2.2.7. Flow Cytometry 39

2.3. Animal experiments 39
2.3.1. Mice 39
2.3.2. Whole body irradiation 39
2.3.3. Virus infection 40

2.4. Statistical analysis 42

3. RESULTS 43

3.1. Clec12A dampens inflammation but enhances ISG expression *in vivo* 43
3.1.1. Clec12A-deficient mice showed excessive sterile inflammation 43
3.1.2. Clec12A-deficent mice have decreased ISG expression in the irradiated thymi 45

3.2. Clec12A positively regulates the global expression of ISGs 46
3.2.1. Clec12A is required for optimal ISGs expression in stimulated BMDC 46
3.2.2. Global transcriptome analysis confirmed the regulatory function of Clec12A 48

3.3. Clec12A modulates IFN-I response independent of IFN-I receptor signaling 51

3.3.1. Clec12A is required for optimal STAT1 phosphorylation 51
3.3.2. Clec12A does not interfere with signaling events initiated by IFNAR engagement 52
3.3.3. Clec12A deficiency leads to reduced IFN-I production 54

3.4. Clec12A amplifies the IFN-I production signaling through activating Src-family kinases 56
3.4.1. Clec12A regulates the TBK1-IRF3 axis of the IFN-I production signaling 56
3.4.2. Clec12A acts on Src-family kinases to regulate IFN-I response 57

3.5. The function of Clec12A in virus infection *in vivo* 60
3.5.1. *Clec12a*$^{-/-}$ mice are more susceptible to LCMV-WE infection 60
3.5.2. *Clec12a*$^{-/-}$ mice are more resistant to LCMV-Docile infection 63
3.5.3. Clec12A is dispensable for IFN-I response during influenza virus infection *in vivo* 64
3.5.4. *Clec12a*$^{-/-}$ mice showed excessive inflammation upon MVA infection 66

4. DISCUSSION 68

4.1. Regulation of IFN-I response by ITAM or ITIM receptors 68

4.2. The point where Clec12A-activated signaling interferes with IFN-I response 71

4.3. Src-family kinases in Clec12A activated signaling 72

4.4. The *in vivo* function of Clec12A during virus infection 75

4.5. Clec12A at the crossroad of inflammation and IFN-I 77

4.6. Conclusion and outlook 79

5. REFERENCES 80

PUBLICATION 97

ACKNOWLEDGEMENTS 98

TABLE AND FIGURE LIST 99

1. Introduction

One central challenge that multi-cellular organisms face is to protect themselves against exogenous or endogenous threats. To meet this challenge, several mechanisms of defense have evolved in both vertebrates and invertebrates. They are collectively called the immune system. The different layers of the immunological defense, which includes multiple dedicated immune organs, various cell types and a vast collection of biological macromolecules, are nicely integrated to face up to the mercurial nature of the intrusions. According to the specificities of defense mechanisms, the immune system can be divided into two major categories: the adaptive immune system and the innate immune system.

1.1. Innate immunity

The innate immune system is more ancient than the adaptive immunity (Kimbrell and Beutler, 2001). Since its activation can happen immediately after the host encounters dangers, it represents the first line of protection and can keep the damage in check until the more specific adaptive immunity develops. The activation of innate immunity relies on an array of germline-encoded pattern recognition receptors (PRRs). These receptors can detect dangers that emerge from both pathogens (pathogen associated molecular pattern, PAMP) or damaged cells (danger associated molecular pattern, DAMP). Well-studied mammalian PRRs include membrane-bound receptors, like Toll-like receptors (TLRs) and C-type lectin receptors (CLRs). There are also PRRs that reside in the cytoplasm, like RIG-I like receptors (RLR) and NOD-like receptors. The list of PRRs gets longer as our understanding of the innate immune response advances (Table 1). Upon recognition of their ligands, PRRs initiate

downstream signaling within the cells. The signals from several PRRs crosstalk with one another to in the end generate a context dependent immune response.

1.1.1. The innate immune cells

The innate immune response involves several effector cells that arise from hematopoietic stem cells. Granulocytes (neutrophil, basophil, eosinophil, mast cell), monocytes, macrophages and dendritic cells (DCs) make up the major population of innate immune cells. They derive from the myeloid lineage during hematopoiesis. Innate lymphoid cells (ILCs) and NK cells, which arise from the lymphoid lineage, are also important players in innate immunity. Neutrophil, monocyte, macrophage and dendritic cell constitute the phagocytic family due to their ability to directly engulf microbes or other damaging particles.

Neutrophils are the most abundant leukocytes in the blood. Under steady condition, they circulate in the bloodstream and survey upcoming dangers. Once take cues from the site of infection or injury, they transmigrate across endothelium in the direction of chemokine gradient. When they reach the affected tissue, neutrophils exert their function by ingesting the damaging microbes and releasing the content stored in their specialized vesicles-a process termed degranulation. Shortly after getting activated, neutrophils die and expel their nuclear content and granules as neutrophil extracellular trap (NET), which can entrap invading pathogens, facilitate their engulfment by phagocytes and directly kill the microbes (Brinkmann et al., 2004). Due to their promptness to action and direct involvement in large numbers, neutrophils are traditionally regarded as the foot soldiers of the innate immune system (Kolaczkowska and Kubes, 2013). Similar to neutrophils, monocytes also quickly respond to chemokine attraction and migrate to endangered tissue. In

addition to working as direct effector cells, monocytes also replenish the classical tissue-resident mononuclear phagocytic pool on demand (Ginhoux and Jung, 2014).

Macrophages are prominent tissue-resident phagocytes and play an important role in microbe-killing, immune regulation and tissue homeostasis maintenance. Tissue macrophages are non-migratory and many of their effector functions concentrate on their vicinity. Because of this attribute, macrophages in different organs exhibit high levels of local adaptation. The pool of tissue resident macrophages has long been believed to be maintained by constant recruitment of blood-circulating monocytes. However, more recent studies have disputed this notion and proposed that in steady state the majority of tissue macrophage population is derived from prenatally seeded embryonic progenitors and maintained by self-renewal. Nevertheless, the macrophage population can be complemented by monocyte-derived macrophages in inflamed tissues (Ginhoux and Jung, 2014; Varol et al., 2015).

Like macrophages, dendritic cells are another group of sentinel phagocytes of the immune system. They are professional antigen presenting cells that induce an immune response against any foreign antigens and enforce tolerance to self-antigens. DCs also scavenge the tissues for invading dangers. However, they differ from macrophages by their high mobility between their resident tissues and lymphoid organs. This feature of DCs also reflects that their major function is to guide the adaptive immune system by reporting the peripheral information. We have gradually realized the heterogeneity within the DC family since its discovery by Ralph Steinman and Zanvil Cohn in the late 1970 (Steinman and Cohn, 1973, 1974). A major division in the DC family was unraveled with the finding of pDCs, which are characterized by their plasma cell-like morphology and their ability to produce huge amount of interferon-α (IFN-α), while still being able to prime T cells as other DCs do (Merad et

al., 2013). They express only limited types of PRRs, including TLR7 and TLR9. To distinguish pDC from the originally described DC, the latter were renamed as classical DC (cDC). cDCs in the lymphoid tissues can be classified by the expression of CD8 on the cell surface (Shortman and Heath, 2010). Their nonlymphoid counterparts are defined by the presence or absence of integrin CD103 (Helft et al., 2010). The lymphoid tissue CD8+ and nonlymphoid CD103+ DCs have the same origin and exert similar functions. They are strategically positioned in the tissue interface to maximize their chance of encountering pathogen or damage derived antigens. Once charged with antigens, they can efficiently migrate to draining lymph nodes and present the antigen to T cells (Helft et al., 2010). Additionally, CD8+ cDCs and CD103+ cDCs have more pronounced ability to load exogenously acquired antigen to MHC I molecule than CD11b+ cDCs (Heath and Carbone, 2009).

Because of their rarity, isolation of primary DCs from mouse tissues with large quantity is often difficult. To address this problem, groups have developed culture system of differentiating hematopoietic precursors in the presence of growth factors. The most commonly used method is to generate bone marrow derived dendritic cells (BMDCs) by differentiating bone marrow cells under the influence of GM-CSF (Lutz et al., 1999). This culturing method will in the end give rise to loosely attached or floating DCs expressing CD11c and high levels of MHC II. The adherent cells in the culture are CD11c and MHC II negative macrophages. However, a recent study illustrates that the DC population from the GM-CSF-driven culture is actually a mixture of DCs and macrophages with CD11c and MHC II expression (Helft et al., 2015). Nevertheless, BMDCs have been widely used in numerous studies. They have been shown to be able to effectively present antigens and resemble migratory DCs *in vivo*. In addition, BMDCs express various PRRs and respond well to microbial

stimuli. Therefore, when used with caution, BMDC is a suitable model for answering fundamental questions regarding the innate immune response.

1.1.2. Pattern recognition receptors

Perceiving both extracellular environment and intracellular content by different innate immune cells is often accomplished by PRRs. The expression of a plethora of PRRs at different cellular compartments ensures that the invading dangers are scanned at various steps. By doing this, the innate immune cells are aware of how much the danger has progressed, and therefore can decide on which measure to take to address the danger.

1.1.2.1. PRR ligands: PAMP and DAMP

The concept of PRR arises from PAMP recognition. Only the most conserved and prevalent structures have been selected to become PAMP by evolution. This maximizes the chance of the innate immune cells recognizing pathogens by using a relatively narrow set of receptors. Lipopolysaccharide (LPS), also known as endotoxin, is the prototype of PAMP. It is one of the most conserved structures of all Gram-negative bacteria, thus a perfect PAMP. LPS consists of three main subunits: lipid A, oligosaccharide core and the distal polysaccharide O-antigen. Lipid A is the unit detected by innate PRRs (Steimle et al., 2016). For a long time, it was believed that TLR4 was the only receptor that recognized LPS in mammalian organisms. Activation of TLR4 initiates signaling cascades that result in the release of pro-inflammatory cytokines and anti-microbial substances. However, it was later discovered that caspase-11 serves as a receptor for intracellular LPS. The activation of caspase-11 leads to inflammasome activation and cell death, which represents a more drastic way of eliminating microbes (Shi et al., 2014). The recognition of the very same PAMP by both the surface expressing TLR4 and intracellular caspase-11

further underlines the importance of the strategic positioning of PRRs. Similar PAMPs derived from microbe structures includes bacterial flagellin, lipoprotein from the bacterial cell walls, β-glucan particle from fungi, and various forms of DNA and RNA from bacteria and viruses (Bardoel and Strijp, 2011).

However, solely detecting PAMPs by PRRs leaves blind spots in the innate immunity, as many pathogens have developed evasion strategies to conceal their PAMP identities or sabotage the PRR signaling. For example, the lipid A with four acyl chains expressed by *Yersinia pestis* at 37 °C (mammalian host temperature) has much poorer immunomodulatory activity than the lipid A with six acyl chains expressed by the bacteria at insect host temperature (Montminy et al., 2006). To overcome this constraint, the innate immune system has another recognition system that relies on sensing DAMP. This strategy allows the innate immune system to detect damage or perturbation caused by the pathogen, instead of directly detecting the pathogen itself (Liston and Masters, 2017). Examples of DAMP include uric acid crystals, extracellular ATP, protein HMGB1 and interleukin-33 (IL-33).

Uric acid is a catabolite of purines derived from DNA and RNA. In most species, uric acid can be further processed by an enzyme, called uricase, into highly soluble allantoin (Kono et al., 2010). Human, however, lack uricase. The fast degradation of DNA and RNA within dying cells leads to accumulation of uric acid. Under certain pathological conditions such as tumor growth, chemotherapy, or virus infection, large scale of cell death will result in high uric acid concentration and uric acid precipitation (Jeha, 2001). The monosodium urate (MSU) crystals, which forms when uric acid precipitates, are strong activators of dendritic cells and have been identified as potent adjuvant for T cell priming (Shi et al., 2003).

PRR	Localization	Key signaling molecues	Main ligands
Toll-like receptors (TLRs) (O'Neill et al., 2013)			
TLR4	Cell surface, endosome	MD2, CD14; MAL, MYD88; TRAM, TRIF; TBK1, IKKs	LPS (Gram-negative bateria), O-linked mannan (Fungi)
TLR3	Endosome	TRIF; TBK1; RIP1, IKKs	Viral dsRNA, synthetic dsRNA (Poly(I:C))
TLR7 or TLR8	Endosome	MYD88; IKKs, IRF7	ssRNA, synthetic imidazoquinoline derivatives
TLR2-TLR1	Cell surface	MAL, MYD88; IKKs	Triacylated lipoprotein (Pam3CSK4, Gram-positive bacteria)
TLR2-TLR6	Cell surface	MAL, MYD88; IKKs	Diacrylated lipoprotein, lipoteichoic acid
TLR5	Cell surface	MYD88, IKKs	Bacterial flagellin
TLR9	Endosome	MYD88; IKKs, IRF7	CpG-DNA
RIG-I like receptors (RLRs) (Chan and Gack, 2016)			
RIG-I	Cytosol	MAVS; TRADDosome; TBK1; RIP1, IKKs	Short dsRNA with 5'-triphosphate or 5'-diphosphate group, LMW poly IC
MDA5			Long dsRNA, HMW poly IC
LGP2		Modulates RIG-I and MDA5 signaling	dsRNA
C-type lectin receptors (Sancho and Reis e Sousa, 2012)			
Dectin-1	Cell surface	hemITAM or ITAM; SFKs, syk; PCKδ; CARD9, BLC10, MALT1	β-Glucan, Vimentin
Dectin-2	Cell surface		High mannose structure (fungi), α-mannan, mannose-capped lipoarabinomannan (mycobacteria)
Mincle	Cell surface		Fungal mannose, trehalose-6'6'-dimycolate (TDM, cord factor), SAP130, dead cells
CLEC9A	Cell surface		F-actin, dead cells
Clec12A	Cell surface		Uric acid crystals, dead cels
CLEC5A	Cell surface	DAP12, syk	Mannose and fucose on flavivirus envelop proteins
DC-SIGN	Cell surface		Mannose glycan of gp120 on HIV virus
NOD-like receptors (NLRs) (Chen et al., 2009)			
NOD1	Cytosol	RIP2, IKKs	Peptidoglycan motif iE-DAP dipeptide (all gram-negative bacteria and certain gram-positive bacteria)
NOD2	Cytosol		Peptidoglycan motif MDP (common to all bacteria)
NLRP3	Cytosol	ASC, caspase-1	Ligand unknown, activators: Bacterial toxin Nigericin, potassium efflux, ATP, various particles etc.
NAIP-NLRC4	Cytosol	ASC, caspase-1	Flagellin and Type III/IV Secretion System components (bacteria)
Other PRRs (Hornung et al., 2009; Shi et al., 2014; Sun et al., 2013)			
cGAS	Cytosol	STING, TBK1, IKKs	Cytosolic DNAs
AIM2	Cytosol	ASC, caspase-1, caspase-11	Cytosolic DNAs
Caspase-11	Cytosol		Intracellular LPS

Table 1: Pattern recognition receptors in the innate immune system.

Summary of selected PRRs, showing their cellular localization, essential mediators in their signaling and reported ligands.

1.1.2.2. Toll-like receptors

The discovery of TLRs has revolutionized our understanding of innate immunity. Initially, innate immunity was only regarded as the initiator of adaptive immunity. Even though the innate immune system was implicated in systematic responses and the induction of innate immune agents, such as tumor necrosis factor (TNF), IL-1β, and IL-6, the exact molecular basis was elusive. The characterization of TLRs both greatly advanced our knowledge of these processes and allowed the discovery of other PRR families.

Toll, a *D. melanogaster* protein, was first found to be homologous to the cytosolic domain of IL-1 receptor 1 (IL-R1), which back then was known to activate nuclear factor-κB signaling and induce pro-inflammatory gene expression. Then in 1996, the essential role of Toll in *D. melanogaster* anti-microbial immune response was validated by the observation that anti-fungal peptide Drosomycin was induced via Toll (Lemaitre et al., 1996). Subsequently in 1997, the mammalian Toll homologue hToll, later renamed as TLR4, was cloned and proved to activate NF-κB and the expression of NF-κB-dependent genes in human monocyte (Medzhitov et al., 1997). Since then, ten human and twelve murine TLRs have been characterized and proven to recognize a variety of PAMPs (Table 1).

TLRs are type I transmembrane receptors and have typical extracellular leucine-rich repeats and intracellular Toll/interleukin-1 receptor homology (TIR) domain (Medzhitov et al., 1997). Binding of ligand causes the dimerization of TLRs and initiates the signaling. Following this, the TIR domains of TLRs engage their respective TIR domain-containing adaptor proteins (Table 1), including myeloid-differentiation primary response protein 88 (MYD88), MYD88-adaptor-like protein (MAL), TIR domain-containing adaptor protein inducing IFNβ (TRIF) and TRIF-related

adaptor molecule (TRAM). MYD88 and TRIF are the main ones among those adaptors molecules. Engagement of MYD88 stimulates the downstream signaling that involves binding between IL-1R-associated kinases (IRAKs) and TNF receptor-associated factor 6 (TRAF6) and eventually leads to the nuclear translocation of NF-κB and the expression of pro-inflammatory cytokines (O'Neill et al., 2013). Similarly, recruitment of TRIF to the TIR domain can also induce NF-κB activation (Hoebe et al., 2003). Additionally, it also activates interferon-regulatory factors (IRFs) (Yamamoto et al., 2002). The nuclear translocation of IRFs results in the expression of type I interferon (IFN-I) related genes. In the case of TLR7 and TLR9 signaling, MYD88, (other than TRIF), was shown to function as the adaptor protein for inducing IFN-I response (Negishi et al., 2006; Schmitz et al., 2007a).

1.1.2.3. RIG-I-Like receptors and cyclic GMP–AMP synthase

RLR are sensors of PAMPs in the form of RNA. The RLR family consists of three proteins: the founding member retinoic acid-inducible gene-I (RIG-I), melanoma differentiation-associated protein 5 (MDA5) and LGP2. These three proteins are structurally characterized by the presence of a central helicase domain and a carboxyl-terminal domain, which are essential for their RNA sensing activity (Andrejeva et al., 2004; Yoneyama et al., 2004). RIG-I and MDA5 also harbor tandem caspase activation and recruitment domain (CARD), which are required for their signaling after binding to their RNA ligands. LGP2, on the other hand, lacks the CARD domain and mainly regulates the RIG-I and MDA5 activity (Yoneyama et al., 2005).

Both RIG-I and MDA5 can recognize synthetic double strand RNA (dsRNA) analogue polyinosinc-polycytidylic acid (polyIC). However, RIG-I is only activated by short dsRNA whereas MDA5 recognize high molecular weight (HMW)-polyIC (Goubau et

al., 2013; Kato et al., 2006). Importantly, the presence of a 5'-triphosphate or 5'-diphosphate group on the RNA is essential for RIG-I recognition, but not for MDA5 (Goubau et al., 2014; Hornung et al., 2006; Pichlmair et al., 2006). The natural ligands of RLR are mainly virus-derived RNA species, even though there are reports that mRNA from bacteria can also activate RIG-I in non-phagocytic cells (Schmolke et al., 2014). As for ligand preferences, RIG-I has been shown to be crucial for the detection of many negative-strand RNA viruses (such as rhabdoviruses, influenza viruses, and arenaviruses), as well as the detection of some positive-strand RNA viruses (such as Japanese encephalitis virus and hepatitis C virus). By contrast, MDA5 recognize RNA from picornaviruses. There are many viral RNA that are sensed by RIG-I and MDA5 depending on the time course of virus replication (Chan and Gack, 2016; Goubau et al., 2013; Schlee, 2013). The ligand spectrum of RLR has certain overlap with TLR ligands (TLR3, TLR7/8). However, there is a fundamental difference in RNA detection between RLRs and TLRs, as RNA-sensing endosomal TLRs recognize extracellular RNAs, while RLRs detect intracellular RNAs from actively replicating viruses (Dixit and Kagan, 2013).

Binding of their respective ligands releases RIG-I and MDA5 from their inactive conformation. RIG-I can be further activated through Lys63-linked polyubiquitination to form a signaling-active tetramer, that subsequently interact and activate the central adaptor mitochondrial antiviral signaling protein (MAVS) on mitochondria. As for MDA5, the activation of MDA5 induces filament formation, which in turn enables interaction with MAVS (Chan and Gack, 2016). MAVS activates TANK binding kinase 1 (TBK1) and the inhibitor of nuclear factor kappa-B kinase (IKK) complex, which activate IRF3 and IRF7, and NF-κB respectively. These transcription factors

eventually work in concert to regulate the gene expression of IFN-Is or IFN-I related genes, as well as many other pro-inflammatory cytokines and chemokines.

Similar to intracellular RNA recognition by RLRs, cytosolic DNA can also be detected by bona fide intracellular DNA sensors cyclic GMP–AMP synthase (cGAS) (Sun et al., 2013). cGAS binds to cytosolic double strand DNA (dsDNA) and generates cyclic GMP-AMP (cGAMP). The second messenger cGAMP subsequently binds to stimulator of interferon genes (STING, an essential adaptor protein for the signaling) and triggers its activation by dimerization and polyubiquitination. Similar to MAVS in RLR signaling, activated STING activates TBK1 and IKK complex and induces signaling cascades that culminate in the expression of IFN-I and proinflammatory genes (Ishikawa and Barber, 2008; Sun et al., 2009).

1.1.2.4. C type lectin receptors

CLRs, defined by the presence of at least one C-type lectin-like domain (CTLD), are a large family of soluble or transmembrane proteins. The prototypic members in this family are characterized by their calcium-dependent carbohydrate binding (lectin) activity. However, many members were later identified based on sequence and structure homology and may no longer have the ability to actually bind calcium and carbohydrate moiety any more (Zelensky and Gready, 2005).

Many CLRs, especially those predominantly expressed on myeloid cells, prove to be key players in pathogen and tissue damage recognition. The ligands of CLRs covers a broad spectrum of pathogen and self-derived molecules (Table 1). Some CLR members, such as Dectin-1 and Dectin-2, mostly recognize microbial PAMPs. Other members, like Clec9a, have been shown to mainly detect self-ligand and dead cells.

In addition, there are CLRs, like Mincle, that recognize both pathogen and endogenous ligands (Sancho and Reis e Sousa, 2012).

Of notice, several CLR genes cluster closely on chromosome 12 in human and chromosome 6 in mouse to form the natural killer receptor gene complex (NKC). Despite recognizing very different ligands, these CLRs use highly conserved signaling modules to execute their functions. Many CLRs have immunoreceptor tyrosine-based activation motif (ITAM), or can couple to adaptors containing such a motif. Crosslinking by ligands of these CLRs triggers tyrosine phosphorylation at their cytoplasmic tails and generates a docking site for the Src-homology 2 (SH2) domain of the spleen tyrosine kinase (SYK). SYK recruited to the receptor undergoes conformational changes, which allows for its autophosphorylation and activation (Mócsai et al., 2010). Active SYK propagates the signaling transduction and lead to myeloid cell activation. One branch of the signaling pathways involves the formation of the CARD9-B-Cell CLL/Lymphoma 10 (BCL10)-Mucosa-associated lymphoid tissue lymphoma translocation protein 1 (MALT1) complex, which is essential for the activation of NF-κB (Gross et al., 2006). For CLRs that harbor immunoreceptor tyrosine-based inhibitory motif (ITIM), or those that can couple to adaptors containing such motifs, the engagement of receptors leads to the phosphorylation of the tyrosine residue within the ITIM. The phosphorylated ITIM serves as a docking site for several phosphatases, such as Src homology 2 domain containing protein tyrosine phosphatase-1/2 (SHP-1/2) and SH2-containing inositol phosphatase (SHIP-1) (Marshall et al., 2004; Richard et al., 2006), which could counteract with activating kinases to keep the cell activation in check (Kanazawa et al., 2002; Neumann et al., 2014).

1.1.2.5. NOD-like receptors and PYHIN family receptors

NLRs are proteins that reside in the cytosol. They typically show a tripartite structure that is comprised of a central nucleotide-binding and oligomerization (NACHT) domain, a C terminal LRR and a variable N terminal effector domain (including CARD, Pyrin domain (PYD), baculovirus inhibitor of apoptosis repeat (BIR) domain and acidic activation (AD) domain etc.). Based on the N terminal effector domain, NLRs can be classified into five subgroups: PYD-containing NLRP, CARD-containing NLRC, BIR-containing NLRB, AD-containing NLRA and NLRX (without homologous effector domain with any other NLR subfamily member) (Ting et al., 2008). NOD1 and NOD2 belong to the NLRC subfamily and are the founding members of NLR (Girardin et al., 2003; Inohara et al., 2003). They recognize bacterial cell wall component and activate NF-κB pathway via receptor-interacting serine/threonine-protein kinase 2 (RIP2) (Strober et al., 2006). Many other NLRs, including NLRP1, NLRP3, NLRC4, are involved in formation of the multiprotein complex inflammasome, which serves as a platform for caspase-1 activation and subsequent secretion of IL-1β and IL-18 (Broz and Dixit, 2016).

Another group of intracellular PRRs are the PYHIN proteins. Under steady state, the PYHINs predominantly localize to the nucleus, with a few exceptions to the cytoplasm. Relocalization of nuclear PYHIN occurs when the cells are stimulated (Schattgen and Fitzgerald, 2011). Each PYHIN protein consists of a PYD and a hematopoietic interferon-inducible nuclear proteins with a 200-amino-acid repeat (HIN-200) domain. The HIN-200 domain is capable of binding DNA. Therefore, PYHINs are important cytosolic DNA sensors. The first PYHIN that was linked to innate immunity is absent in melanoma 2 (AIM2), which was identified as a receptor

for DNA-induced inflammasome activation. Other PYHINs, like IFI16, was found to activate type I interferon via STING, similar as cGAS.

1.2. Type I interferon

Interferon was initially described in 1957 by Alick Isaacs and Jean Lindenmann and was the first cytokine to be identified (Isaacs and Lindenmann, 1957). Decades later, it was discovered that “interferon” is not one protein, but rather a family of proteins that can be divided into three subgroups according to their receptors: namely type I, II and III interferon. IFN-I is the largest interferon family. In human, the IFN-I consists of IFN-α, IFN-β, IFN-ε, IFN-κ and IFN-ω, all of which represent a single protein, except for IFN-α, that is comprised of 13 subtypes. All nucleated cells are capable of producing IFN-α and IFN-β, however with variable amount. The type II interferon has only one member IFNγ and the type III interferon is made up of three members, IFN-λ1, IFN-λ2, and IFN-λ3, also known as IL-29, IL-28A, and IL-28B, respectively.

1.2.1. Type I interferon signaling

All interferons signal via the Janus Kinase (JAK)-signal transducer and transactivator (STAT) signaling pathway. Three of the four known JAKs are involved in interferon signaling, with JAK1 and TYK2 being involved in IFN-I signaling. There are seven STATs in mammals, and STAT1 and STAT2 are most important in IFN-I signaling (Figure 1).

Following binding to IFN-I, IFNAR transmits a signal across the plasma membrane to activate JAKs. This happens instantly as the JAKs and other IFN-I signaling components are already present at baseline (Larner et al., 1984; Schneider et al., 2014). Type I interferon receptor (IFNAR) is a heterodimer consisting of two subunits: IFNAR1 and IFNAR2, which associate with JAK1 and tyrosine kinase 2 (TYK2) respectively. The JAKs couple to IFNAR with an inactive conformation and get activated by trans-phosphorylating neighboring JAKs when brought together by

interferon receptor ligation. The activated JAKs in turn tyrosine phosphorylate the interferon receptor and generate a SH2 domain-binding site.

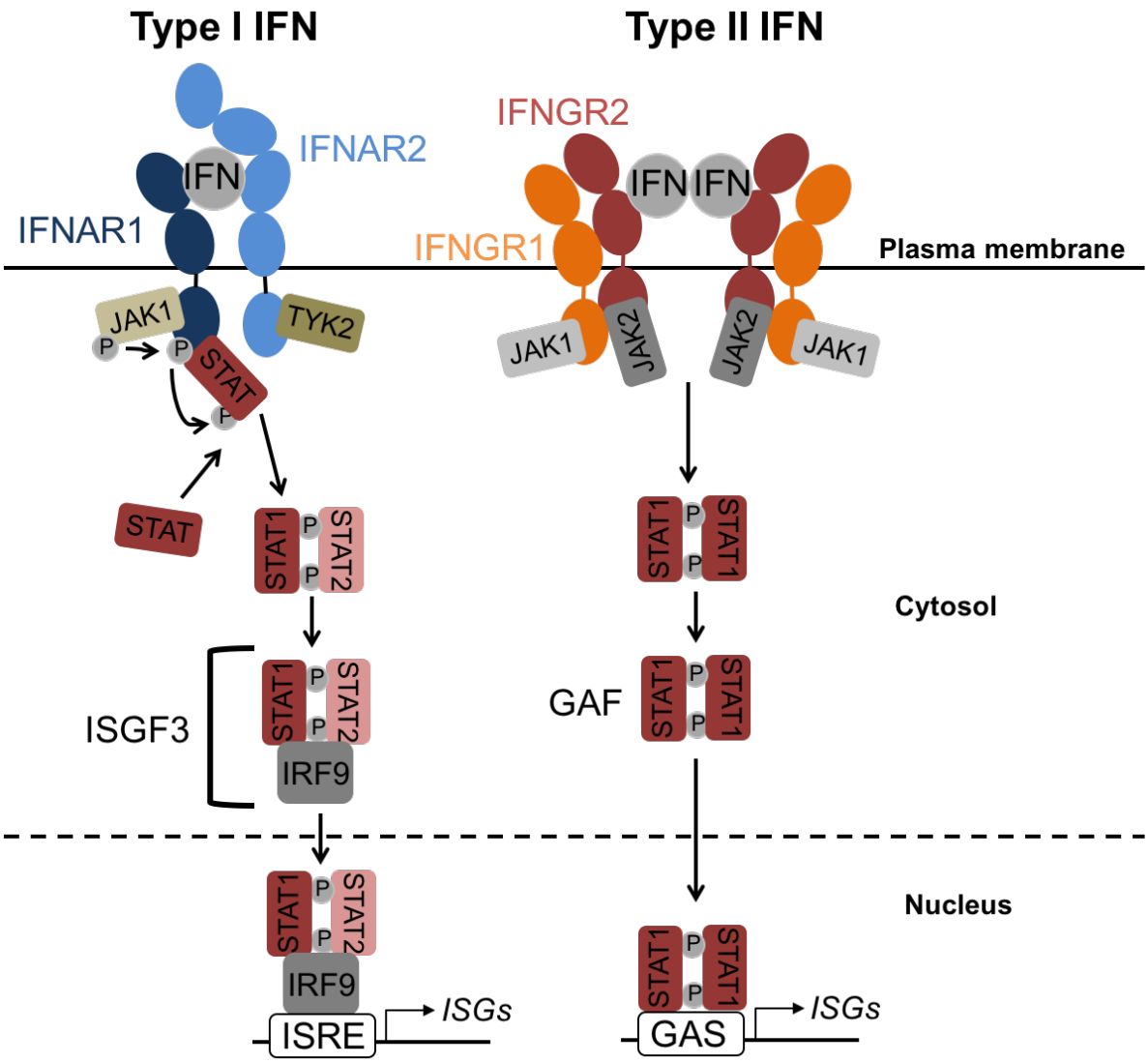

Figure 1: The interferon signaling cascade.

Type I interferon activate the IFN-α receptor 1 (IFNAR1) and 2 (IFNAR2) heterodimer, while type II interferon bind dimers of heterodimers consisting of IFN-γ receptor 1(IFNGR1) and 2 (IFNGR2). Ligation of those receptors triggers phosphorylation of the respective pre-associated JAKs, which in turn phosphorylate the receptors, creating a docking site for STATs. STATs recruited to the receptors will be activated by phosphorylation. STAT1 and STAT2 form heterodimer after activation by type I interferon ligation and further recruit IRF9 to form the IFN-stimulated gene factor 3 (ISGF3). STAT1 activated by type II interferon forms homodimer. Both the ISGF3 and STAT1 homodimer are transcriptionally active and can translocate to the nucleus and regulate the expression of genes containing their respective binding site, namely IFN-stimulated response element (ISRE) and gamma-activated sequence (GAS). Adapted from (Schneider et al., 2014)

The exposed binding site on IFNAR recruits and phosphorylates STAT1 and STAT2. The phosphorylated STAT1/STAT2 are then released from the receptor and form a heterodimer, which helps to reveal their nuclear localization signal and facilitates their nuclear translocation (Melen et al., 2001). The STAT1/STAT2 heterodimer also interact with IRF9. The three proteins form a complex called interferon-stimulated gene factor 3 (ISGF3) (Fu et al., 1990), which can bind the consensus motif interferon-stimulated response element (ISRE) and regulate the transcription of a huge set of interferon-stimulated genes (ISGs) (Levy et al., 1988).

1.2.2. The production of type I interferon

The production of IFN-I can have a biphasic mode. The initial phase is represented by the primary production of IFN-β and IFN-α4 as a result of PRR signaling. The second phase, on the other hand, occurs when the autocrine IFN-I activates IFNAR and triggers the expression of all IFN-I subtypes (Sato et al., 2000). In light of this, the study of primarily produced IFNβ induction could provide great insight into the regulation of IFN-I response after innate immune activation. The promoter region of IFN-β contains four cis regulatory elements called positive regulatory domain (PRD) I, II, III and IV (Kim and Maniatis, 1997). These domain binds to IRFs, NF-κB and AP-1, which all together form enhanceosome to facilitate the initiation of IFN-β transcription (Agalioti et al., 2000). However, TNF-α, which robustly activates NF-κB and AP-1 but not IRFs, can only weakly (if at all) activate *Ifnb* promoter (Reis et al., 1989; Yarilina et al., 2008), indicating that the IRFs are the real master regulators of *Ifnb* transcription.

Nine IRFs members, namely IRF1-9, constitutes the IRF family. Among them, IRF1, IRF3, IRF5, and IRF7 have been reported to positively regulate primary IFN-I expression (del Fresno et al., 2013; Miyamoto et al., 1988; Sato et al., 2000).

Especially IRF3 and IRF7 are well studied and prove to play critical role in inducing IFN-I downstream of several PRR signalings. IRF3 resides in the cytosol and is constitutively expressed. The phosphorylation of IRF3 at serine residues 396 and 386 prove to be essential for turning on its transcriptional activity (Mori et al., 2004; Servant et al., 2003), either by releasing its auto-inhibitory state (Qin et al., 2003) or by inducing active IRF3 homodimer or heterodimer with IRF7 (Takahasi et al., 2003). IRF7 is highly homologous to IRF3. The expression of IRF7, by contrast, is extremely low at steady state. However, it can be greatly induced in the presence of IFN-I, indicating its role in the feed-forward loop of IFN-I production (Marié et al., 1998; Sato et al., 2000). Compared to IRF3, IRF7 is also short-lived and is quickly degraded through the ubiquitin-dependent pathway to avoid the collateral damage from IFN-I overproduction (Yu et al., 2005). In addition, in the specialized IFN-I producing cell pDC, the IFN-I production is mainly mediated by IRF7, while IRF3 seems to be dispensable. Meanwhile, the TLRs on pDC utilize MYD88, rather than TRIF, to induce IFN-I response by directly interacting with IRF7 (Honda et al., 2005).

Major PRR families all have members that are known to control the expression of IFN-Is by regulating the activity of IRF3 and IRF7. Despite the variable upstream signaling events, they all seem to achieve this by acting on TBK1 (Figure 2). Key adaptors in PRR signaling, including TRIF in TLR, MAVS in RLR and STING in cGAS and PYHINs, are known to recruit or directly interact with TBK1 (Ishikawa and Barber, 2008; Liu et al., 2015; Sato et al., 2003). TBK1 encompasses a catalytic kinase domain (KD), a ubiquitin-like domain (ULD), and a scaffolding/dimerization domain (SDD). It can be recruited to discrete signaling platforms. This recruitment results in high local concentrations of TBK1, which facilitates its trans-autophosphorylation at serine residue S172 and activation (Ma et al., 2012). Active

TBK1 can directly phosphorylate IRF3 and IRF7 at their serine residues and trigger their transcriptional activity (Fitzgerald et al., 2003; McWhirter et al., 2004; Sharma et al., 2003). Given its critical role in IFN-I induction, the activity of TBK1 is tightly regulated through dephosphorlation, polyubiquitination or kinase activity modulation (Zhao, 2013).

1.2.3. The functions of type I interferon

IFN-Is are pleiotropic cytokines. Their most prominent function is to establish anti-viral state in virus-infected cells by inducing the expression of ISGs. Many of these ISGs have been individually characterized and prove to be essential in combating viral infection by interfering with key steps in the virus replication cycle. For example, proteins from the IFN-inducible transmembrane (IFITM) family block cell entry by interacting with viruses that transit from late endosome or lysosome to cytosol (Brass et al., 2009; Huang et al., 2011), and IFN-induced proteins with tetratricopeptide repeats (IFIT) inhibit protein translation and can sequester specific viral RNAs (Diamond and Farzan, 2013; Pichlmair et al., 2011). In addition, viperin, also known as RSAD2, is induced by IFN-I and can inhibit budding of enveloped viruses (Szretter et al., 2011; Wang et al., 2007). Many key signaling molecules, such as IRF7 and STAT1, are also induced by IFN-I and thus, also considered as ISGs (Sato et al., 2000).

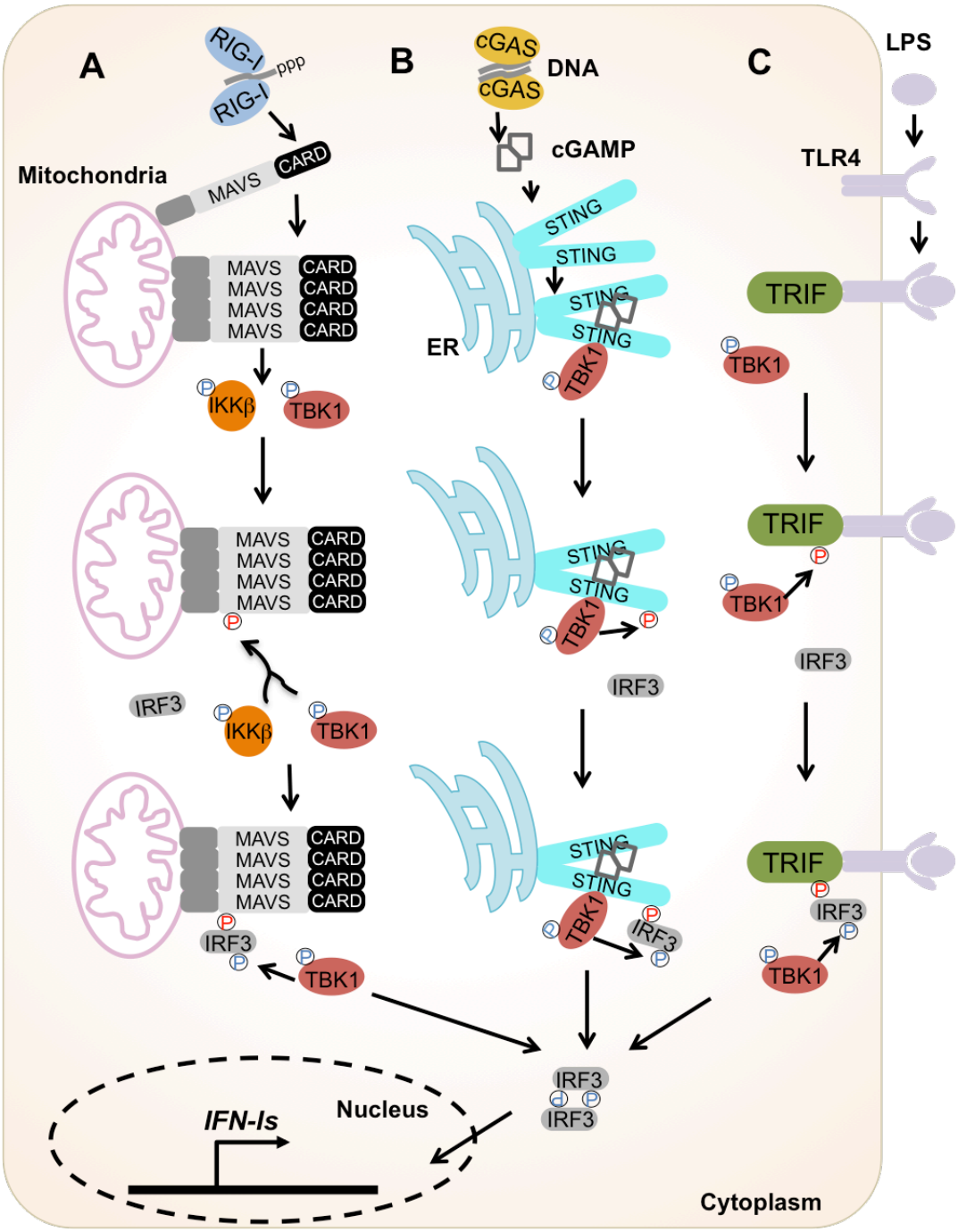

Figure 2: IFN-I production signaling downstream of various PRRs converge on TBK1

Upon ligand binding, RIG-I, cGAS and TLR4 activate their adaptors MAVS, STING and TRIF respectively through distinct mechanisms. Active MAVS aggregates and TRIF indirectly recruit and activate kinases TBK1 and IKK, whereas STING directly binds and activates TBK1. In return, the activated kinases phosphorylate those adaptors proteins at their pLxIS motif (p: hydrophilic, x: any amino acid), providing a docking site for the positively charged C terminal region of IRF3. Subsequently, TBK1 activates IRF3 in its proximity through serine phosphorylation. Adapted from (Liu et al., 2015).

In addition, IFN-Is are known to have modulatory effects in various autoimmune diseases. It has been reported that commensals in the gut can induce IFN-I production by activating TLR9, which protects the mice against experimental colitis. Moreover, IFNAR deficient mice are extremely susceptible to DSS-induced colitis (Katakura et al., 2005). In addition to intestinal inflammation, other diseases that are driven by T helper 1 (TH1) and TH17 response, such as multiple sclerosis and arthritis, also benefit from recombinant IFN administering. By contrast, systemic lupus erythematosus and psoriasis are improved by IFN-I inhibition (González-Navajas et al., 2012).

Similar to its disparate roles in autoimmune diseases, IFN-I seems to also be a double-edged sword in anti-bacterial response. Depending on the bacterial replication strategy, the virulent factors and route of infection, IFN-I directs variable outcomes of bacterial infection (Boxx and Cheng, 2016). IFN-I is shown to exacerbate infection of *Listeria monocytogenes*, *Francicella tularensis* and *Salmonella enterica* serovar Typhi by inducing death of immune cells and by inhibiting anti-bacterial inflammatory responses (Henry et al., 2010; O'Connell et al., 2004; Perkins et al., 2015). On the other hand, IFN-I provides protection against infection of *Helicobacter pylori*, mainly by inducing chemotactic ISG, CXCL10 (Watanabe et al., 2010).

1.3. Clec12A

CLec12A, also known as myeloid inhibitory C-type lectin receptor (MICL) or dendritic cell-associated lectin 2 (DCAL-2), is an inhibitory C-type lectin receptor found in the NKC. It is predominantly expressed on myeloid cells, but can also be found on murine B cells (Kasahara and Clark, 2012; Marshall et al., 2006; Pyż et al., 2008). As a type II transmemrane protein, it contains one extracellular CTLD at its C terminus and a short cytoplasmic tail at its N terminus. Importantly, an ITIM motif (IVYANL) was identified at the N terminus of Clec12A. When the tyrosine phorsphorylation in the ITIM is unspecifically induced by sodium pervanadate treatment, the receptor recruits phosphatases SHP1/2, implying it can transduce inhibitory signals (Marshall et al., 2006).

Early studies indicated the presence of endogenous ligands for Clec12A. Recombinant murine Clec12a protein was reported to bind cell preparations isolated from heart, kidney, lung, liver and spleen (Pyż et al., 2008). Further research identified Clec12a as a DAMP sensing receptor. It binds to corpse of the dead cells in those cell preparations. More specifically, Clec12A detects uric acid crystals released from dead cells, even though the existence of other endogenous ligands can not be excluded (Neumann et al., 2014). Consistently, a recent study claim that Clec12A can recognize damaged membranes, as proven by the colocalization of Clec12A with membrane-damage marker LC3 (Begun et al., 2015).

There is accumulating evidence showing that Clec12A can regulate inflammation (Figure 3). The Clec12A-deficient neutrophils produce much more respiratory oxygen species (ROS) when activated by uric acid crystals. In line with this, the Clec12A-deficient mice recruit many more inflammatory cells when uric acid crystals are

injected or local cell death is introduced into those animals (Neumann et al., 2014). Meanwhile, Clec12A-deficient mice showed increased susceptibility to collagen antibody-induced arthritis. This finding is further corroborated by the identification of anti-Clec12A autoantibody in rheumatoid arthritis patients (Redelinghuys et al., 2016).

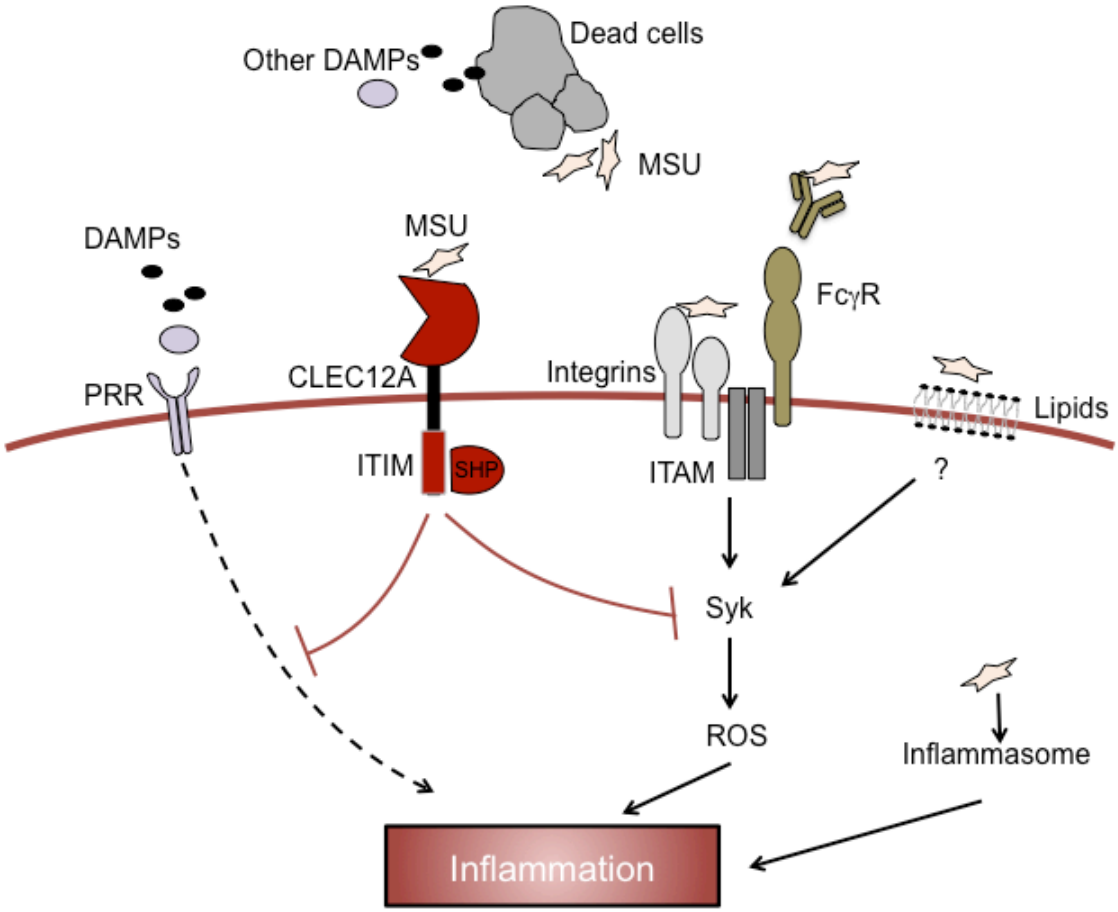

Figure 3: Clec12A controls inflammation upon recognizing MSU crystal and dead cells

Uric acid can be released by dead cells and forms MSU crystals in appropriate extracellular milieu. The MSU crystal (opsonized by antibodies) can bind to integrin and cell surface Fc receptors that are coupled to ITAM containing adaptors, or directly interacts with membrane lipid, leading to ROS production through syk activation. In mouse bone marrow cells, Clec12A, upon sensing dead cells and MSU crystals, can counteract the activating signals and keep the ROS production in check, thereby controlling excessive inflammation. In addition, it is largely dispensable for the MSU induced inflammasome activation and IL-1β production. Adapted from (Yamasaki, 2014)

1.4. Purpose of the study

The research of individual PRRs have greatly advanced our knowledge of the innate immune system. However, PRRs do not work in isolation. The cross talk and regulation between PRRs ensure that the innate immune cells generate context-dependent response. This notion is supported by the fact that ITAM and ITIM-containing receptors can cross talk with PRRs that initiate the interferon response (Huynh et al., 2012; Rahim et al., 2013; Troegeler et al., 2017). As Clec12a has been identified as a DAMP-sensing receptor with an ITIM motif, it is interesting to consider whether it can integrate cues from dying and damaged cells to subsequently alert the cells by regulating the interferon response. This would ensure that the innate immune cells mount a more effective and controlled response.

Through taking advantage of the Clec12A deficient mice generated by our laboratory, this study will:

1. Explore the possible link between Clec12A and PRR induced interferon.

2. Dissect the signaling events of Clec12A regulating IFN-I response.

3. Define the role of Clec12A *in vivo* during infection.

2. Material and methods

2.1. Cell culture

2.1.1. Bone marrow derived dendritic cell culture

Cells were handled aseptically under the filtered cell culture hood (BDK Luft- und Reinraumtechnik GmbH), and were cultured at 37 °C/5% CO_2 in a humidified incubator (BINDER GmbH). All centrifugation steps were performed at 400 *g* for 5 min at 4 °C. Cells were enumerated by using the LUNA™ automated cell counter (Logos Biosystems).

Murine bone marrow was used to differentiate dendritic cells according to previously described protocol with minor modification (Boudreau et al., 2008; Lutz et al., 1999). Briefly, 22-gauge needle was inserted into femur and tibiae bones to flush out the bone marrow into R5 medium (RPMI supplemented with 5% FBS). Erythrocytes were lysed with G-DEX II RBC lysis buffer (Intron Biotechnology) and 5 million bone marrow cells were seeded into 10 cm non-treated petri dish (Sarstedt) in 10 ml complete RPMI supplemented with 10% FBS (PAN), 50 μM beta-mercaptoethanol, 100 U/ml penicillin, 100 mg/ml streptomycin and 20 ng/ml recombinant GM-CSF (immunotools). 10 ml of additional medium was given on day three. 10 ml of old medium was replaced with fresh medium on day six. On day nine, non-adherent and loosely adherent cells were collected by pipetting. Cells were washed once with R5 before stimulation.

2.1.2. Cell treatment and stimulation

Cells were kept in R5 during stimulation. Lipofectamine 2000™ (Invitrogen) was used to transfect 5'-triphosphate dsRNA (3pRNA, InvivoGen) into BMDCs. 3pRNA and

Lipofectamine 2000 at the ratio of 1 μg:2 μl was added into Opti-MEM™ (Gibco) separately for 5 minutes before they were mixed and incubated for another 20 minutes. If not otherwise indicated, the following concentration of stimuli were used: MSU 500 μg/ml, LPS (ultrapure, from *E. coli* 0111:B4) 50 ng/ml, CpG-ODN 1826 (InvivoGen) 0.5 μM, 3pRNA 0.4 μg/ml for gene expression analysis and 2 μg/ml for immunoblot analysis, recombinant interferon β (Mammalian expressed, PBL assay science) 200 U/ml.

For IFNAR blocking, cells were pretreated with IFNAR1 monoclonal antibody (MAR1-5A3, eBioscience) or mouse IgG1 isotype control (eBioscience) at 10 μg/ml for 1 hour before stimulation. For inhibitor treatment, BMDCs were preincuated with PP2 (Calbiochem), Wortmannin (Cell Signaling), Cytochalasin D (Sigma), MCC950 (Cayman Chemical), CA-074 Me (Enzo Life Sciences), IRAK1/4 (Sigma) and chloroquine (Sigma) or mock treated with DMSO for 1 hour before stimulation.

2.2. Molecular biology

2.2.1. MSU crystal preparation

1.68 g uric acid (Sigma) was added to 500 ml sodium hydroxide (20 mM) solution and was subsequently heated up to 70 °C for 20 minutes. If uric acid did not dissolve well, add 200-500 μl of 1 M sodium hydroxide solution. Then cool down the solution to 60-40 °C and adjust the PH to 7.1 with 1 M sodium hydroxide solution. Add sodium chloride to final concentration of 20 mM to facilitate crystallization. Incubate the solution for 2 weeks with gentle rotation under the dark. Two weeks later, collect the crystals by filtering with 0.22 μm Stericup® Filter Units (Millipore). Wash the crystals with 800ml absolute ethanol. Dry the crystals under the hood and resuspend in PBS.

2.2.2. RNA extraction

Stimulated cells were centrifuged to remove supernatant. RLT plus (Qiagen) buffer was directly added to lyse the cells. For isolating RNA from tissues, the Tissuelyser II (Qiagen) and steal beads (Qiagen) were used to disrupt and homogenize samples. Genomic DNA was removed by using the genomic DNA removal column (Qiagen). Total RNA was then extracted by using the RNeasy plus mini kit (Qiagen) according to the manufacturer's instruction. RNA was either directly reverse transcribed or flash frozen in liquid nitrogen and store at -80 °C.

2.2.3. Real time quantitative PCR

Total RNA was first reversed transcribed into cDNA by using the ProtoScript® II Reverse Transcriptase (NEB), random primer (Invitrogen) and 10 mM dNTP mix (Biozym). Transcribed cDNA was diluted 1:5 to 1:10 before gene expression quantification.

SYBR Green I core kit (Eurogentec) and the LightCycler 480 real-time PCR system were used for subsequent gene expression quantification. If not otherwise indicated, the expression of target genes was calculated as the ration of the real-time signals of the target genes to that of *Hprt*.

qPCR master mix:

10x qPCR buffer	2 µl
$MgCl_2$ (50 mM)	1.4 µl
dNTP (5 mM each)	0.8 µl
SYBR green solution	0.6 µl
Hot Start Gold Taq	0.1 µl
Water	7.1 µl

Primer mix (forward and reverse, 1 μM) 3 μl

Diluted cDNA 5 μl

qPCR program: Taq hot start, 95 °C for 10 minutes; denaturation, 95 °C for 15 seconds, annealing 60 °C for 20 seconds, extension 72 °C for 40 seconds, 40 cycles; melting curve.

Primers

Ifit3	5'-GATTTCTGAACTGCTCAGCCC-3'
	5'-TCCCGGTTGACCTCACTCAT-3'
Irf7	5'-ATGCACAGATCTTCAAGGCCTGGGC-3'
	5'-GTGCTGTGGAGTGCACAGCGGAAGT-3'
Hprt	5'-CAGTCCCAGCGTCGTGATTAG-3'
	5'-GCAAGTCTTTCAGTCCTGTCCA-3'
LCMV-NP	5'-CGCACAGTGGATCCTAGGC-3'
	5'-GCTGACTTCAGAAAAGTCCAACC-3'
β-actin	5 '-CACACCCGCCACCAGTTCG-3'
	5'-CACCATCACACCCTGGTGC-3'

2.2.4. RNA-seq and gene set enrichment analysis

The quality of purified total RNA samples from BMDCs were checked by using the 2200 Tapestation system (Agilent Technologies). Samples with RIN value more than 9.0 were submitted to the Genomics & Proteomics Core Facility at the DKFZ (Heidelberg, Germany), where they were subjected to library preparation where it was subjected to library preparation using the Illumina TruSeq RNA sample preparation kit v2. Libraries were pooled (5 samples per lane) and sequenced on an Illumina HiSeq 2000 (50 base pair single-end reads).

The RNA-seq data were analyzed by using the Tuxedo pipeline (Trapnell et al., 2012). The reads were mapped to the mm9 mouse genome assembly downloaded from UCSC by using Tophat (v2.1.1). Fragments per kilobase of transcript per million mapped reads (FPKM) values of all samples from were quantified by using cuffquant (v2.2.0). FPKM values from different conditions were normalized by using cuffnorm (v2.2.0) to account for the inter-sample variation. FPKM values of selected genes were clustered by hierarchical clustering and plotted by using the Morpheus software. Additionally, lists of differentially regulated genes for the WT versus knockout samples in each condition were generated by using Cuffdiff (v2.2.0). Differentially regulated genes with FDR of no greater than 0.1 from all conditions were complied and used for subsequent gene set enrichment analysis (GSEA).

GSEA analysis was done with the javaGSEA tool (Broad institute). Complied list of gene expression FPKM value were compared against the MSigDB gene set collection H (hallmark gene sets, 50 gene sets in total) and C7 (immunologic signatures, 4872 gene sets in total). The settings used are as follows: number of permuations, 1000; permutation type, gene set; collapse dataset to gene symbols, true; chip platform, ENSEMBL_mouse_gene.chip (from Broad institute); enrichment statistic, weighted; metric for ranking genes, log2 ratio of classes; size of gene sets, 15-500.

2.2.5. Immunoblotting

Stimulated cells were washed with ice cold 1xPBS and lysed in 2x Laemmli buffer or 1x NP-60 buffer with phosphatase and protease inhibitors (Roche). Samples directly lysed in laemmli buffer were cooked at 95 °C for 10 minutes before loading. Cells that were lysed in NP-40 buffer was incubated at 4 °C for 30min and centrifuged at 12000 g for 20 minutes at 4 °C to remove the genomic DNA and debris. The protein

concentration in the supernatant was determined by BCA protein assay (Thermo Scientific™ Pierce™). Equal amount of protein across samples was mixed with Laemmli buffer and cooked at 95 °C for 10 minutes before loading. Denatured protein samples were loaded onto 10-12 percent Bis-Tris polyacrylamide gels and proteins separated by application of 130 V for 1-2 hours in 1x MOPS buffer. Proteins were transferred from gels to nitrocellulose membrane (GE Healthcare) by application of 0.4 mA for 2 hours in 1x transfer buffer. The efficiency of transfer was checked by soaking the membrane in Ponceau S and subsequent rinsing with deionized water. After blocking the membrane in blocking buffer (5% BSA in TBST) for 1 hour at room temperature, primary antibodies diluted in blocking buffer (supplemented with 0.1% sodium azide) were applied overnight at 4 °C. The membrane was washed in 1x TBST buffer for at least 3 times at room temperature, each at least half an hour, and incubated with respective horseradish peroxidase (HRP)-coupled secondary antibody diluted in 1x TBST for 1 hour at room temperature. The membrane was again washed 3 times with 1x TBST. Normal or enhanced chemiluminescent substrate (Thermo Scientific™ Pierce™ or Amersham™ ECL™ Prime) was added on top of the membrane before it was imaged with the cooled charge-coupled device (CCD) camera (Intas). 1 to 30 minutes exposures were taken depending on the signal intensity. Images were inverted, so that the signal was black instead of white. In cases of detecting the total protein levels of the respective phosphorylated proteins or detecting proteins with similar molecular weight, the membranes were stripped before re-blotting. For membrane stripping, the membrane was washed once with 1x TBST after developing and put into 1x stripping buffer. The buffer was then heated up in an 80 °C water bath for 20 minutes with gentle shaking in between.

Primary and antibodies used:

phospho-STAT1 Y701,	CST #9167, rabbit	1:1000
STAT1	CST #9172, rabbit	1:1000
phospho-NF-κB p65 S536	CST #3033, rabbit	1:1000
phospho-TBK1/NAK S172	CST #5483, rabbit	1:2000
phospho-IRF3 S396	CST #4947, rabbit	1:1000
IRF3	CST #4302, rabbit	1:1000
phospho-Src family Y416	CST #2101, rabbit	1:2000
TBK1	sc-73115, mouse	1:1000
Src	sc-5266, mouse	1:1000
S100A9	R&D MAB2065, rat	2 μg/ml
β-actin	Sigma A5060, rabbit	1:10000

2.2.6. Cytokine and LDH Measurement

Cells were stimulated with indicated stimuli for 6 hours. The cell free supernatant was collected by centrifugation. Level of IFN-α was measure by the Mouse IFN Alpha ELISA Kit (PBL assay science) and the level of IFN-β was measure by the High Sensitivity Mouse IFN Beta ELISA Kit (PBL assay science) according to manufacturer's instructions. Absorbance at 450 nm was measured using the Mithas plate reader, and concentrations were interpolated from the standard curve by using Graphpad prism.

LDH in cell free supernatant was determined by CytoTox 96® NonRadioactive Cytotoxicity Assay (Promega). Maximal relseas of LDH was determined by measuring LDH levels in the supernatant of cells lysed with Triton X-100.

2.2.7. Flow Cytometry

Single cells suspension was centrifuged to remove the supernatant. Cell pellet was wash with FACS buffer (PBS with 3% FBS and 0.05% sodium azid) before they were incubated with Fc-block (1:200, anti-CD16/CD32 ebioscience) and the fixable viability dye (ebioscience) in PBS at 4 °C for 20 minutes. Subsequently, the cells were washed again with FACS buffer and stained with the appropriate surface markers in FACS buffer at 4 °C for 20 minutes. After washing with FACS buffer, the cells were resuspended in FACS buffer and acquired on a FACSCanto II (BD). FACS data were analyzed by using Flowjo software (Tree Star, Inc.) For staining Clec12A on BMDC, the APC conjugated antibody (Clone 5D3, Biolegend) was used.

2.3. Animal experiments

2.3.1. Mice

Clec12A deficient mice were generated by conventional gene-targeting method (Neumann et al., 2014). A neomycin cassette was recombined to replace the exon 1 and 2 encoding the N-terminal part of Clec12a protein. The mice were backcrossed to C57BL/6J for more than 10 generations and kept under specific pathogen-free condition in the Zentrum für Präklinische Forschung facility. Groups of sex and age matched mice were cohoused for at least 4 weeks before they were used for *in vivo* experiments.

2.3.2. Whole body irradiation

WT and *Clec12a*$^{-/-}$ mice were whole body-irradiated with 1 Gy of X-rays. Fourteen hours later, the thymus was excise and meshed through 100μM cell strainer. The thymocytes were either analyzed by flow cytometry or subjected to RNA extraction as described (Neumann et al., 2014).

For gelatin zymography, the supernatant of meshed thymus was mixed with 4X non-reducing sample buffer (Pierce™) and loaded onto 12% polyacrylamide gel with 0.1% gelatin. Run the gel with 1x Tris-Glycine SDS running buffer. The gel was then washed sequentially with 2.5% Triton X-100 and zymography buffer (200 mM NaCl, 5 mM $CaCl_2$, 50 mM Tris-HCl PH 7.4) before it was placed into zymography buffer and incubated at 37 °C overnight. The gel was finally stained with Coomassie Brilliant Blue G-250 Dye (Thermo scientific). Areas of protease activity will appear as clear bands against a dark blue background where the protease has digested the substrate.

2.3.3. Virus infection

For acute LCMV infection, mice were intravenously injected with $2x10^6$ plaque forming unit (PFU) of LCMV-WE stain through the tail vein. Mice were weight and monitored daily for health and survival. In addition, serum samples were collected on day 2, day 8 and day 14-post infection by submandibular bleeding. The levels of viral NP genes in the mouse liver on day 14-post infection were quantified by real-time PCR. Serum AST and ALT activity was measured in the Institut für Klinische Chemie und Pathobiochemie, Klinikum rechts der Isar.

Chronic LCMV infection was performed by Vikas Duhan at Universität Duisburg-Essen. Briefly mice were infected with $2x10^4$ PFU of LCMV-docile stain. Serum samples were collected at different time points after infection. Serum titer of virus was determined by plaque assay as previously described (Duhan et al., 2016).

For MVA virus infection, $5x10^7$ $TCID_{50}$ of MVA-OVA virus (MVA-mBNbc126; Batch #Prod.05A13, Bavarian Nordic) were intravenously injected though the tail vein. Serum samples were taken before infection, 6 hours and 24 hours after infection for

cytokine analysis. After 7 days, mice were sacrificed and blood was taken for serum preparation out of the heart. Spleen was taken out and meshed. Splenocytes were stained and analyzed by flow cytometry.

Staining I

Fixable viability dye	eFluor 506	eBioscience
CD3	FITC	eBioscience (145-2C11)
CD4	APC-cy7	eBioscience (GK1.5)
CD8	Pacific blue	eBioscience (53-6.7)
OVA dextramers H-2 Kb (SIINFEKL)	PE	Immudex
B8 dextramers H-2 Kb (TSYKFESV)	APC	Immudex

Staining II

Fixable viability dye	eFluor 506	eBioscience
CD19	APC-cy7	eBioscience (1D3)
CD11b	Pacific blue	eBioscience (M1/70)
Clec12A	APC	Biolegend (5D3)
CD49b	PE	eBioscience (DX5)

Anne Louise Hansen at Aarhus University, Denmark performed the influenza infection experiments. Briefly, male mice were intranasally infected with $1x10^4$ PFU influenza PR8. Mice were weighed and monitored daily for health and survival. On day 6, bronchoalveolar lavage fluid was collected from the mice and single cell suspension of the lung was prepared by enzymatic digestion. The level of IFN-I bioactivity in the cell free supernatant of the lavage fluid was determined by using the L929 cell based assay as described (Holm et al., 2016). The degree of neutrophil and monocyte infiltration was assessed by flow cytometry.

Staining

ZombieNIR fixable viability dye		Biolegend
CD11b	BV421	Biolegend (M1/70)
CD11c	PE	eBioscience (N418)
Ly6G	BV785	Biolegend (1A8)
Ly6C	PE	eBioscience (HK1.4)

2.4. Statistical analysis

Data were analyzed and plotted by using Graphpad Prism (Graphpad software). As indicated in the figure legends, unpaired two-tailed t tests assuming normal distributions and unequal variances or unpaired two-tailed Mann-Whitney tests were used when two groups were compared. Analysis across more than two groups within a single dataset was performed using one-way ANOVA with post hoc Tukey's test.

3. Results

3.1. Clec12A dampens inflammation but enhances ISG expression *in vivo*

3.1.1. Clec12A-deficient mice showed excessive sterile inflammation

Injured or damaged cells that are not cleared promptly will expose DAMPs, and can subsequently trigger sterile inflammation. A previous study of death-sensing CLR Mincle used an irradiation-induced sterile inflammation model to probe its in vivo function. In this model, mice receive a low dosage of whole body irradiation. $CD4^+CD8^+$ double-positive cells in mouse thymus are prone to cell death. Therefore, the x-ray exposure will generate massive cell death of the thymocytes, which can be sensed by Mincle. This lead to a transient infiltration of neutrophils into the thymus, causing a local sterile inflammation (Yamasaki et al., 2008).

Since Clec12A is an ITIM containing receptor that also recognizes dead cells, we asked if it counteracts with the ITAM-containing Mincle to keep the sterile inflammation in check. To test this possibility, we applied 1Gy irradiation to both WT and *Clec12a*$^{-/-}$ mice. 14 hours later, we analyzed the percentage of neutrophils in the total thymocytes by FACS. From a barely detectable level before irradiation to around 0.2% after irradiation, we indeed observed a clear infiltration of neutrophils into the WT thymus (Figure 3A). Meanwhile, we noticed that the percentage of neutrophils in the irradiated *Clec12a*$^{-/-}$ mice almost doubled, supporting the negative regulatory function of Clec12A under the sterile inflammation setting (Figure 3A).

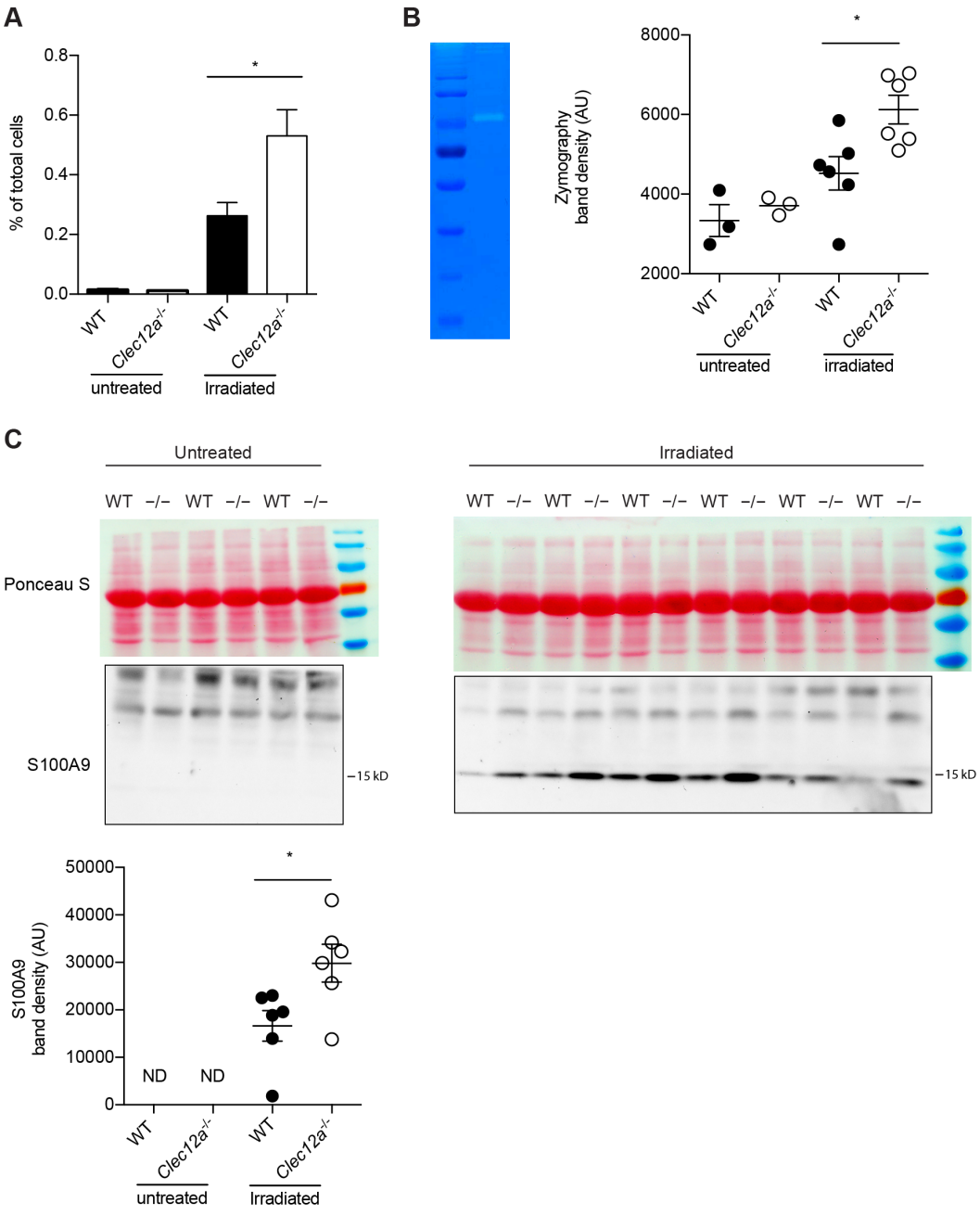

Figure 3: Clec12A dampens sterile inflammation *in vivo*

WT and *Clec12a*$^{-/-}$ mice were given whole body irradiation. 14 hours later the thymus was taken out and meshed through a 100 μM cell strainer. A) Percentage of CD11b^{+}Gr1^{hi} neutrophil in the single thymocyte preparation was determined by flow cytometry. Data are mean+SEM of 12 mice. B) Supernatant of meshed thymus was subjected to zymography assay. Left image shows the representative image of the assay and the right one shows the band density quantified by using ImageJ. C) The level of S100A9 in the supernatant was assessed by immunoblotting. Equal loading was controlled by Ponceau S staining. Densitometric quantification was done by using ImageJ. B,C) Data are depicted as mean±SEM. ND, not detected, * $p<0.05$.

Acute inflammation is often accompanied by neutrophil degranulation and concomitant liberation of various proteinase and anti-microbial peptides (Lacy, 2006). To further confirm the increased inflammation in the irradiated *Clec12a*$^{-/-}$ mice, we next tested the interstitial matrix metalloproteinases (MMPs) activity in the thymus by gelatin zymography. The MMPs in the supernatant of meshed thymus degraded the gelatin in the SDS-PAGE gel and therefore left a band after Coomassie blue staining (Figure 3B). Quantification of the band density revealed that the thymus of irradiated *Clec12a*$^{-/-}$ mice contained significantly more MMPs (Figure 3B). Considering that the alarmin S100A9 has been identified as a biomarker for local inflammation (Vogl et al., 2014), we additionally determined the protein level of S100A9 in the thymus supernatant by western blotting. As expected, S100A9 was only detected by western blottting in the inflamed thymus after irradiation (Figure 3C). Accordingly, the thymus of *Clec12a*$^{-/-}$ mice have significantly more of this alarmin protein (Figure 3C). Together, we conclude that the Clec12A dampens excessive sterile inflammation induced by cell death.

3.1.2. Clec12A-deficent mice have decreased ISG expression in the irradiated thymi

In addition to measuring the levels of proteinases and alarmin in the thymus interstices, we analyzed the expression levels of proinflammatory cytokines and chemokines in the irradiated thymus. As expected, the thymus of *Clec12a*$^{-/-}$ mice expressed increased level of *Tnf* and *Cxcl1* (Neumann et al., 2014), further supporting the negative regulatory function of Clec12A in inflammation.

Besides inducing sterile inflammation, irradiation has been shown to activate the type I interferon response (Deng et al., 2014a). Therefore, we additionally measured the transcription of putative ISGs. To our surprise, the expression of *Ifit3* and *Irf7*, which

are known to be induced by IFN-I, were significantly reduced in the *Clec12a*$^{-/-}$ mice thymus. This implies that Clec12A is required for optimal ISG expression (Figure 4).

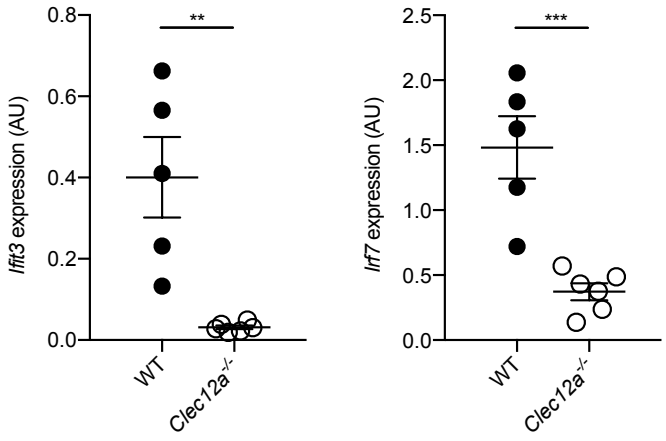

Figure 4: *Clec12a*$^{-/-}$ mice showed reduced ISG expression in irradiated thymi

QPCR analysis of ISG expression in thymi from mice that received 1Gy whole body irradiation. Results are relative to those of *Hprt* expression. Data are depicted as mean±SEM. Representative data of two independent experiments are shown. ** p<0.01, *** p<0.01.

3.2. Clec12A positively regulates the global expression of ISGs

3.2.1. Clec12A is required for optimal ISGs expression in stimulated BMDC

To further determine the function of Clec12A in regulating ISGs, we next used the more simplified in vitro BMDC model, which highly expresses Clec12A on the cell surface (Figure 5A). Activating Clec12A with its known ligand MSU alone did not initiate ISG transcription (Figure 5B), indicating that Clec12A plays a modulatory function. In light of this, we transfected BMDCs with RIG-I agonist 5′-triphosphate RNA (3pRNA) to activate the IFN-I response and induce *Ifit3* and *Irf7* expression. We also added MSU crystals to the culture to ensure the activation of Clec12A. As expected, transfecting the WT cells with 3pRNA efficiently induced the expression of both *Ifit3* and *Irf7* (Figure 5B and 5C), whereas the transcription of both genes was significantly compromised in the *Clec12a*$^{-/-}$ BMDCs (Figure 5C)—recapitulating the

reduced expression of ISGs in the irradiated thymi of *Clec12a*$^{-/-}$ mice *in vivo* (Figure 4). It is important to note that *Clec12a*$^{-/-}$ BMDCs express suboptimal levels of both *Ifit3* and *Irf7* even in the absence of MSU, indicating the existence of additional ligands (Figure 5C). This is not totally surprising, as treating dead cells with uricase did not completely abrogate the binding of Clec12A to dead cells (Neumann et al., 2014).

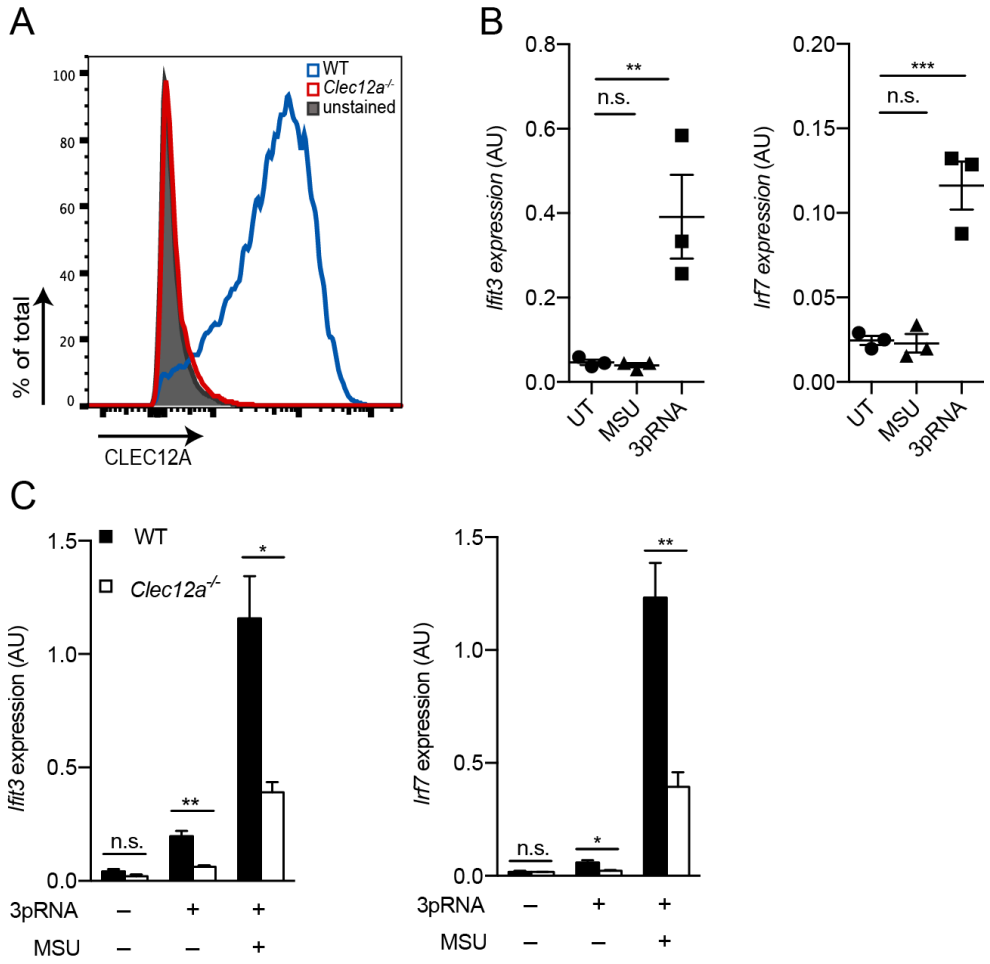

Figure 5: Clec12A is required for optimal ISG expression in BMDC

A) FACS analysis of the surface expression of Clec12A on BMDC. B) Relative expressions of *Ifit3* and *Irf7* in WT BMDCs stimulated with MSU or 3pRNA for 3 hours. C) WT and Clec12a$^{-/-}$ BMDCs were stimulated with MSU crystal (500 μg/ml) for 20 minutes followed by transfection with 3pRNA (0.4 μg/ml) for 3 hours. Gene expression relative to *Hprt* were analyzed QPCR. Representative experiment is shown from at least 3 independent experiments. B, C) Data are depicted as mean±SEM (B) or mean+SEM (C) with n=3. n.s., not significant, * p<0.05, ** p<0.01, *** p<0.001.

3.2.2. Global transcriptome analysis confirmed the regulatory function of Clec12A

To determine whether Clec12A specifically regulates the expression of *Ifit3* and *Irf7* or regulates the general transcription of ISGs, we investigated the transcriptome profile of BMDCs in various treatment groups. Untreated WT and *Clec12a*$^{-/-}$ BMDCs together with those stimulated with either 3pRNA alone or co-stimulated with MSU were subjected to high through-put RNA sequencing. Initial analysis of the transcriptome of cells co-stimulated with 3pRNA and MSU revealed that *Ifit3* and *Irf7* were indeed among the top 100 down-regulated genes in the *Clec12a*$^{-/-}$ BMDCs (Figure 6). Furthermore, several additional putative ISGs were also found to be significantly down-regulated in the *Clec12a*$^{-/-}$ BMDCs, including *Isg15* (Skaug and Chen, 2010), *Usp18* (Ritchie et al., 2004), *Rsad2 (Viperin)* (Seo et al., 2011), chemokine *Cxcl10* (Trinchieri, 2010) and other members of the IFIT family *Ifit1* and *Ifit2* (Diamond and Farzan, 2013)(Figure 6).

Next, we evaluated the sequencing data by using an unbiased gene set enrichment analysis. We started with comparing the differentially regulated genes of the MSU and 3pRNA co-stimulated samples with 4263 gene sets in the MSigDB C7 immunologic signature gene sets collection. From this analysis, we identified 140 gene sets that were significantly enriched in the WT BMDCs and 10 gene sets that were significantly enriched in the *Clec12a*$^{-/-}$ BMDCs (FDR<25%). Interestingly, genes that are induced by Newcastle disease virus infection or LPS treatment were significantly enriched in the WT BMDCs (within top 70 gene sets out of 4263) (Figure 7A). As these conditions are known to activate IFN-I response and induce global expression of ISGs, these findings further support our hypothesis that Clec12A plays a positive regulatory role in IFN-I response. Additionally, we compared the same expression dataset with the MSigDB gene set collection H with 50 gene sets. In line

with the previous findings, the gene induced by IFN-α treatment was significantly enriched in WT BMDCs, whereas the NF-κB gene set did not exhibit enrichment in either phenotype class (Figure 7B). This indicates that the regulatory function of Clec12A is specific.

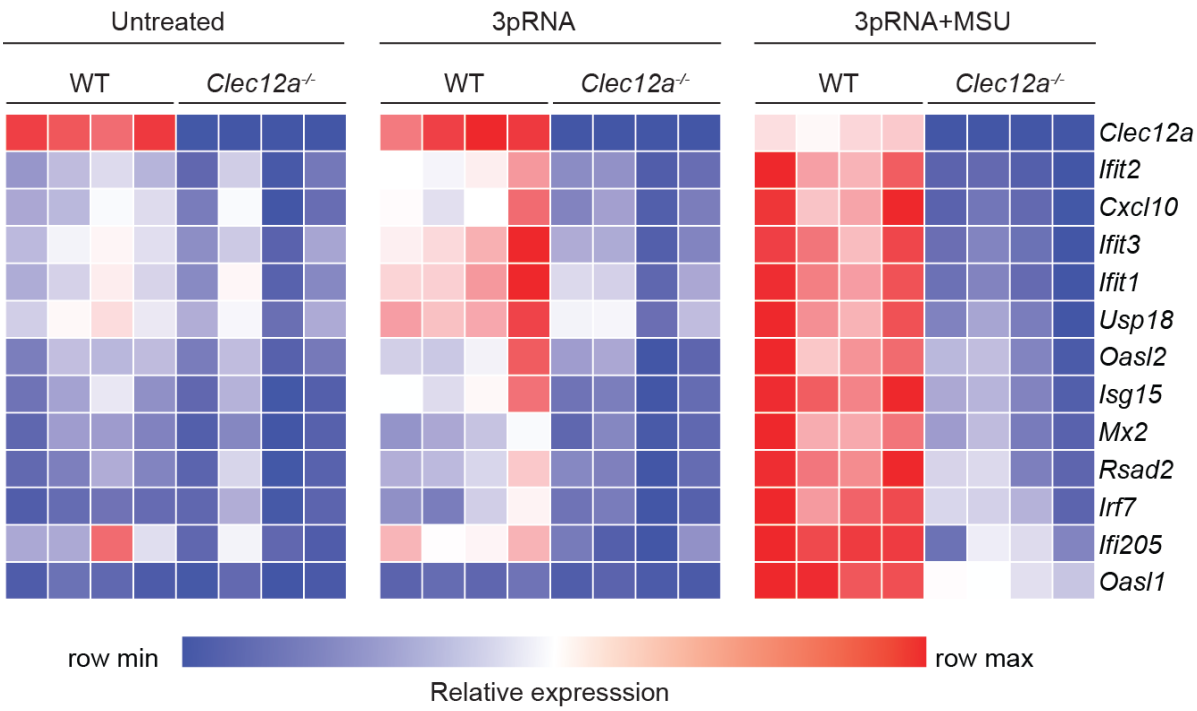

Figure 6: Clec12A regulates ISG expression at global level

Heatmap showing the expression of *Clec12a* and putative ISGs that are among the top 100 most down-regulated genes in the co-stimulated *Clec12a*$^{-/-}$ BMDCs versus WT BMDCs. Data shown are relative FPKM values of individual biological replicates in the RNA-seq.

Furthermore, we also applied the above-mentioned MSigDB C7 analysis to the genesets that are constituted by significantly regulated genes in the untreated and 3pRNA treated samples. In contrast, the untreated samples have no significant enrichment of any tested gene set (Figure 7A). Notably, the gene expression profile of 3pRNA stimulated samples showed a similar pattern of enrichment as the co-stimulated samples, albeit with less significance (Figure 7A).

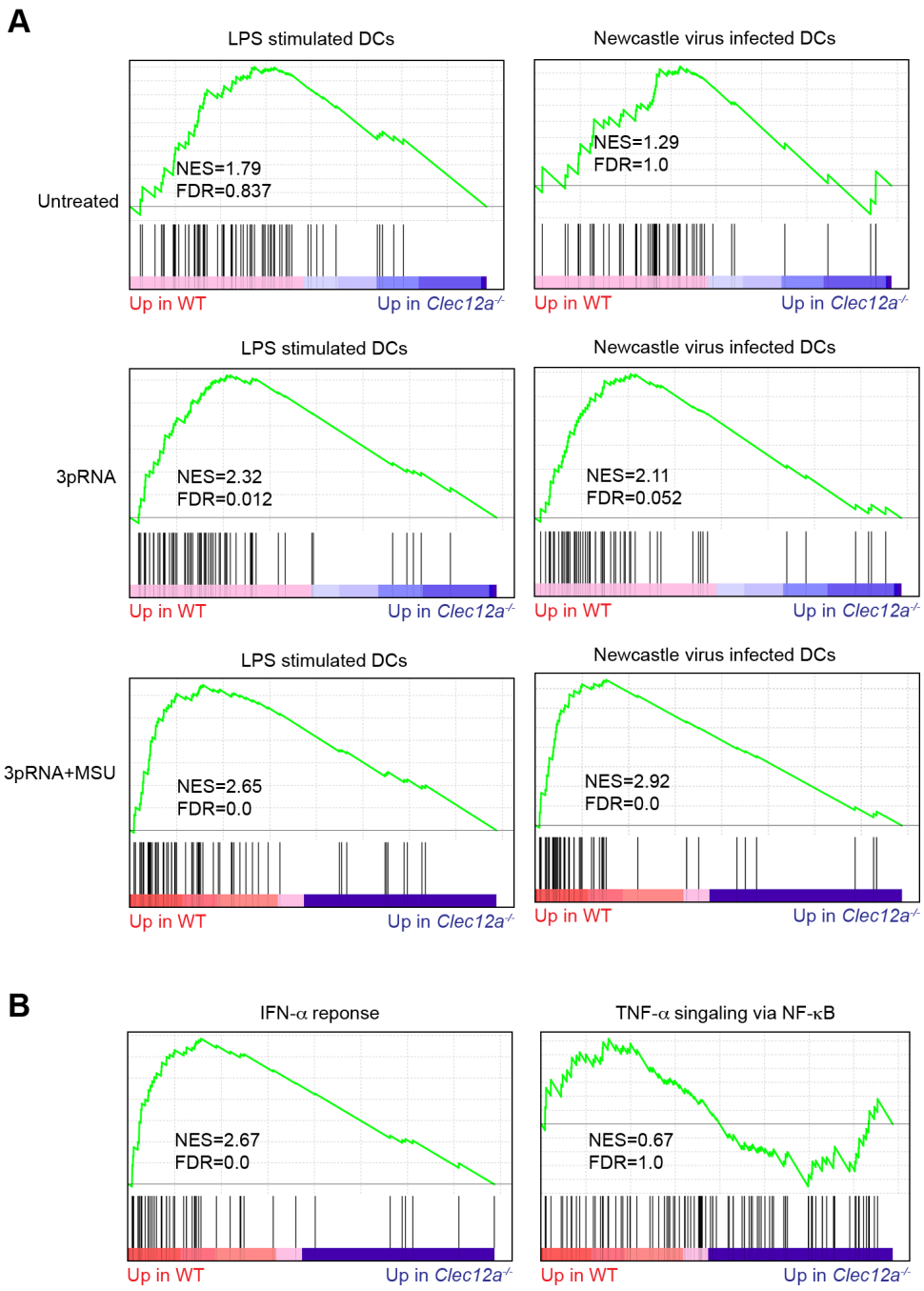

Figure 7: Clec12A regulates genes with IFN-I signature

A) Gene set enrichment analysis plots of the differentially expressed genes in the untreated, 3pRNA treated and co-stimulated WT versus *Clec12a*$^{-/-}$ BMDCs. The expression dataset was compared with MSigDB gene set collection C7 (immunological signature, 4872 gene sets). B) Gene set enrichment analysis plots of the differentially expressed genes in the co-stimulated WT versus *Clec12a*$^{-/-}$ BMDCs. The expression dataset was compared with MSigDB gene set collection H (Hallmark gene sets, 50 gene sets). NES: normalized enrichment score, FDR: false discovery rate.

3.3. Clec12A modulates IFN-I response independent of IFN-I receptor signaling

3.3.1. Clec12A is required for optimal STAT1 phosphorylation

ISGs have a consensus cis-regulatory element at their promoter region, namely ISRE (Levy et al., 1988). The occupation of ISRE by ISGF3 proves to be essential for the initiation of ISG transcription upon IFNAR engagement. In order to dissect the mechanism of Clec12A regulating ISG expression, we assessed the activation status of ISGF3 by checking the phosphorylation of STAT1, which is included in the ISGF3 complex. Transfecting BMDCs for 2 hours with 3pRNA indeed induced the phosphorylation of STAT1 at the tyrosine residue Y701 (Figure 8A), which is important for its transcriptional activity (Sadzak et al., 2008). In line with the decreased ISG expression, the same treatment induced less STAT1 phosphorylation in the *Clec12a*$^{-/-}$ BMDCs (Figure 8A). Interestingly, the addition of MSU crystal to the culture further increased the level of STAT1 phosphorylation of WT cells, consistent with the positive effect of Clec12A (Figure 8A). By contrast, the level of p65 phosphorylation did not differ between WT and *Clec12a*$^{-/-}$ cells (Figure 8A). The observation is in line with the findings from the gene set enrichment that Clec12A does not affect the NF-κB signaling.

To further determine if the regulatory function of Clec12A is restricted to the RIG-I activated IFN-I response, we additionally co-stimulated the cells MSU together with LPS or CpG-ODN type B. In accordance with previous reports (Kawai et al., 2001; Schmitz et al., 2007b), both stimuli activated the IFN-I response and STAT1 phosphorylation in BMDCs as well (Figure 8B). Moreover, the absence of Clec12A

resulted in a marked reduction in the STAT1 phosphorylation when the cells were co-stimulated with MSU together either TLR ligand. (Figure 8B).

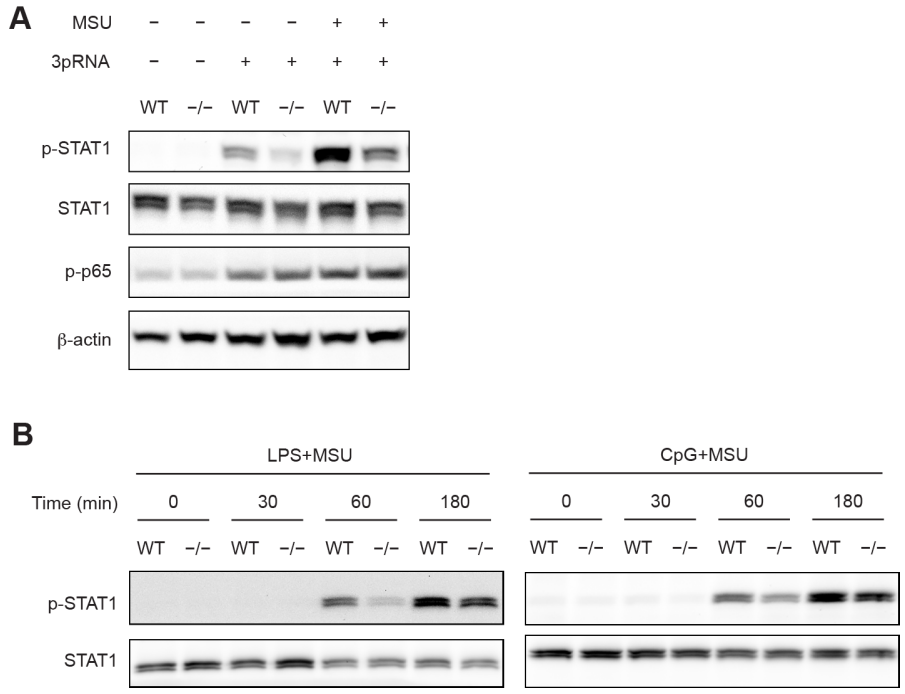

Figure 8: Clec12A is required for optimal STAT1 phosphorylation

A) WT and *Clec12a*$^{-/-}$ BMDCs were stimulated with MSU crystal (500 μg/ml) for 20 minutes followed by transfection with 3pRNA (2 μg/ml) for 2 hours. Total cell lysates were subjected to immunoblotting for the activation of IFN-I signaling (p-STAT1 Y701 and total STAT1) and NF-kB (p-p65 S536). Equal loading was control by β-actin. B) WT and *Clec12a*$^{-/-}$ BMDCs were stimulated with MSU crystal (500 μg/ml) for 20 minutes followed by stimulation with LPS (50 ng/ml) or CpG (0.5 μM) for indicated time. Total cell lysates were subjected to immunoblotting for the activation of IFN-I signaling (p-STAT1 Y701 and total STAT1). Data are representative of 3 independent experiments.

3.3.2. Clec12A does not interfere with signaling events initiated by IFNAR engagement

Several ITAM or ITIM containing receptors have been reported to regulate the signaling after IFNAR engagement. In order to test if Clec12A, an ITIM-containing receptor, also interferes with IFN-I signaling, we treated the BMDCs with increasing doses of recombinant IFN-β. IFN-β quickly activated the IFNAR, as indicated by the Y701 phosphorylation of STAT1 (Figure 9A), and triggered the transcription of *Ifit3*

and *Irf7* (Figure 9B). However, both the IFNAR activated STAT1 phosphorylation and ISG (*Ifit3* and *Irf7*) transcription were intact with the deficiency of Clec12A (Figure 9A and 9B). Therefore, we conclude that Clec12A does not directly interfere with the signaling triggered by IFNAR activation.

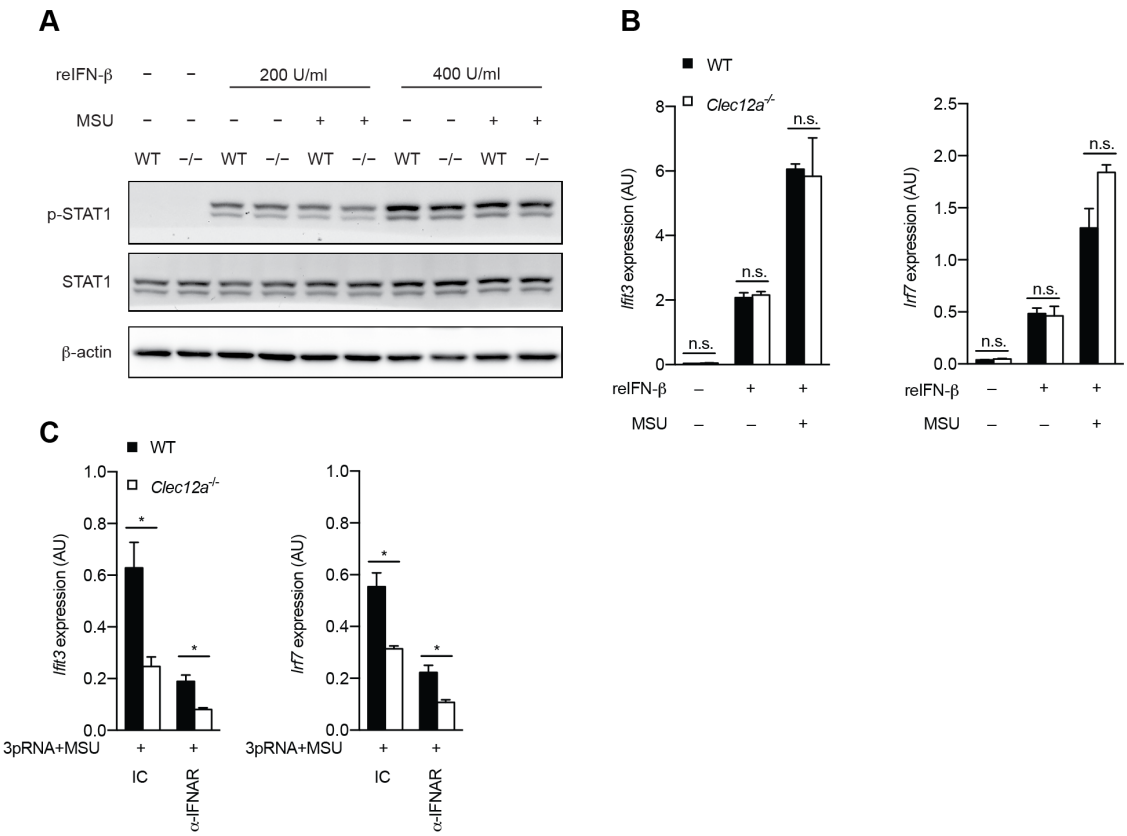

Figure 9: Clec12A does not regulate the signaling triggered by IFNAR engagement

A) WT and *Clec12a*$^{-/-}$ BMDCs were left untreated (-) or stimulated with MSU crystal (500 μg/ml) for 20 minutes followed by treatment with increasing doses of recombinant IFN-β for 30 minutes. Total cell lysates were subjected to immunoblotting for pSTAT1 Y701 and total STAT1. Equal loading was determined by β-actin. Data shown are representative of two independent experiments B) WT and *Clec12a*$^{-/-}$ BMDCs were stimulated with MSU crystal (500 μg/ml) for 20 minutes followed by treatment with 200 U/ml recombinant IFN-β for 2 hours. Relative gene expression was analyzed by QPCR. C) WT and *Clec12a*$^{-/-}$ BMDCs were pretreated with IFNAR blocking antibody (α-IFNAR) or respective isotype control (IC). Subsequently, cells were stimulated with MSU crystal (500 μg/ml) for 20 minutes followed by transfection with 3pRNA (0.4 μg/ml) for 3 hours. Relative gene expression was analyzed by QPCR. Data are depicted as mean+SEM with n≥3. Representative data from two independent experiments are shown. * $p<0.05$.

To further corroborate this conclusion, we pretreated BMDCs with an IFNAR blocking antibody or respective isotype control, followed by co-stimualtion with MSU and 3pRNA. As expected, blockage of IFNAR greatly comprised RIG-I induced transcription of *Ifit3* and *Irf7* (Figure 9C), implying the 3pRNA transfection indeed triggered the autocrine secretion of IFN-I, which accounted for the major part of ISG induction through IFNAR. However, there was clearly a residual portion of 3pRNA induced ISG expression that was independent of IFNAR (Figure 9C). Most importantly, blocking IFNAR failed to abrogate the differential expression of *Ifit3* and *Irf7* between WT and *Clec12a*$^{-/-}$ cells after co-stimulation (Figure 9C). Collectively, these data proved that Clec12A regulates ISG expression independently of IFNAR signaling.

3.3.3. Clec12A deficiency leads to reduced IFN-I production

As Clec12A acts upstream of IFNAR to regulate IFN-I response, we next tested if Clec12A modulates the production of IFN-I. To this end, we measured IFN-β in the cell free supernatant of 3pRNA-stimulated BMDCs. Indeed, the IFN-β production was impaired in the *Clec12a*$^{-/-}$ cells (Figure 10A). Reminiscent to the STAT1 phosphorylation (Figure 9A), the level of 3pRNA induced IFN-β production was also further increased by the addition of MSU crystals (Figure 10A). Moreover, the *Clec12a*$^{-/-}$ BMDCs also showed a defect in IFN-β production upon MSU plus LPS or CpG-ODN co-stimulation (Figure 10B). Co-stimulating BMDCs with 3pRNA and MSU is known to initiate pyroptosis. However, 3pRNA and MSU co-stimulation caused similar levels of cell death in WT and *Clec12a*$^{-/-}$ cells (Figure 10C), as determined by the amount of lactate dehydrogenase (LDH) released into the supernatant when the cells die. Therefore, the decreased IFN-I response in *Clec12a*$^{-/-}$ cells was not due to increased cell death.

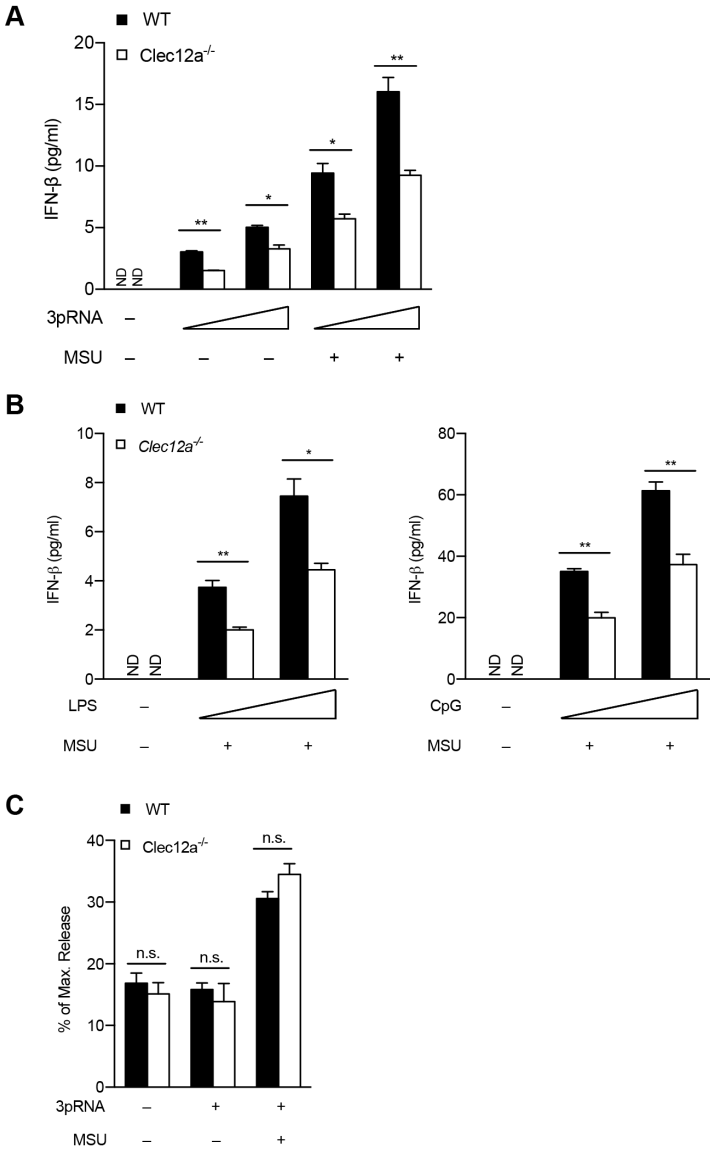

Figure 10: Clec12A positively regulates IFN-β production and does not affect MSU-induced cell death

A) WT and Clec12a$^{-/-}$ BMDCs were left untreated (-) or stimulated with MSU crystal (500 μg/ml) for 20 minutes, followed by stimulation with increasing doses of 3pRNA (0.2 μg/ml, 0.5 μg/ml), B) LPS (50 ng/ml, 100 ng/ml) or CpG-ODN (0.5 μM, 1 μM) for 8 hours. The level of IFN-β in the supernatants were analyzed by ELISA. Data are depicted as mean+SEM with n=3. C) Cells were stimulated as in A), the relative LDH levels in the supernatant as compared to cells lysed with Triton X-100 were determined. A-D) Data are depicted as mean+SEM with n=3. Representative results from two independent experiments are shown.

3.4. Clec12A amplifies the IFN-I production signaling through activating Src-family kinases

3.4.1. Clec12A regulates the TBK1-IRF3 axis of the IFN-I production signaling

IRF3 has long been regarded as the master transcription factor for RIG-I induced primary IFN-I production (Sato et al., 2000). Given that Clec12A regulates IFN-β production, it is conceivable that Clec12A also regulates the transcriptional activity of IRF3. Indeed, western blot showed that the phosphorylation of IRF3 at serine residue S396 was impaired in the 3pRNA transfected *Clec12a*$^{-/-}$ BMDCs (Figure 11). In RIG-I induced IFN-I production signaling cascade, IRF3 is directly phosphorylated and activated by serine kinase TBK1 (Liu et al., 2015). Therefore, the reduced IRF3 phosphorylation would indicate impaired TBK1 activity. In line with this postulation, the serine phosphorylation of TBK1 at S172 also showed a defect in the absence of Clec12A in BMDCs (Figure 11).

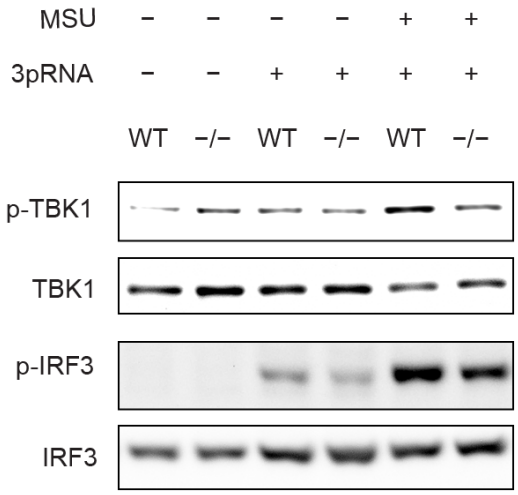

Figure 11: Clec12A amplifies the TBK1-IRF3 signaling axis of RIG-I activation

WT and *Clec12a*$^{-/-}$ BMDCs were stimulated with MSU crystal (500 μg/ml) for 20 minutes followed by transfection with 3pRNA (2 μg/ml) for 2 hours. Total cell lysates were subjected to immunoblotting for p-IRF3 S396, total IRF3, p-TBK1 S172 and total TBK1. Data are representative of 3 independent experiments.

3.4.2. Clec12A acts on Src-family kinases to regulate IFN-I response

Recently, several studies have reported the role of Src-family kinases (SFKs) in regulating IFN-I response. SFK is a family of tyrosine kinases consisting of nine family members. They are involved in ITAM and ITIM receptor signaling. The kinase activity of SFK is regulated by the activating tyrosine phosphorylation within their kinase domain, e.g. Y416 of c-src. The phosphorylation of the Y416 motif releases them from the auto-inhibitory conformation and activates their kinase activity. To determine if SFKs provide the link between Clec12A and IFN-I response, we first assessed the activating status of SFKs. Indeed, compared to *Clec12a*$^{-/-}$ cells, stimulating the WT BMDC with Clec12A ligand MSU led to higher level of SFK phosphorylation at the Y416 motif (Figure 12A). To test if the activated SFKs can subsequently modulate IFN-I response, we treated the BMDCs with SFK inhibitor PP2 prior to 3pRNA and MSU stimulation. The inhibition of SFK brought down the phosphorylation of both TBK1 and IRF3 in the WT BMDCs to the same levels as in *Clec12a*$^{-/-}$ cells (Figure 12B). In addition, blocking SFK activity by PP2 also greatly inhibited the expression level of *Ifit3* and *Irf7*. Most importantly, PP2 abrogated the enhancement of *Ifit3* and *Irf7* transcription in WT BMDC compared to *Clec12a*$^{-/-}$ cells (Figure 12C). Together, these experiments indicate that Clec12A amplifies IFN-I producing signaling by acting on SFKs.

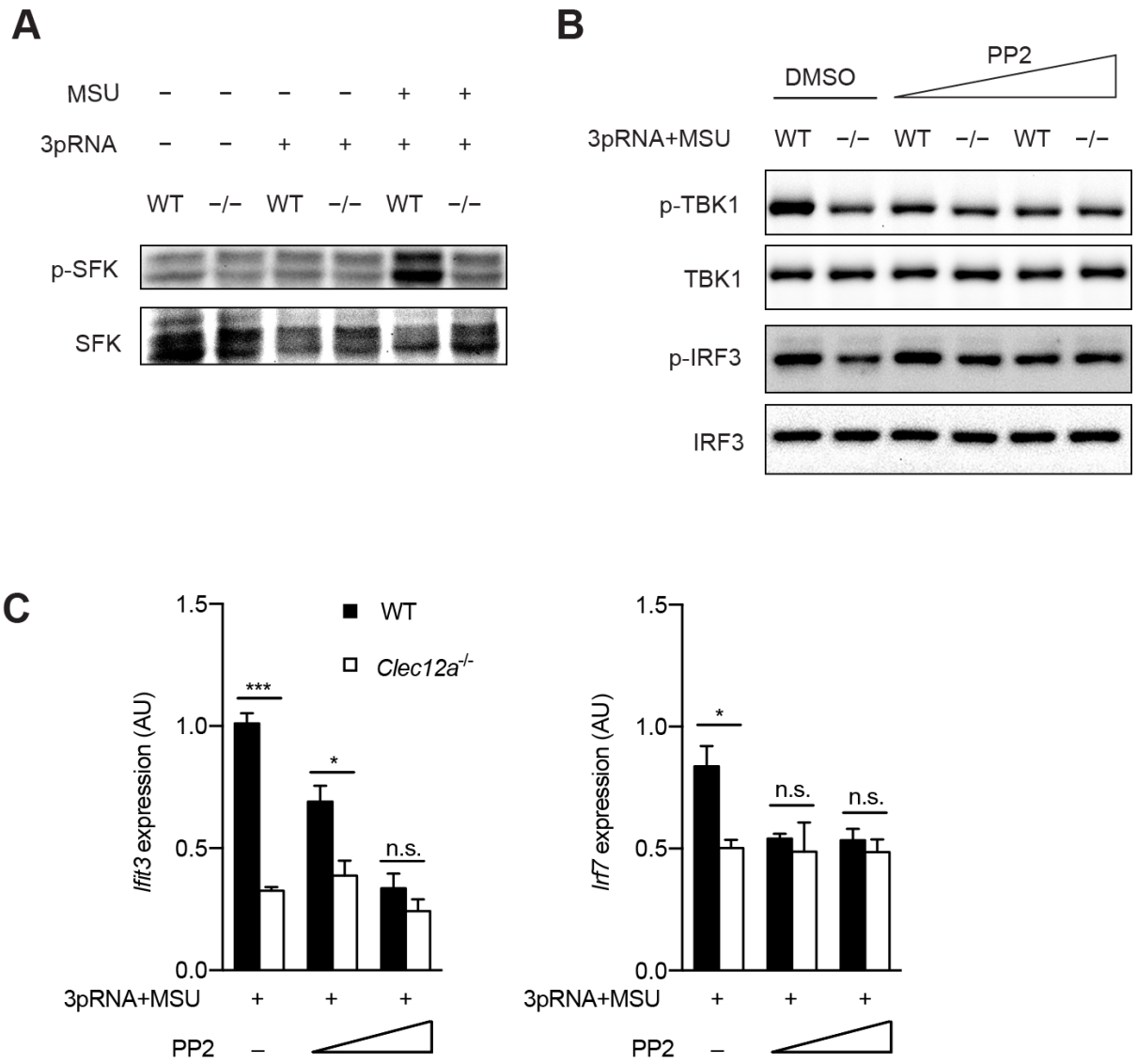

Figure 12: Clec12A amplifies the TBK1-IRF3 axis by modulating SFK activity

A) WT and *Clec12a*$^{-/-}$ BMDCs were stimulated with MSU crystal (500 μg/ml) for 20 minutes followed by transfection with 3pRNA (2 μg/ml) for 2 hours. Total cell lysates were subjected to immunoblotting for p-SFK Y416 and total SFK. Data are representative of 3 independent experiments. B) WT and *Clec12a*$^{-/-}$ BMDCs were pretreated with SFK inhibitor PP2 (2.5 μM, 5 μM) for 1 hour followed by co-stimulated with both MSU crystal (500 μg/ml) and 3pRNA (2 μg/ml) for 2 hours. Total cell lysates were subjected to immunoblotting for p-IRF3 S396, total IRF3, p-TBK1 S172 and total TBK1. C) Cell were pretreated as in B), followed by co-stimulation with MSU crystal (500 μg/ml) and 3pRNA (0.4 μg/ml) for 3 hours. Gene expression relative to *Hprt* was analyzed by QPCR and was depicted as mean+SD with n n≥3. B, C) Data are representative of two independent experiments.

To gain additional information on other signaling pathways that are implicated in the regulatory effect of Clec12A on the IFN-I response, we pretreated the BMDCs with a additional panel of inhibitors and evaluated the expression of *Ifit3* after MSU and 3pRNA co-stimulation. The targets of those inhibitors include actin polymerization, endosome acidification and NLRP3, which are all important players in the MSU induced response. Clearly, blocking actin polymerization compromised the positive role of Clec12A in regulating IFN-I response, thereby leading to similar level of *Ifit3* expression in the WT and *Clec12a*$^{-/-}$ BMDCs after MSU and 3pRNA co-stimulation. Meanwhile NLRP3 and endosome acidification are not involved (Figure 13).

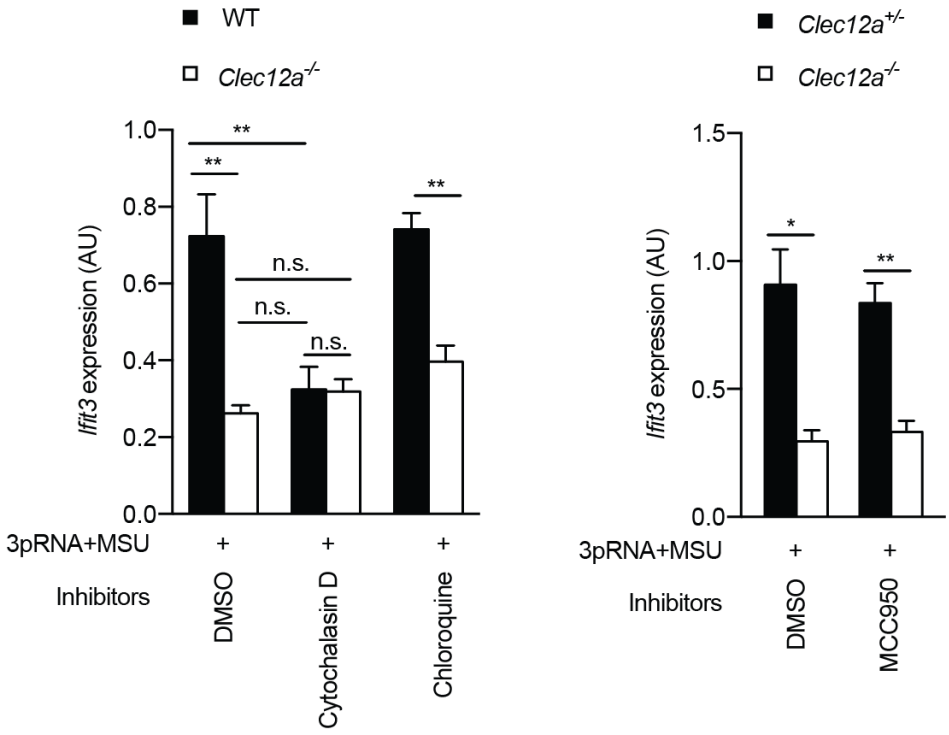

Figure 13: PI3K and actin polymerization mediate the positive effect of Clec12A on IFN-I response

WT and *Clec12a*$^{-/-}$ BMDCs were pretreated with Cytochalasin D (10 μM), Chloroquine (10 μM), MCC950 (10 μM) or DMSO for 1 hour before they were stimulated with both MSU crystal (500 μg/ml) and 3pRNA (2 μg/ml) for 3 hours. The relative expression of *Ifit3* were quantified by QPCR. Data are expression of mean+SEM of data from at least three mice. n.s. not significant, *p<0.05, **p<0.01, ***p<0.001.

3.5. The function of Clec12A in virus infection *in vivo*

The IFN-I response constitutes a pivotal part of the first line defense against viral infection. Deficiency in this response leads to increased host susceptibility to many viral infections (Asgari et al., 2017; Everitt et al., 2012; Spanier et al., 2014). Nevertheless, recent studies also highlight the immunomodulatory role of IFN-I in viral infection and point out that IFN-I response could be exploited by certain viruses to sustain persistent infection. As the above data demonstrates the involvement of Clec12A in IFN-I regulation, it is conceivable that the *Clec12a*$^{-/-}$ mice would respond differently to viral infection compared to WT mice. To test this, we applied several *in vivo* virus infection models to the *Clec12a*$^{-/-}$ mice, including DNA and RNA viruses, as well as both acute and chronic infections.

3.5.1. *Clec12a*$^{-/-}$ mice are more susceptible to LCMV-WE infection

Lymphocytic choriomeningitis virus (LCMV) is the prototypic arenavirus. The genome of LCMV contains two segments of negative single stranded RNAs. It is known that LCMV infection induces RIG-I/MDA5 dependent IFN-I production (Zhou et al., 2010). The commonly used LCMV strains in research includes the Amstrong strain, the Clone 13, the WE strain and the Docile strain. Amstrong and WE strain cause acute infection while C13 and Docile cause chronic infection in mice (Duhan et al., 2016).

Used as an acute virus infection model, we intravenously injected $2x10^6$ PFU of LCMV-WE into the WT and *Clec12a*$^{-/-}$ mice and monitored the mice for 14 days. By looking at the weight curve, it is apparent that the infected mice initially become sick on day 2, followed by a quick recovery. However, the mice got severely diseased again on day 8, probably due to immunopathology caused by a cytotoxic T cell response and chronic inflammation (Figure 14A). This pattern of weight loss is

consistent with the known effect of LCMV infection in mice (Cornberg et al., 2013). During the experimental course, we bled the mice on day 2, day 8 and day 14 of infection. Interestingly, analysis of the day 2 serum samples revealed that the *Clec12a*$^{-/-}$ mice produced much less IFN-α—implying a reduced IFN-I response in these mice (Figure 14B).

Moreover, given that LCMV-WE is known to cause liver pathology (Beier et al., 2015; Lukashevich et al., 2003), we specifically assessed the liver damage caused by LCMV-WE infection by measuring the levels of serum aspartate aminotransferase (AST) and alanine aminotransferase (ALT) on day 8 and 14 post infection. Both the WT and *Clec12a*$^{-/-}$ mice similarly showed massive liver damage on day 8. Nevertheless, the WT mice seem to fully recover at the experiment endpoint, whereas the *Clec12a*$^{-/-}$ mice still maintained a high level of liver damage (Figure 14C). Finally, the increased number of LCMV NP genes in the liver homogenates of *Clec12a*$^{-/-}$ mice indicates that the mice have compromised ability to clear the virus (Figure 14D).

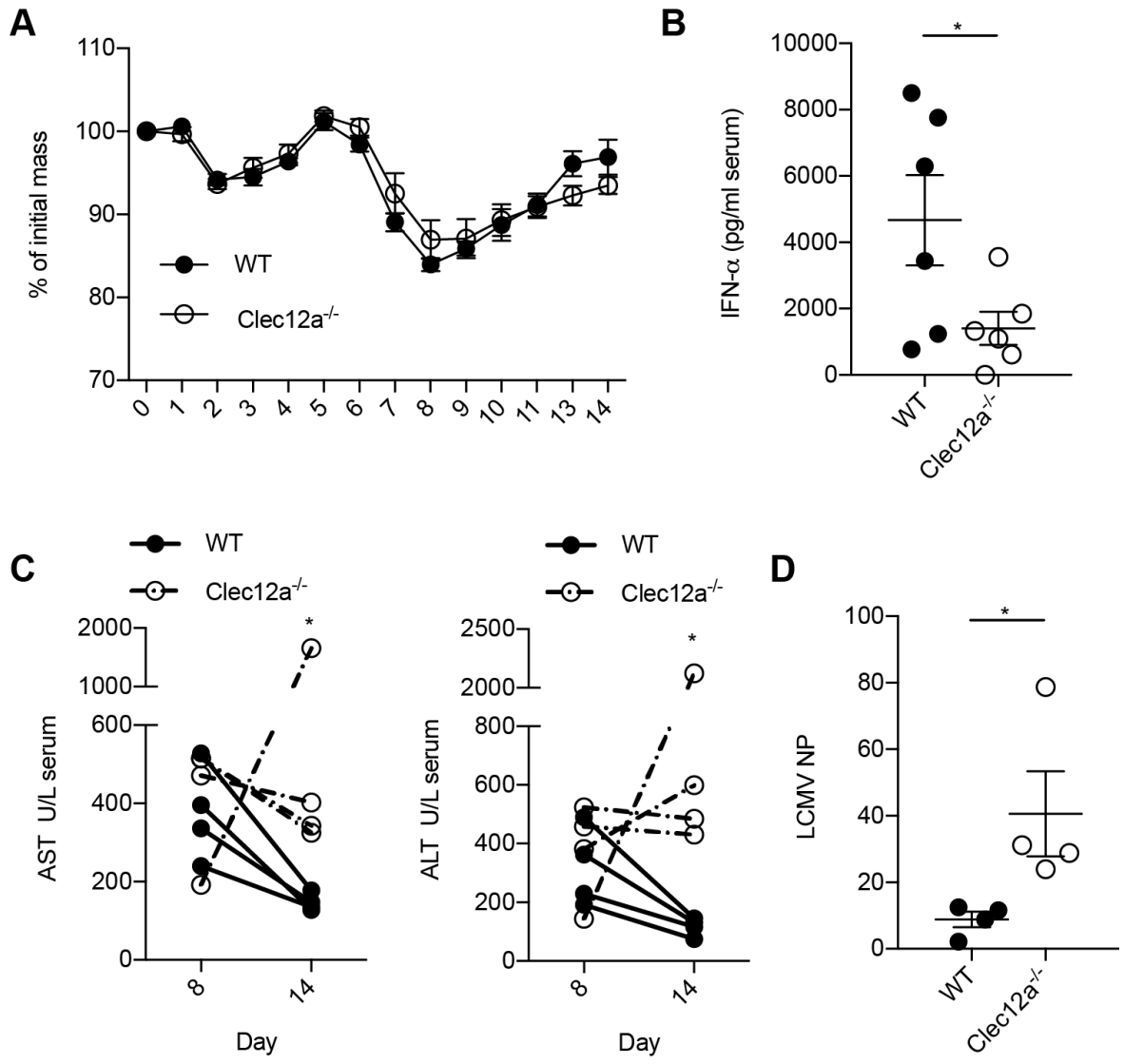

Figure 14: Clec12A is required for optimal IFN-I production and protection against acute LCMV infection

Cohoused WT and *Clec12a*$^{-/-}$ mice were infected with 2x10^6 PFU of LCMV-WE. A) The mice were monitored and weighed every 24 hours for 2 weeks and bled on day 2, 8,14 to collect serum samples. B) The levels of IFN-α in the serum samples on day 2 were determined by ELISA. C) The levels of AST and ALT in the serum samples on day 8 and day 14 were analyzed. D) The amount of LCMV-NP gene in the liver homogenates was assessed by QPCR. Data are normalized to the level of β-actin mRNA of mouse liver tissues. A, B, D) Data are depicted as mean±SEM. B-D) Each circle represents value from one mouse. C) Data from one mouse are connected. *p<0.05.

3.5.2. *Clec12a*$^{-/-}$ mice are more resistant to LCMV-Docile infection

We next established a chronic virus infection model to further probe the role of Clec12A in regulating IFN-I response *in vivo*. IFN-I has been shown to have contrasting effects on the outcome of acute and chronic LCMV infections. During acute infection, the direct anti-viral effect of IFN-I is dominant. Therefore, the defect of IFN-I leads to increased susceptibility and pathology (Müller et al., 1994). On the contrary, LCMV virus causing chronic infection has been reported to exploit the IFN-I response for their benefit. IFN-I induced by chronic LCMV infection upregulates IL-10 production and PD-L1 expression within the myeloid compartment. These modulatory effects of IFN-I will lead to T cell exhaustion and suppression of anti-viral response. Diminishing the IFN-I signaling in this case confers protection as well as faster virus clearance (Teijaro et al., 2013; Wilson et al., 2013).

Clec12a$^{-/-}$ and WT control mice were intravenously infected with $2x10^4$ PFU of LCMV-Docile. Similar to the acute LCMV infection, the mice become sick on day 8 of infection (Figure 15A). By contrast, the *Clec12a*$^{-/-}$ mice lost significantly less weight than the WT controls, indicating increased resistance to the chronic LCMV infection conferred by the Clec12A deficiency (Figure 15A). Nevertheless, the *Clec12a*$^{-/-}$ mice again showed decreased production of IFN-α (Figure 15B), implying that the regulatory function of Clec12A in IFN-I production is not dependent on the chronicity of LCMV infection. Additionally, the infection indeed caused chronic infection in both the *Clec12a*$^{-/-}$ and WT control mice, as the viremia in those mice lasted for more than two months. However, 4 out of 5 *Clec12a*$^{-/-}$ mice already cleared the virus on day 70, whereas only 1 WT control did (Figure 15C), further confirming the increased resistance to chronic LCMV infection in *Clec12a*$^{-/-}$ mice.

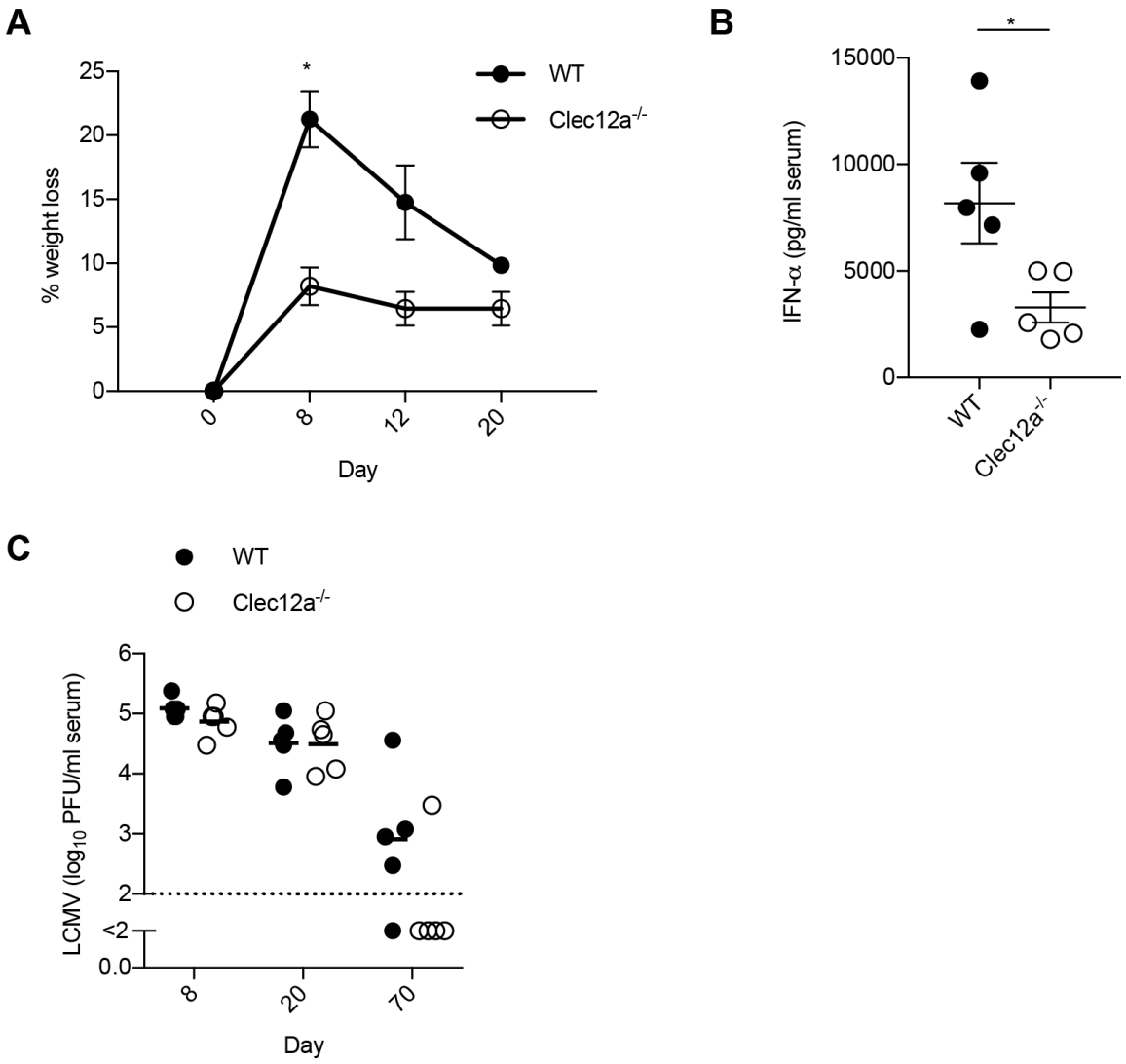

Figure 15: *Clec12a*$^{-/-}$ mice are more resistant to chronic LCMV infection

Cohoused WT and *Clec12a*$^{-/-}$ mice were infected with 2x10^6 PFU of LCMV-Docile intravenously. A) The weight of mice was monitored. B) The IFN-α levels in serum samples on day 2 were analyzed by ELISA. C) The virus titers in the blood on indicated days were determined by plaque assay. A, B) Data are depicted as mean±SEM. B, C) Each circle represents value from one mouse. *p<0.05.

3.5.3. Clec12A is dispensable for IFN-I response during influenza virus infection *in vivo*

In addition to LCMV virus infection, we took advantage of the influenza virus infection, another RNA virus infection model that are known to rely on RIG-I activation for IFN-I production, to investigate the *in vivo* function of Clec12A. In collaboration with Anne Hansen at Aarhus University, we intranasally infected the WT

and *Clec12a*$^{-/-}$ mice with H1N1 influenza strain PR8 and monitored the mice for 6 days. Both WT and *Clec12a*$^{-/-}$ mice similarly lost around 10% of body weight as compared to the uninfected controls, indicating Clec12A is not important for the overall disease progression of influenza virus infection (Figure 16A). Closer examination of local IFN-I level in the bronchoalveolar lavage fluid revealed that the *Clec12a*$^{-/-}$ mice did not produce a significantly different level of IFN-I from the WT animals (Figure 16B). Furthermore, the degree of inflammation in the lung after virus infection did not differ between WT and *Clec12a*$^{-/-}$ mice, as indicated by similar levels of inflammatory cell infiltration that were determined through FACS analysis (Figure 16C). Collectively, and in contrary to LCMV infection, Clec12A is not required for influenza virus induced IFN-I response in a complex infection model *in vivo* and does not majorly affect the anti-viral response of the host.

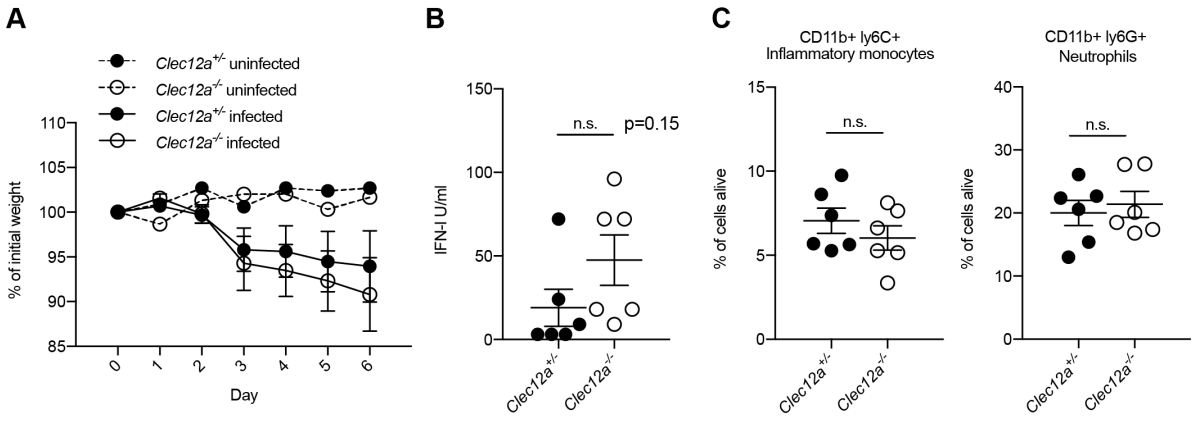

Figure 16: Clec12A is not required for the IFN-I response induced by influenza virus infection

WT and *Clec12a*$^{-/-}$ mice were infected with 1x10^4 PFU of Influenza strain PR8 intranasally. A) The weight of infected mice and the uninfected controls were monitors for 6 days. Data are mean±SEM of 9 mice for the infected group. The uninfected control contains only 1 mouse of each genotype. B) The level of IFN-I in the cell free bronchoalveolar fluid of mice on day 6 after infection were determined by IFN-I bioactivity assay. C) The inflammatory cell infiltration in the lung of mice on day 6 after infection were determined by FACS. Cells were pre-gated on viable CD11c negative cell population. B, C) Each circle represents value from one mouse. n.s., not significant.

3.5.4. *Clec12a*$^{-/-}$ mice showed excessive inflammation upon MVA infection

To further explore the function of Clec12A *in vivo*, we infected the mice with modified vaccinia Ankara (MVA), which is a DNA virus belongs to the poxvirus family. The virus was highly attenuated, therefore can be used as a vaccine and vaccine vector. The virus was engineered to express ovalbumin. As expected, systematic infection with 5×10^7 $TCID_{50}$ of the virus by intravenous injection did not cause overt disease in the mice. Moreover, the virus induced similar level of IFN-α production in Clec12A$^{+/-}$ and *Clec12a*$^{-/-}$ mice 6h after infection (Figure 17A). FACS analysis of the splenocytes 7 days post infection revealed that the B cell, T cell and NK cell population, as well as the OVA and MVA specific T cells population in the spleens of *Clec12a*$^{-/-}$ mice did not significantly differ from their heterozygous littermate controls (Figure 17B and 17C). By contrast, a population of CD11b^{hi}-expressing cells, predicted to be neutrophils according to their higher SSC value, were significantly increased in the *Clec12a*$^{-/-}$ mice, indicating that Clec12A controls excessive inflammation caused by viral infection (Figure 17D). These results are in line with our observations with the sterile inflammation model, where the mice showed increased influx of inflammatory cells into the irradiated thymi (Figure 3A).

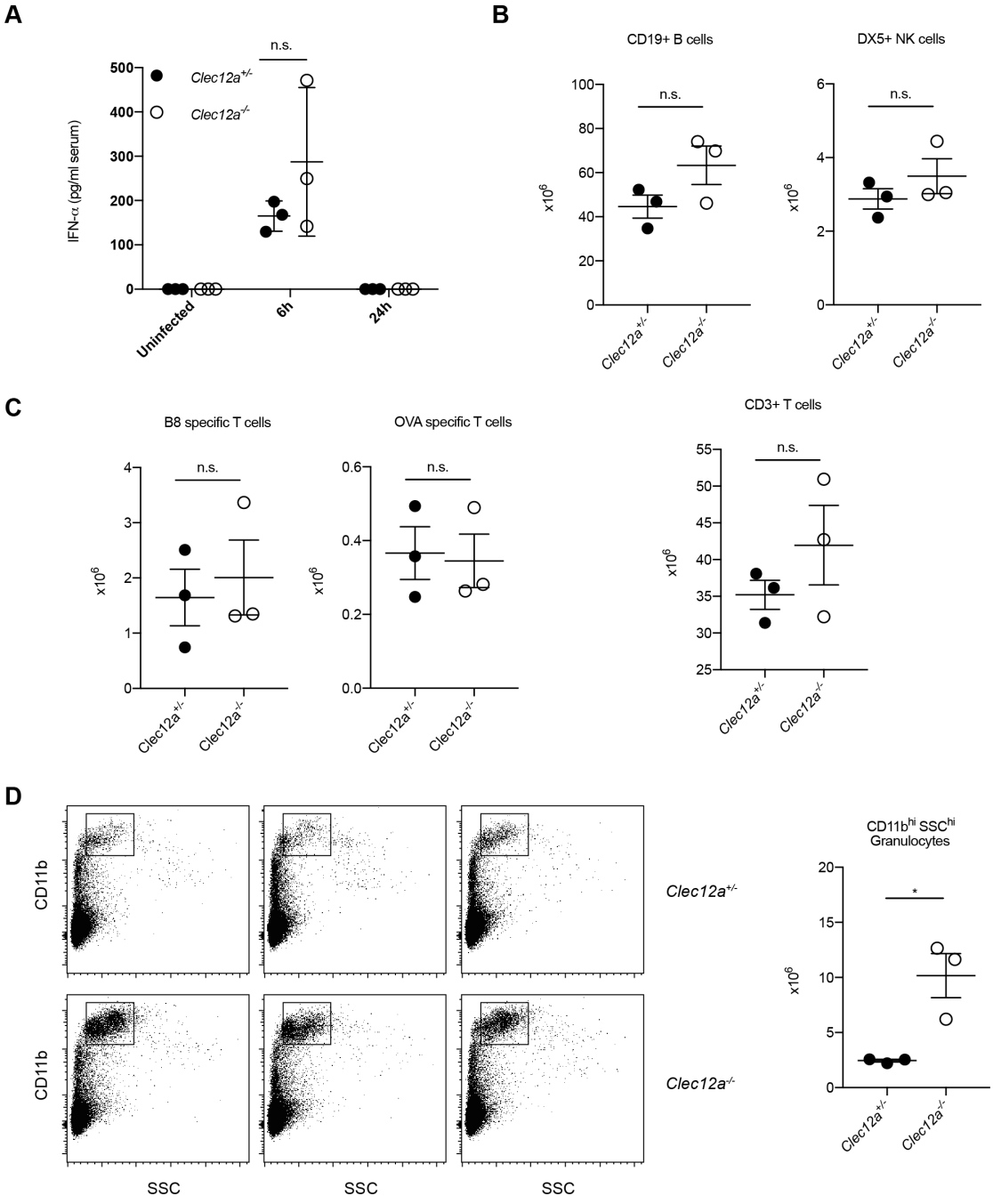

Figure 17: Clec12A controls inflammation induced by MVA infection

Clec12a$^{-/-}$ mice and their heterozygous littermates were intravenously infected with 5x10^7 $TCID_{50}$ of MVA-OVA. A) Serum samples were taken before infection, 6 hours post infection and 24hours post infection. IFN-α levels were assayed by ELISA. B, C) 7 days after infection, mice were sacrificed and the total number of CD19$^+$ B cells, DX5$^+$ NK cells, CD3$^+$ T cells, CD11b$^+$ cells, as well as B8 or OVA-loaded dextramer positive CD8$^+$ T cells in the spleen were analyzed by FACS. D) CD11b and SSC plot of each mouse are shown. A-D) Data are depicted as mean±SEM. Each circle represents value from one mouse. *p<0.05.

4. Discussion

Collectively, the results stated above establish the positive regulatory function of Clec12A in IFN-I response. As what would be predicted with its ITIM motif, Clec12A can down modulate the activation status of innate immune cells in a sterile inflammation model. These observations indicate its importance in preventing immunopathology triggered by uncontrolled inflammation. On the other hand, Clec12A supports the optimal induction of ISGs through regulating events that lead to IFN-I production. Specifically, Clec12A activates SFKs, which act on TBK1 to amplify the IFN-I producing pathway and ensure optimal production of IFN-I. This model is summarized in the below schematic figure (Figure 18). In line with our *in vitro* findings, the Clec12A knockout mice showed impaired IFN-I production in response to both acute and chronic LCMV infection. Furthermore, the pathological outcomes of Clec12A deficient mice correlate with the known function of IFN-I in both virus infection models. This study of death-sensing Clec12A provide evidence that the immune cells can simultaneously fine-tune different defensive arms to generate a context dependent response.

4.1. Regulation of IFN-I response by ITAM or ITIM receptors

The initial observation of decreased ISG expression in the irradiated *Clec12a*$^{-/-}$ thymocytes is interesting. Little is known about how the interferon response is initiated in the irradiated thymus. However, studies on tumor radiotherapy have demonstrated that ionizing radiation can shape the innate immune response through modulating IFN-I response, and subsequently affecting anti-tumor adaptive immunity (Burnette et al., 2011). In addition, it has been shown that the anti-tumor immune response conferred by radiotherapy is largely compromised in STING-

deficient mice (Deng et al., 2014b). Additionally, the cGAMP-STING-IRF3 signaling axis within the intratumoral CD11c+ cell population accounted for the sensing of damaged DNA after radiotherapy. It is possible that the damaged DNA in the irradiated thymus is similarly sensed and initiates an IFN-I response.

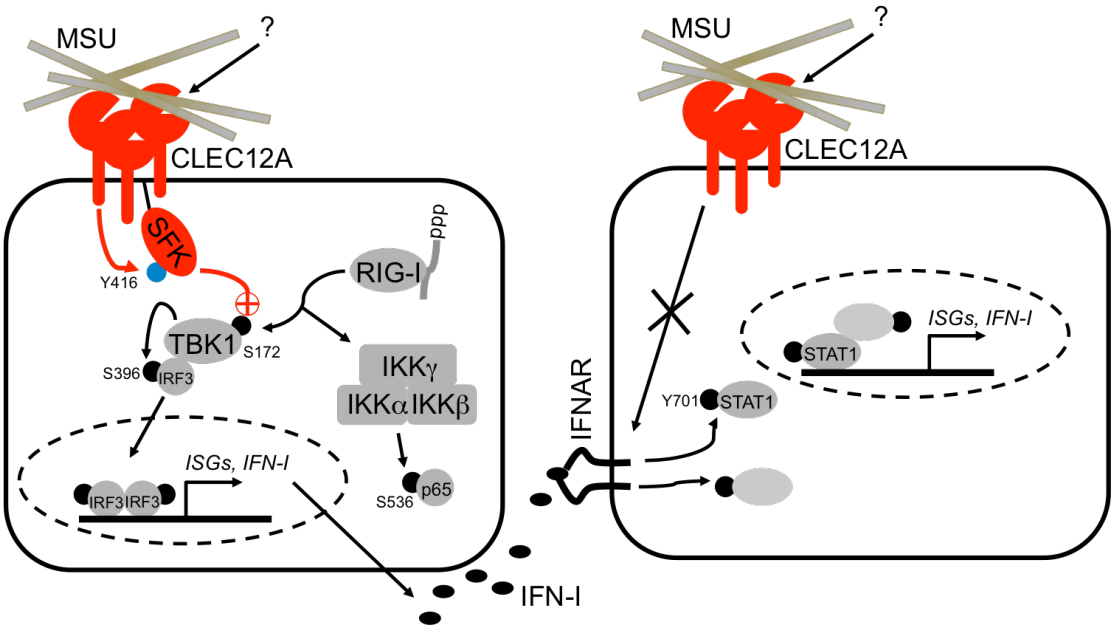

Figure 18: Clec12A positively regulates RIG-I activated IFN-I response

Clec12A, in response to MSU or unknown ligand, activates SFKs. SFKs subsequently positively regulate the TBK1-IRF3 signaling axis activated by RIG-I ligation—thereby enhancing the transcription of ISGs and production of IFN-I. Meanwhile, the signaling branch of NF-κB, which is also activated by RIG-I ligation, is not affected by Clec12A. The autocrine or paracrine IFN-I binds to IFN-I receptor IFNAR and trigger the phosophorylation of STAT1 at Y701. This enables STAT1 to translocate into the nucleus and induce ISG expression. Moreover, Clec12A does not regulate events after IFNAR engagement.

Next in a much-simplified *in vitro* primary cell model, we were able to recapitulate the regulatory effect of Clec12A on IFN-I response. Through combining gene set enrichment analysis of our high throughput sequencing data and biochemical studies *in vitro*, we established the positive role of CLEC1A in regulating IFN-I response. According to the ITAM and ITIM paradigm, Clec12A is predicted to play an inhibitory role in immune cell signaling due to the ITIM motif in its cytoplasmic tail. However,

Clec12A performs the opposite function in IFN-I signaling. This is not surprising for several reasons. ITAM-containing receptors have been shown to negatively regulate IFN-I signaling. For example, integrin CD11b is reported to negatively regulate TLR activated IFN-I response (Han et al., 2010). The outside-in signaling of CD11b activates syk, which then promotes the Cbl-b mediated degradation of TRIF, and hampers TLR-mediated IFN-I response. In line with this, another study showed that pre-ligation of ITAM-coupled β_2 integrin directly inhibits the proximal signaling by IFNAR (Huynh et al., 2012). Therefore, it is conceivable that the ITIM of Clec12A recruits phosphatases that counteract with the signaling of ITAM receptors to positively regulate the IFN-I response indirectly. Secondly, it is possible that Clec12A regulates IFN-I response independently of its ITIM motif. We have demonstrated above that SFKs are necessary for the regulatory function of Clec12A. As the activation of SFKs by CLR ligation precedes ITIM phosphorylation, it is likely that the signal from Clec12A activation diverges at the point of SFKs. On one hand, the Clec12A activated SFKs phosphorylate ITIM to relay inhibitory signaling and on the other hand directly activate another branch of signaling cascade that supports IFN-I response. To dissect if the ITIM motif are required for its regulatory function in IFN-I response, and to determine which of the formerly mentioned hypothesis is true, further experiments that express Clec12A mutant (with mutated ITIM motif) in Clec12A knock-out cell lines will be needed.

In addition to Clec12A, two other ITIM-containing CLRs—Ly46Q and DCIR—are reported to positively regulate the IFN-I response. Ly46Q is a CLR highly expressed on pDCs. The deficiency of Ly46Q on pDC results in decreased IFN-α production by pDCs. The regulatory function of Ly46Q requires an intact ITIM motif at its cytoplasmic tail (Rahim et al., 2013). Another inhibitory CLR involved in IFN-I

regulation is dendritic cell immunoreceptor (DCIR). By using the same in vitro primary cell model BMDC, it has been shown that DCIR is required for sustained ISG expression and IFN-I signaling activated by *mycoplasma tuberculosis* infection. This very same study claims DCIR expression grants the optimal IFN-I signaling in DC to prevent excessive Th1 response during in vivo *mycoplasma tuberculosis* infection (Troegeler et al., 2017). The link between DCIR and IFN-I response established in this study by RNA-seq and GSEA greatly resembles what we observed with Clec12A. However, the regulatory mechanisms utilized by these two inhibitory CLRs seem to be quite different. The Y701 phosphorylation of STAT1 after TLR activation is not altered in the DCIR deficient cells, whereas it is decreased when Clec12A is absent. Secondly, DCIR regulates the IFN-I receptor proximal signaling without affecting the production of IFN-Is, whereas Clec12A regulates IFN-I producing pathways upstream of IFNAR ligation.

4.2. The point where Clec12A-activated signaling interferes with IFN-I response

Recombinant IFN-β similarly activates IFN-I response in WT and *Clec12a*$^{-/-}$ BMDCs in terms of STAT1 phosphorylation and ISG expression. Therefore, our data clearly shows that Clec12A regulates signaling events independent of IFNAR engagement. Furthermore, inhibiting IFNAR by administering a blocking antibody did not abrogate the difference of 3pRNA induced ISG expression seen between WT and *Clec12a*$^{-/-}$ cells. This implies that Clec12A modulates IFN-I production.

In addition, we observed that Clec12A deficiency results in compromised IFN-I production by different PRR activation, including RIG-I (3pRNA stimulated), TLR4 (LPS stimulated) and TLR9 (CpG-ODN stimulated). This prompted us to speculate that Clec12A may regulate IFN-I production signaling events that are common among

these PRRs. The receptor proximal signaling of IFN-I production by TLR4 and RIG-I are quite different. Even though certain events, such as polyubiquitination, are critical for many of those PRR induced receptor proximal signaling, the fact that the NF-κB pathway is not affected excludes the possibility that Clec12A interfere with those early steps.

For IFN-I production, TLR4 and RIG-I relay the upstream signaling to their respective adaptor proteins TRIF and MAVS. From this point on, the different IFN-I producing pathways start to engage similar signaling modules (Figure 2). The adapter proteins first recruit kinase TBK1 (also IKKβ in the case of RIG-I) and get phosphorylated by TBK1 at their conserved pLxIS motif. Subsequently, the phosphorylated adapter proteins recruit IRF3 and draw it within close proximity to TBK1, to allow TBK1 to directly phosphorylate and activate IRF3(Liu et al., 2015). Therefore, Clec12A is most likely to come into play at the point of TBK1 activation. Although the identity of adaptor protein in the signaling of TLR9 induced IFN-I production is not clear, it has been reported that TBK1 is similarly activated (Clark et al., 2011).

4.3. Src-family kinases in Clec12A activated signaling

SFKs are one of the major signaling molecule families that operate in the proximal signaling pathways in innate immune cells. These signaling pathways including signaling of immunoreceptors, C-type lectin receptors, integrins, G protein-coupled receptors and many others (Lowell, 2011). The SFKs have certain redundancy in signaling and in most cases only the deficiency of several kinases together produces a profound effect (Lowell, 2004).

As indicated by the increased activating tyrosine phosphorylation (the Y416 motif of Src), stimulating the BMDCs with MSU crystal significantly induced the kinase activity

of SFKs. In this case, the full induction of SFK kinase activity clearly depends on Clec12A, as the *Clec12a*$^{-/-}$ cells showed a marked defect of SFK Y416 phosphorylation. However, it remains unclear how the SFK kinase activity is triggered. In the case of T lymphocytes, the phosphatase CD45 can release the Lck from the catalytic inactive “tail-bite” conformation by removing the inhibitory Y505 phosphorylation. Meanwhile, CD45 can also inhibit the activating Y398 phosphorylation, which is triggered by intermolecular autophosphorylation in response to Y505 dephosphorylation. As the Y398 phosphorylation is required for the full activation of Lck, the dual function of CD45 keeps the SFK activity at basal level under steady state. When T lymphocytes encounters an antigen, CD45 is excluded from the immunological synapse and separated from Lck. Such a process could locally prevent the inactivation of Lck, thereby leading to T cell activation (Rhee and Veillette, 2012). Similarly, when dectin-1 binds its ligand β-glucan in the particulate form (but not in soluble monomer form) they cluster to the “phagocytic synapse”. This structure also excludes CD45 and harbors activated SFKs and syk at its core (Goodridge et al., 2011). As Clec12a only recognizes MSU in its crystal form, it is possible that the binding of MSU crystal by Clec12A generates a similar signaling synapse to activate SFKs.

Treating the cells with SFK inhibitor PP2 blocks the difference of p-TBK1, p-IRF3 and ISG expression between WT and *Clec12a*$^{-/-}$ cells. These results indicate that SFK is a key mediator between Clec12A and the IFN-I producing pathway. In several studies, SFKs has been implicated in regulating the IFN-I response. In HEK293 cells, Sendai virus infection triggers Src activation, which promotes IFN-β production. Specifically, Src interact with TRAF3 to modulate the RIG-I mediated IFN-I production signaling (Johnsen et al., 2009). In addition, a recent study showed that the serine

kinase activity of TBK1 could be negatively regulated by its phosphorylation at Tyr354/394, which is catalyzed by several SFKs (Lck, Fgr and Hck) in epithelial cell lines, HEK293 cells, lymphocytic cell lines and Raw264.7. The authors of this study also demonstrated that IFN-I induces SFK expression, proposing that SFKs constitute a negative feedback mechanism of anti-viral immune response (Liu et al., 2017). In addition, it has been shown that the serine kinase activity of TBK1 could be regulated by tyrosine phosphorylation at site Y179. However, the Y179 phosphorylation seems to positively regulate TBK1 activation. Moreover, the Y179 phosphorylation is mediated specifically by Src, but not other SFKs (Li et al., 2017).

The data obtained from this study best supports the notions that SFKs positively regulate TBK1 activity, as the adding of PP2 impaired the IFN-I response, including the TBK1 serine phosphorylation at S172. Our study and that of Li et al's focused on short stimulation. Therefore, it is likely that the negative regulation of IFN-I by Lck, Fgr and Hck requires much longer duration of time to happen, whereas the more immediate positive effect of Src is dominates during short stimulation. The ITIM motif of Clec12A is likely to be phosphorylated by SFKs. Therefore, we can not discriminate whether SFKs that are activated by Clec12A directly affect TBK1 activity, or they indirectly modulate TBK1 via ITIM. Since there is no inhibitor targets each single SFK members, we would need amenable cell line tools to further dissect the mechanism.

In addition to PP2, we treated the cells with several other inhibitors, aiming to get more information about the signaling pathways that are engaged by Clec12A to modulate IFN-I response. Our data showed that cytochalasin D (actin polymerization inhibitor) treatment can block the difference of *Ifit3* expression seen between WT and *Clec12a*$^{-/-}$ cells, whereas MCC950 (NLRP3 inhibitor) and chloroquine (endosomal

acidification/autophagy inhibitor) treatment did not. As SFK, and actin polymerization are involved in cell adhesion and phagocytosis, it is plausible that Clec12A may also regulate these processes. The exact details surrounding these processes and their relationship to the IFN-I response still need to be determined.

4.4. The *in vivo* function of Clec12A during virus infection

Since we initially observed that Clec12A regulates the RIG-I activated IFN-I response, we explored the *in vivo* function of Clec12A by using two strains of LCMV viruses, that are known to activate the RIG-I-MAVS IFN-I production pathway (Wang et al., 2012; Zhou et al., 2010). The deficiency of Clec12A in mice leads to a decrease in serum IFN-α levels following infection with both LCMV strains. These results nicely fit together with our *in vitro* observations. LCMV is known to infect a wide range of cell types, including cDC and pDC (Teijaro et al., 2013). Meanwhile, it has been shown that the RNA from LCMV can induce IFN-I production in both cDC and pDC (Zhou et al., 2010). As the IFN-I production signaling is quite different in these two cell types, discriminating the responsible cell type by crossing the mice to IFN-β-YFP reporter mice (Teijaro et al., 2013) could help to gain further insight into the regulatory function of Clec12A *in vivo*. In contrast to LCMV infection, the deficiency of Clec12A does not affect the production of IFN-I in mice infected with influenza virus and MVA virus. As there are many parameters that are not directly comparable among these different virus infection models, it is challenging to establish the reason for this observation. For example, the mice were inoculated with influenza virus intranasally (rather than systematically), thereby inducing local response mainly restricted to the lung. In the case of MVA, the virus is highly attenuated, inducing only a weak and transient IFN-I response.

As previously reported, infecting mice with LCMV-WE induces considerable liver damage(Beier et al., 2015; Lukashevich et al., 2003). Initially, both the *Clec12a*$^{-/-}$ mice and the WT control showed a similar degree of liver damage. However, by the experiment endpoint, the WT mice are fully recovered, while the *Clec12a*$^{-/-}$ mice did not. As LCMV is not cytolytic, immunopathology is most like to account for the liver damage. However, the *Clec12a*$^{-/-}$ mice show a decreased virus clearance. As the CTL response should efficiently limit the virus replication, this observation would refute the idea that the increased immunopathology is caused by increased CTL response. Therefore, it is more likely that excessive inflammation is responsible for the increased liver damage in the knock out mice. In support of this possibility, we have observed markedly increased infiltration of neutrophils in the spleen of MVA infected knock out mice. Meanwhile, Clec12A does not seem to affect the adaptive immune response, as there are no major differences in the T and B cells compartment between WT and *Clec12a*$^{-/-}$ mice following MVA and LCMV-Docile infection.

In addition, the deficiency of Clec12A conferred significant protection against chronic LCMV infection. Chronic LCMV infection can induce robust IFN-I production, which initiates a immunosuppressive program that includes IL-10 production and up-regulation of PD-1 ligand in myeloid cells (Teijaro et al., 2013; Wilson et al., 2013). It would be interesting to investigate if the IL-10 level in the serum and PD-1 ligand expression on DCs differ between the WT and *Clec12a*$^{-/-}$ mice after LCMV-Docile infection. Considering the knowledge of disparate effects of IFN-I in determining host come in acute and chronic LCMV infection (that is IFN-I benefit the host during acute LCMV infection and is detrimental during chronic infection), the pattern of

pathological outcomes of *Clec12a*$^{-/-}$ mice upon LCMV-WE and Docile infection again suggests a positive role of Clec12A in regulating IFN-I response *in vivo*.

4.5. Clec12A at the crossroad of inflammation and IFN-I

Inflammation and IFN-I response are important forces in the innate immune response. Several reports have demonstrated the counter-regulatory relationship between these two types of innate immune response. During influenza infection, blocking the production or signaling of prostaglandin E2 (an important mediator of inflammation) by pharmacological inhibition or genetic deletion provides protection against the virus both *in vivo* and *in vitro*. The PI3K-AKT pathway mediates the inhibitory effect of prostaglandin E2 on IFN-I (Coulombe et al., 2014). Similarly, during *mycobacteria tuberculosis* infection, IL-1β has been reported to limit excessive IFN-I response by inducing eicosanoid species, including prostaglandin E2 (Mayer-Barber et al., 2014). On the other hand, IFN-I has been shown to inhibit MSU, alum or nigericin triggered NLRP3 inflammasome activity through unknown mechanism, and block alum induced inflammatory cell migration *in vivo* (Guarda et al., 2011). Moreover, monocytes isolated from multiple sclerosis patients who received recombinant interferon treatment show decreased NLRP3 inflammasome activation by alum (Guarda et al., 2011). Nevertheless, IFN-I is required for NLRP3 and AIM2 inflammasome activation in response to intracellular bacteria infection as it induces small GTPases to expose bacterial PAMPs (Man et al., 2016; Meunier et al., 2014; Rathinam et al., 2012).

In vivo analysis of thymocytes from mice that received a low-dose irradiation revealed that Clec12A simultaneously suppresses sterile inflammation and supports ISG transcription. Transcriptome analysis of *in vitro* stimulated BMDCs uncovered a

positive role for Clec12A in regulating the IFN-I response. Meanwhile, previous work in our lab has demonstrated that in isolated neutrophils, Clec12A prevents excessive ROS production, which is a potent mediator of acute inflammation. In line with this, we observed *Clec12a*$^{-/-}$ BMDCs stimulated with MSU produce significantly greater amount of prostaglandin E2, and express more chemokine genes such as *Cxcl1*, *Cxcl2* and *nos2*, which generates nitric oxide to mediate inflammation (data not shown). This evidence, from both *in vivo* and *in vitro* experiments, suggests that Clec12A is able to sense the biological context and instruct the innate immune cells to downplay the inflammatory response to prevent immunopathology, while amplifying IFN-I response to initiate the cell intrinsic response. In the case of an infection, this role of Clec12A could be strategically beneficial. At the early stage of bacterial or viral invasion, before the pathogen has established its replication, triggering inflammatory responses to attract professional phagocytes would be effective as those cells are specially equipped to engulf and killing those extracellular intruders. However, when the pathogens finally get access to the cell and start to initiate cell damage, the risk of inflammation causing immunopathology will outweigh its potential pathogen-killing function. At this point, the damage caused by the pathogen will activate Clec12A, which will halt inflammation and simultaneously amplify the IFN-I response. The IFN-I response is a more effective force to eradicate intracellular pathogens as it induces ISGs that interfere with pathogen replication and initiate cell death, which will destroy the venue of pathogen multiplication.

4.6. Conclusion and outlook

The detection of DAMP by PRRs makes it possible for the innate immune cell to constantly gauge the progression of the immune response, thereby improving the efficiency of the immune response as well as minimizing collateral damage. Several CLRs, like CLEC9A and Mincle, have been implicated in the recognition of DAMPs. Clec12A is another CLR that can sense dead cell corpse and MSU crystals. The results presented in this thesis demonstrate that the recognition of DAMP by Clec12A could positively regulate the IFN-I production pathway. As IFN-I plays an important role in the anti-microbial immune response, this study contributes mechanistic insight into immune modulation by DAMP during infection.

It is interesting to see that the genetic deletion of Clec12A provides significant protection to the chronic LCMV infection. Further investigation into the role of Clec12A in clinically relevant chronic infections, such as Hepatitis C virus or HIV infection, will be of great interest. As MSU is the ligand for Clec12A, it is possible that uric acid levels could be targeted for therapy against chronic virus infection. In addition, as discussed above, the anti-tumor immune response induced by radiotherapy has been reported to depend on successful induction of IFN-I response. Integrating our observation that Clec12A modulate both IFN-I and inflammatory response in the thymus after whole body irradiation, this raises the possibility that Clec12A is also involved in radiotherapy-induced anti-tumor immune response.

5. References

Agalioti, T., Lomvardas, S., Parekh, B., Yie, J., Maniatis, T., and Thanos, D. (2000). Ordered recruitment of chromatin modifying and general transcription factors to the IFN-beta promoter. Cell *103*, 667–678.

Andrejeva, J., Childs, K.S., Young, D.F., Carlos, T.S., Stock, N., Goodbourn, S., and Randall, R.E. (2004). The V proteins of paramyxoviruses bind the IFN-inducible RNA helicase, mda-5, and inhibit its activation of the IFN-beta promoter. Proc. Natl. Acad. Sci. U. S. A. *101*, 17264–17269.

Asgari, S., Schlapbach, L.J., Anchisi, S., Hammer, C., Bartha, I., Junier, T., Mottet-Osman, G., Posfay-Barbe, K.M., Longchamp, D., Stocker, M., et al. (2017). Severe viral respiratory infections in children with IFIH1 loss-of-function mutations. Proc. Natl. Acad. Sci. U. S. A. *114*, 8342–8347.

Bardoel, B.W., and Strijp, J.A.G. (2011). Molecular battle between host and bacterium: recognition in innate immunity. J. Mol. Recognit. *24*, 1077–1086.

Begun, J., Lassen, K.G., Jijon, H.B., Baxt, L.A., Goel, G., Heath, R.J., Ng, A., Tam, J.M., Kuo, S.-Y., Villablanca, E.J., et al. (2015). Integrated Genomics of Crohn's Disease Risk Variant Identifies a Role for CLEC12A in Antibacterial Autophagy. Cell Rep. *11*, 1905–1918.

Beier, J.I., Jokinen, J.D., Holz, G.E., Whang, P.S., Martin, A.M., Warner, N.L., Arteel, G.E., and Lukashevich, I.S. (2015). Novel Mechanism of Arenavirus-Induced Liver Pathology. PLoS One *10*, e0122839.

Boudreau, J., Koshy, S., Cummings, D., and Wan, Y. (2008). Culture of myeloid dendritic cells from bone marrow precursors. J. Vis. Exp. e769–e769.

Boxx, G.M., and Cheng, G. (2016). The Roles of Type I Interferon in Bacterial Infection. Cell Host Microbe *19*, 760–769.

Brass, A.L., Huang, I.-C., Benita, Y., John, S.P., Krishnan, M.N., Feeley, E.M., Ryan,

B.J., Weyer, J.L., van der Weyden, L., Fikrig, E., et al. (2009). The IFITM proteins mediate cellular resistance to influenza A H1N1 virus, West Nile virus, and dengue virus. Cell *139*, 1243–1254.

Brinkmann, V., Reichard, U., Goosmann, C., Fauler, B., Uhlemann, Y., Weiss, D.S., Weinrauch, Y., and Zychlinsky, A. (2004). Neutrophil Extracellular Traps Kill Bacteria. Science (80-.). *303*, 1532–1535.

Broz, P., and Dixit, V.M. (2016). Inflammasomes: mechanism of assembly, regulation and signalling. Nat. Rev. Immunol. *16*, 407–420.

Burnette, B.C., Liang, H., Lee, Y., Chlewicki, L., Khodarev, N.N., Weichselbaum, R.R., Fu, Y.-X., and Auh, S.L. (2011). The efficacy of radiotherapy relies upon induction of type I interferon-dependent innate and adaptive immunity. Cancer Res. *71*, 2488–2496.

Chan, Y.K., and Gack, M.U. (2016). Viral evasion of intracellular DNA and RNA sensing. Nat. Rev. Microbiol. *14*, 360–373.

Chen, G., Shaw, M.H., Kim, Y.-G., and Nuñez, G. (2009). NOD-Like Receptors: Role in Innate Immunity and Inflammatory Disease. Annu. Rev. Pathol. Mech. Dis. *4*, 365–398.

Clark, K., Takeuchi, O., Akira, S., and Cohen, P. (2011). The TRAF-associated protein TANK facilitates cross-talk within the IkappaB kinase family during Toll-like receptor signaling. Proc. Natl. Acad. Sci. U. S. A. *108*, 17093–17098.

Cornberg, M., Kenney, L.L., Chen, A.T., Waggoner, S.N., Kim, S.-K., Dienes, H.P., Welsh, R.M., and Selin, L.K. (2013). Clonal exhaustion as a mechanism to protect against severe immunopathology and death from an overwhelming CD8 T cell response. Front. Immunol. *4*, 475.

Coulombe, F., Jaworska, J., Verway, M., Tzelepis, F., Massoud, A., Gillard, J., Wong, G., Kobinger, G., Xing, Z., Couture, C., et al. (2014). Targeted prostaglandin E2 inhibition enhances antiviral immunity through induction of type I interferon and apoptosis in macrophages. Immunity *40*, 554–568.

Deng, L., Liang, H., Xu, M., Yang, X., Burnette, B., Arina, A., Li, X.-D., Mauceri, H.,

Beckett, M., Darga, T., et al. (2014a). STING-dependent cytosolic DNA sensing promotes radiation-induced type I interferon-dependent antitumor immunity in immunogenic tumors. Immunity *41*, 843–852.

Deng, L., Liang, H., Xu, M., Yang, X., Burnette, B., Arina, A., Li, X.-D., Mauceri, H., Beckett, M., Darga, T., et al. (2014b). STING-Dependent Cytosolic DNA Sensing Promotes Radiation-Induced Type I Interferon-Dependent Antitumor Immunity in Immunogenic Tumors. Immunity *41*, 843–852.

Diamond, M.S., and Farzan, M. (2013). The broad-spectrum antiviral functions of IFIT and IFITM proteins. Nat. Rev. Immunol. *13*, 46–57.

Dixit, E., and Kagan, J.C. (2013). Intracellular pathogen detection by RIG-I-like receptors. Adv. Immunol. *117*, 99–125.

Duhan, V., Khairnar, V., Friedrich, S.-K., Zhou, F., Gassa, A., Honke, N., Shaabani, N., Gailus, N., Botezatu, L., Khandanpour, C., et al. (2016). Virus-specific antibodies allow viral replication in the marginal zone, thereby promoting CD8+ T-cell priming and viral control. Sci. Rep. *6*, 19191.

Everitt, A.R., Clare, S., Pertel, T., John, S.P., Wash, R.S., Smith, S.E., Chin, C.R., Feeley, E.M., Sims, J.S., Adams, D.J., et al. (2012). IFITM3 restricts the morbidity and mortality associated with influenza. Nature *484*, 519–523.

Fitzgerald, K.A., McWhirter, S.M., Faia, K.L., Rowe, D.C., Latz, E., Golenbock, D.T., Coyle, A.J., Liao, S.-M., and Maniatis, T. (2003). IKKε and TBK1 are essential components of the IRF3 signaling pathway. Nat. Immunol. *4*, 491–496.

del Fresno, C., Soulat, D., Roth, S., Blazek, K., Udalova, I., Sancho, D., Ruland, J., and Ardavín, C. (2013). Interferon-β production via Dectin-1-Syk-IRF5 signaling in dendritic cells is crucial for immunity to C. albicans. Immunity *38*, 1176–1186.

Fu, X.Y., Kessler, D.S., Veals, S.A., Levy, D.E., and Darnell, J.E. (1990). ISGF3, the transcriptional activator induced by interferon alpha, consists of multiple interacting polypeptide chains. Proc. Natl. Acad. Sci. U. S. A. *87*, 8555–8559.

Ginhoux, F., and Jung, S. (2014). Monocytes and macrophages: developmental pathways and tissue homeostasis. Nat. Rev. Immunol. *14*, 392–404.

Girardin, S.E., Boneca, I.G., Viala, J., Chamaillard, M., Labigne, A., Thomas, G., Philpott, D.J., and Sansonetti, P.J. (2003). Nod2 Is a General Sensor of Peptidoglycan through Muramyl Dipeptide (MDP) Detection. J. Biol. Chem. *278*, 8869–8872.

González-Navajas, J.M., Lee, J., David, M., and Raz, E. (2012). Immunomodulatory functions of type I interferons. Nat. Rev. Immunol. *12*, 125.

Goodridge, H.S., Reyes, C.N., Becker, C.A., Katsumoto, T.R., Ma, J., Wolf, A.J., Bose, N., Chan, A.S.H., Magee, A.S., Danielson, M.E., et al. (2011). Activation of the innate immune receptor Dectin-1 upon formation of a “phagocytic synapse”. Nature *472*, 471–475.

Goubau, D., Deddouche, S., and Reis e Sousa, C. (2013). Cytosolic Sensing of Viruses. Immunity *38*, 855–869.

Goubau, D., Schlee, M., Deddouche, S., Pruijssers, A.J., Zillinger, T., Goldeck, M., Schuberth, C., Van der Veen, A.G., Fujimura, T., Rehwinkel, J., et al. (2014). Antiviral immunity via RIG-I-mediated recognition of RNA bearing 5′-diphosphates. Nature *514*, 372–375.

Gross, O., Gewies, A., Finger, K., Schäfer, M., Sparwasser, T., Peschel, C., Förster, I., and Ruland, J. (2006). Card9 controls a non-TLR signalling pathway for innate anti-fungal immunity. Nature *442*, 651–656.

Guarda, G., Braun, M., Staehli, F., Tardivel, A., Mattmann, C., Förster, I., Farlik, M., Decker, T., Du Pasquier, R.A., Romero, P., et al. (2011). Type I interferon inhibits interleukin-1 production and inflammasome activation. Immunity *34*, 213–223.

Han, C., Jin, J., Xu, S., Liu, H., Li, N., and Cao, X. (2010). Integrin CD11b negatively regulates TLR-triggered inflammatory responses by activating Syk and promoting degradation of MyD88 and TRIF via Cbl-b. Nat. Immunol. *11*, 734–742.

Heath, W.R., and Carbone, F.R. (2009). Dendritic cell subsets in primary and secondary T cell responses at body surfaces. Nat. Immunol. *10*, 1237–1244.

Helft, J., Ginhoux, F., Bogunovic, M., and Merad, M. (2010). Origin and functional heterogeneity of non-lymphoid tissue dendritic cells in mice. Immunol. Rev. *234*, 55–

75.

Helft, J., Böttcher, J., Chakravarty, P., Zelenay, S., Huotari, J., Schraml, B.U., Goubau, D., and Reis e Sousa, C. (2015). GM-CSF Mouse Bone Marrow Cultures Comprise a Heterogeneous Population of CD11c+MHCII+ Macrophages and Dendritic Cells. Immunity *42*, 1197–1211.

Henry, T., Kirimanjeswara, G.S., Ruby, T., Jones, J.W., Peng, K., Perret, M., Ho, L., Sauer, J.-D., Iwakura, Y., Metzger, D.W., et al. (2010). Type I IFN Signaling Constrains IL-17A/F Secretion by γδ T Cells during Bacterial Infections. J. Immunol. *184*.

Hoebe, K., Du, X., Georgel, P., Janssen, E., Tabeta, K., Kim, S.O., Goode, J., Lin, P., Mann, N., Mudd, S., et al. (2003). Identification of Lps2 as a key transducer of MyD88-independent TIR signalling. Nature *424*, 743–748.

Holm, C.K., Rahbek, S.H., Gad, H.H., Bak, R.O., Jakobsen, M.R., Jiang, Z., Hansen, A.L., Jensen, S.K., Sun, C., Thomsen, M.K., et al. (2016). Influenza A virus targets a cGAS-independent STING pathway that controls enveloped RNA viruses. Nat. Commun. *7*, 10680.

Honda, K., Yanai, H., Negishi, H., Asagiri, M., Sato, M., Mizutani, T., Shimada, N., Ohba, Y., Takaoka, A., Yoshida, N., et al. (2005). IRF-7 is the master regulator of type-I interferon-dependent immune responses. Nature *434*, 772–777.

Hornung, V., Ellegast, J., Kim, S., Brzozka, K., Jung, A., Kato, H., Poeck, H., Akira, S., Conzelmann, K.-K., Schlee, M., et al. (2006). 5’-Triphosphate RNA Is the Ligand for RIG-I. Science (80-.). *314*, 994–997.

Hornung, V., Ablasser, A., Charrel-Dennis, M., Bauernfeind, F., Horvath, G., Caffrey, D.R., Latz, E., and Fitzgerald, K.A. (2009). AIM2 recognizes cytosolic dsDNA and forms a caspase-1-activating inflammasome with ASC. Nature *458*, 514–518.

Huang, I.-C., Bailey, C.C., Weyer, J.L., Radoshitzky, S.R., Becker, M.M., Chiang, J.J., Brass, A.L., Ahmed, A.A., Chi, X., Dong, L., et al. (2011). Distinct Patterns of IFITM-Mediated Restriction of Filoviruses, SARS Coronavirus, and Influenza A Virus. PLoS Pathog. *7*, e1001258.

Huynh, L., Wang, L., Shi, C., Park-Min, K.-H., and Ivashkiv, L.B. (2012). ITAM-Coupled Receptors Inhibit IFNAR Signaling and Alter Macrophage Responses to TLR4 and Listeria monocytogenes. J. Immunol. *188*, 3447–3457.

Inohara, N., Ogura, Y., Fontalba, A., Gutierrez, O., Pons, F., Crespo, J., Fukase, K., Inamura, S., Kusumoto, S., Hashimoto, M., et al. (2003). Host Recognition of Bacterial Muramyl Dipeptide Mediated through NOD2. J. Biol. Chem. *278*, 5509–5512.

Isaacs, A., and Lindenmann, J. (1957). Virus Interference. I. The Interferon. Proc. R. Soc. London B Biol. Sci. *147*.

Ishikawa, H., and Barber, G.N. (2008). STING is an endoplasmic reticulum adaptor that facilitates innate immune signalling. Nature *455*, 674–678.

Jeha, S. (2001). Tumor lysis syndrome. Semin. Hematol. *38*, 4–8.

Johnsen, I.B., Nguyen, T.T., Bergstroem, B., Fitzgerald, K.A., and Anthonsen, M.W. (2009). The tyrosine kinase c-Src enhances RIG-I (retinoic acid-inducible gene I)-elicited antiviral signaling. J. Biol. Chem. *284*, 19122–19131.

Kanazawa, N., Okazaki, T., Nishimura, H., Tashiro, K. e. i., Inaba, K., Miyachi, Y., and Tsubata, T. (2002). DCIR Acts as an Inhibitory Receptor Depending on its Immunoreceptor Tyrosine-Based Inhibitory Motif11A preliminary report of these results was presented by the first author at the 61st annual meeting of SID in Chicago in the session “General Immunology”. J. Invest. Dermatol. *118*, 261–266.

Kasahara, S., and Clark, E.A. (2012). Dendritic cell-associated lectin 2 (DCAL2) defines a distinct CD8α- dendritic cell subset. J. Leukoc. Biol. *91*, 437–448.

Katakura, K., Lee, J., Rachmilewitz, D., Li, G., Eckmann, L., and Raz, E. (2005). Toll-like receptor 9-induced type I IFN protects mice from experimental colitis. J. Clin. Invest. *115*, 695–702.

Kato, H., Takeuchi, O., Sato, S., Yoneyama, M., Yamamoto, M., Matsui, K., Uematsu, S., Jung, A., Kawai, T., Ishii, K.J., et al. (2006). Differential roles of MDA5 and RIG-I helicases in the recognition of RNA viruses. Nature *441*, 101–105.

Kawai, T., Takeuchi, O., Fujita, T., Inoue, J., Mühlradt, P.F., Sato, S., Hoshino, K., and

Akira, S. (2001). Lipopolysaccharide Stimulates the MyD88-Independent Pathway and Results in Activation of IFN-Regulatory Factor 3 and the Expression of a Subset of Lipopolysaccharide-Inducible Genes. J. Immunol. *167*.

Kim, T.K., and Maniatis, T. (1997). The mechanism of transcriptional synergy of an in vitro assembled interferon-beta enhanceosome. Mol. Cell *1*, 119–129.

Kimbrell, D.A., and Beutler, B. (2001). The evolution and genetics of innate immunity. Nat. Rev. Genet. *2*, 256–267.

Kolaczkowska, E., and Kubes, P. (2013). Neutrophil recruitment and function in health and inflammation. Nat. Rev. Immunol. *13*, 159–175.

Kono, H., Chen, C.-J., Ontiveros, F., and Rock, K.L. (2010). Uric acid promotes an acute inflammatory response to sterile cell death in mice. J. Clin. Invest. *120*, 1939–1949.

Lacy, P. (2006). Mechanisms of degranulation in neutrophils. Allergy Asthma. Clin. Immunol. *2*, 98–108.

Larner, A.C., Jonak, G., Cheng, Y.S., Korant, B., Knight, E., Darnell, J.E., and Jr (1984). Transcriptional induction of two genes in human cells by beta interferon. Proc. Natl. Acad. Sci. U. S. A. *81*, 6733–6737.

Lemaitre, B., Nicolas, E., Michaut, L., Reichhart, J.M., and Hoffmann, J.A. (1996). The dorsoventral regulatory gene cassette spätzle/Toll/cactus controls the potent antifungal response in Drosophila adults. Cell *86*, 973–983.

Levy, D.E., Kessler, D.S., Pine, R., Reich, N., and Darnell, J.E. (1988). Interferon-induced nuclear factors that bind a shared promoter element correlate with positive and negative transcriptional control. Genes Dev. *2*, 383–393.

Li, X., Yang, M., Yu, Z., Tang, S., Wang, L., Cao, X., and Chen, T. (2017). The tyrosine kinase Src promotes phosphorylation of the kinase TBK1 to facilitate type I interferon production after viral infection. Sci. Signal. *10*, eaae0435.

Liston, A., and Masters, S.L. (2017). Homeostasis-altering molecular processes as mechanisms of inflammasome activation. Nat. Rev. Immunol. *17*, 208–214.

Liu, S., Cai, X., Wu, J., Cong, Q., Chen, X., Li, T., Du, F., Ren, J., Wu, Y.-T., Grishin, N. V., et al. (2015). Phosphorylation of innate immune adaptor proteins MAVS, STING, and TRIF induces IRF3 activation. Science (80-.). *347*, aaa2630-aaa2630.

Liu, S., Chen, S., Li, X., Wu, S., Zhang, Q., Jin, Q., Hu, L., Zhou, R., Yu, Z., Meng, F., et al. (2017). Lck/Hck/Fgr-mediated tyrosine phosphorylation negatively regulates TBK1 to restrain innate antiviral responses. Cell Host Microbe *21*, 754–768.e5.

Lowell, C. (2004). Src-family kinases: rheostats of immune cell signaling. Mol. Immunol. *41*, 631–643.

Lowell, C.A. (2011). Src-family and Syk kinases in activating and inhibitory pathways in innate immune cells: signaling cross talk. Cold Spring Harb. Perspect. Biol. *3*, a002352.

Lukashevich, I.S., Tikhonov, I., Rodas, J.D., Zapata, J.C., Yang, Y., Djavani, M., and Salvato, M.S. (2003). Arenavirus-mediated liver pathology: acute lymphocytic choriomeningitis virus infection of rhesus macaques is characterized by high-level interleukin-6 expression and hepatocyte proliferation. J. Virol. *77*, 1727–1737.

Lutz, M.B., Kukutsch, N., Ogilvie, A.L., Rössner, S., Koch, F., Romani, N., and Schuler, G. (1999). An advanced culture method for generating large quantities of highly pure dendritic cells from mouse bone marrow. J. Immunol. Methods *223*, 77–92.

Ma, X., Helgason, E., Phung, Q.T., Quan, C.L., Iyer, R.S., Lee, M.W., Bowman, K.K., Starovasnik, M.A., and Dueber, E.C. (2012). Molecular basis of Tank-binding kinase 1 activation by transautophosphorylation. Proc. Natl. Acad. Sci. U. S. A. *109*, 9378–9383.

Man, S.M., Karki, R., Sasai, M., Place, D.E., Kesavardhana, S., Temirov, J., Frase, S., Zhu, Q., Malireddi, R.K.S., Kuriakose, T., et al. (2016). IRGB10 Liberates Bacterial Ligands for Sensing by the AIM2 and Caspase-11-NLRP3 Inflammasomes. Cell *167*, 382–396.e17.

Marié, I., Durbin, J.E., and Levy, D.E. (1998). Differential viral induction of distinct interferon-alpha genes by positive feedback through interferon regulatory factor-7. EMBO J. *17*, 6660–6669.

Marshall, A.S.J., Willment, J.A., Lin, H.-H., Williams, D.L., Gordon, S., and Brown, G.D. (2004). Identification and characterization of a novel human myeloid inhibitory C-type lectin-like receptor (MICL) that is predominantly expressed on granulocytes and monocytes. J. Biol. Chem. *279*, 14792–14802.

Marshall, A.S.J., Willment, J.A., Pyż, E., Dennehy, K.M., Reid, D.M., Dri, P., Gordon, S., Wong, S.Y.C., and Brown, G.D. (2006). Human MICL (CLEC12A) is differentially glycosylated and is down-regulated following cellular activation. Eur. J. Immunol. *36*, 2159–2169.

Mayer-Barber, K.D., Andrade, B.B., Oland, S.D., Amaral, E.P., Barber, D.L., Gonzales, J., Derrick, S.C., Shi, R., Kumar, N.P., Wei, W., et al. (2014). Host-directed therapy of tuberculosis based on interleukin-1 and type I interferon crosstalk. Nature *511*, 99–103.

McWhirter, S.M., Fitzgerald, K.A., Rosains, J., Rowe, D.C., Golenbock, D.T., and Maniatis, T. (2004). IFN-regulatory factor 3-dependent gene expression is defective in Tbk1-deficient mouse embryonic fibroblasts. Proc. Natl. Acad. Sci. U. S. A. *101*, 233–238.

Medzhitov, R., Preston-Hurlburt, P., and Janeway, C.A. (1997). A human homologue of the Drosophila Toll protein signals activation of adaptive immunity. Nature *388*, 394–397.

Melen, K., Kinnunen, L., and Julkunen, I. (2001). Arginine/lysine-rich structural element is involved in interferon-induced nuclear import of STATs. J. Biol. Chem. *276*, 16447–16455.

Merad, M., Sathe, P., Helft, J., Miller, J., and Mortha, A. (2013). The Dendritic Cell Lineage: Ontogeny and Function of Dendritic Cells and Their Subsets in the Steady State and the Inflamed Setting. Annu. Rev. Immunol. *31*, 563–604.

Meunier, E., Dick, M.S., Dreier, R.F., Schürmann, N., Broz, D.K., Warming, S., Roose-Girma, M., Bumann, D., Kayagaki, N., Takeda, K., et al. (2014). Caspase-11 activation requires lysis of pathogen-containing vacuoles by IFN-induced GTPases. Nature *509*, 366–370.

Miyamoto, M., Fujita, T., Kimura, Y., Maruyama, M., Harada, H., Sudo, Y., Miyata, T.,

and Taniguchi, T. (1988). Regulated expression of a gene encoding a nuclear factor, IRF-1, that specifically binds to IFN-beta gene regulatory elements. Cell *54*, 903–913.

Mócsai, A., Ruland, J., and Tybulewicz, V.L.J. (2010). The SYK tyrosine kinase: a crucial player in diverse biological functions. Nat. Rev. Immunol. *10*, 387–402.

Montminy, S.W., Khan, N., McGrath, S., Walkowicz, M.J., Sharp, F., Conlon, J.E., Fukase, K., Kusumoto, S., Sweet, C., Miyake, K., et al. (2006). Virulence factors of Yersinia pestis are overcome by a strong lipopolysaccharide response. Nat. Immunol. *7*, 1066–1073.

Mori, M., Yoneyama, M., Ito, T., Takahashi, K., Inagaki, F., and Fujita, T. (2004). Identification of Ser-386 of interferon regulatory factor 3 as critical target for inducible phosphorylation that determines activation. J. Biol. Chem. *279*, 9698–9702.

Müller, U., Steinhoff, U., Reis, L.F., Hemmi, S., Pavlovic, J., Zinkernagel, R.M., and Aguet, M. (1994). Functional role of type I and type II interferons in antiviral defense. Science *264*, 1918–1921.

Negishi, H., Fujita, Y., Yanai, H., Sakaguchi, S., Ouyang, X., Shinohara, M., Takayanagi, H., Ohba, Y., Taniguchi, T., and Honda, K. (2006). Evidence for licensing of IFN- -induced IFN regulatory factor 1 transcription factor by MyD88 in Toll-like receptor-dependent gene induction program. Proc. Natl. Acad. Sci. *103*, 15136–15141.

Neumann, K., Castiñeiras-Vilariño, M., Höckendorf, U., Hannesschläger, N., Lemeer, S., Kupka, D., Meyermann, S., Lech, M., Anders, H.-J., Kuster, B., et al. (2014). Clec12a Is an Inhibitory Receptor for Uric Acid Crystals that Regulates Inflammation in Response to Cell Death. Immunity *40*, 389–399.

O'Connell, R.M., Saha, S.K., Vaidya, S.A., Bruhn, K.W., Miranda, G.A., Zarnegar, B., Perry, A.K., Nguyen, B.O., Lane, T.F., Taniguchi, T., et al. (2004). Type I Interferon Production Enhances Susceptibility to Listeria monocytogenes Infection. J. Exp. Med. *200*.

O'Neill, L.A.J., Golenbock, D., and Bowie, A.G. (2013). The history of Toll-like receptors - redefining innate immunity. Nat. Rev. Immunol. *13*, 453–460.

Perkins, D.J., Rajaiah, R., Tennant, S.M., Ramachandran, G., Higginson, E.E., Dyson, T.N., and Vogel, S.N. (2015). Salmonella Typhimurium Co-Opts the Host Type I IFN System To Restrict Macrophage Innate Immune Transcriptional Responses Selectively. J. Immunol. *195*.

Pichlmair, A., Schulz, O., Tan, C.P., Naslund, T.I., Liljestrom, P., Weber, F., and Reis e Sousa, C. (2006). RIG-I-Mediated Antiviral Responses to Single-Stranded RNA Bearing 5'-Phosphates. Science (80-.). *314*, 997–1001.

Pichlmair, A., Lassnig, C., Eberle, C.-A., Górna, M.W., Baumann, C.L., Burkard, T.R., Bürckstümmer, T., Stefanovic, A., Krieger, S., Bennett, K.L., et al. (2011). IFIT1 is an antiviral protein that recognizes 5′-triphosphate RNA. Nat. Immunol. *12*, 624–630.

Pyż, E., Huysamen, C., Marshall, A.S.J., Gordon, S., Taylor, P.R., and Brown, G.D. (2008). Characterisation of murine MICL (CLEC12A) and evidence for an endogenous ligand. Eur. J. Immunol. *38*, 1157–1163.

Qin, B.Y., Liu, C., Lam, S.S., Srinath, H., Delston, R., Correia, J.J., Derynck, R., and Lin, K. (2003). Crystal structure of IRF-3 reveals mechanism of autoinhibition and virus-induced phosphoactivation. Nat. Struct. Biol. *10*, 913–921.

Rahim, M.M.A., Tai, L.-H., Troke, A.D., Mahmoud, A.B., Abou-Samra, E., Roy, J.G., Mottashed, A., Ault, N., Corbeil, C., Goulet, M.-L., et al. (2013). Ly49Q positively regulates type I IFN production by plasmacytoid dendritic cells in an immunoreceptor tyrosine-based inhibitory motif-dependent manner. J. Immunol. *190*, 3994–4004.

Rathinam, V.A.K., Vanaja, S.K., Waggoner, L., Sokolovska, A., Becker, C., Stuart, L.M., Leong, J.M., and Fitzgerald, K.A. (2012). TRIF licenses caspase-11-dependent NLRP3 inflammasome activation by gram-negative bacteria. Cell *150*, 606–619.

Redelinghuys, P., Whitehead, L., Augello, A., Drummond, R.A., Levesque, J.-M., Vautier, S., Reid, D.M., Kerscher, B., Taylor, J.A., Nigrovic, P.A., et al. (2016). MICL controls inflammation in rheumatoid arthritis. Ann. Rheum. Dis. *75*, 1386–1391.

Reis, L.F., Ho Lee, T., and Vilcek, J. (1989). Tumor necrosis factor acts synergistically with autocrine interferon-beta and increases interferon-beta mRNA levels in human fibroblasts. J. Biol. Chem. *264*, 16351–16354.

Rhee, I., and Veillette, A. (2012). Protein tyrosine phosphatases in lymphocyte activation and autoimmunity. Nat. Immunol. *13*, 439–447.

Richard, M., Thibault, N., Veilleux, P., Gareau-Pagé, G., and Beaulieu, A.D. (2006). Granulocyte macrophage-colony stimulating factor reduces the affinity of SHP-2 for the ITIM of CLECSF6 in neutrophils: A new mechanism of action for SHP-2. Mol. Immunol. *43*, 1716–1721.

Ritchie, K.J., Hahn, C.S., Kim, K. Il, Yan, M., Rosario, D., Li, L., de la Torre, J.C., and Zhang, D.-E. (2004). Role of ISG15 protease UBP43 (USP18) in innate immunity to viral infection. Nat. Med. *10*, 1374–1378.

Sadzak, I., Schiff, M., Gattermeier, I., Glinitzer, R., Sauer, I., Saalmüller, A., Yang, E., Schaljo, B., and Kovarik, P. (2008). Recruitment of Stat1 to chromatin is required for interferon-induced serine phosphorylation of Stat1 transactivation domain. Proc. Natl. Acad. Sci. U. S. A. *105*, 8944–8949.

Sancho, D., and Reis e Sousa, C. (2012). Signaling by Myeloid C-Type Lectin Receptors in Immunity and Homeostasis. Annu. Rev. Immunol. *30*, 491–529.

Sato, M., Suemori, H., Hata, N., Asagiri, M., Ogasawara, K., Nakao, K., Nakaya, T., Katsuki, M., Noguchi, S., Tanaka, N., et al. (2000). Distinct and Essential Roles of Transcription Factors IRF-3 and IRF-7 in Response to Viruses for IFN-α/β Gene Induction. Immunity *13*, 539–548.

Sato, S., Sugiyama, M., Yamamoto, M., Watanabe, Y., Kawai, T., Takeda, K., and Akira, S. (2003). Toll/IL-1 Receptor Domain-Containing Adaptor Inducing IFN-β (TRIF) Associates with TNF Receptor-Associated Factor 6 and TANK-Binding Kinase 1, and Activates Two Distinct Transcription Factors, NF-κB and IFN-Regulatory Factor-3, in the Toll-Like Receptor …. J. Immunol. *171*.

Schattgen, S.A., and Fitzgerald, K.A. (2011). The PYHIN protein family as mediators of host defenses. Immunol. Rev. *243*, 109–118.

Schlee, M. (2013). Master sensors of pathogenic RNA – RIG-I like receptors. Immunobiology *218*, 1322–1335.

Schmitz, F., Heit, A., Guggemoos, S., Krug, A., Mages, J., Schiemann, M., Adler, H.,

Drexler, I., Haas, T., Lang, R., et al. (2007a). Interferon-regulatory-factor 1 controls Toll-like receptor 9-mediated IFN-β production in myeloid dendritic cells. Eur. J. Immunol. *37*, 315–327.

Schmitz, F., Heit, A., Guggemoos, S., Krug, A., Mages, J., Schiemann, M., Adler, H., Drexler, I., Haas, T., Lang, R., et al. (2007b). Interferon-regulatory-factor 1 controls Toll-like receptor 9-mediated IFN-β production in myeloid dendritic cells. Eur. J. Immunol. *37*, 315–327.

Schmolke, M., Patel, J.R., de Castro, E., Sánchez-Aparicio, M.T., Uccellini, M.B., Miller, J.C., Manicassamy, B., Satoh, T., Kawai, T., Akira, S., et al. (2014). RIG-I detects mRNA of intracellular Salmonella enterica serovar Typhimurium during bacterial infection. MBio *5*, e01006-14.

Schneider, W.M., Chevillotte, M.D., and Rice, C.M. (2014). Interferon-stimulated genes: a complex web of host defenses. Annu. Rev. Immunol. *32*, 513–545.

Seo, J.-Y., Yaneva, R., and Cresswell, P. (2011). Viperin: a multifunctional, interferon-inducible protein that regulates virus replication. Cell Host Microbe *10*, 534–539.

Servant, M.J., Grandvaux, N., TenOever, B.R., Duguay, D., Lin, R., and Hiscott, J. (2003). Identification of the minimal phosphoacceptor site required for in vivo activation of interferon regulatory factor 3 in response to virus and double-stranded RNA. J. Biol. Chem. *278*, 9441–9447.

Sharma, S., tenOever, B.R., Grandvaux, N., Zhou, G.-P., Lin, R., and Hiscott, J. (2003). Triggering the Interferon Antiviral Response Through an IKK-Related Pathway. Science (80-.). *300*.

Shi, J., Zhao, Y., Wang, Y., Gao, W., Ding, J., Li, P., Hu, L., and Shao, F. (2014). Inflammatory caspases are innate immune receptors for intracellular LPS. Nature *514*, 187–192.

Shi, Y., Evans, J.E., and Rock, K.L. (2003). Molecular identification of a danger signal that alerts the immune system to dying cells. Nature *425*, 516–521.

Shortman, K., and Heath, W.R. (2010). The CD8 $^{+}$ dendritic cell subset. Immunol. Rev. *234*, 18–31.

Skaug, B., and Chen, Z.J. (2010). Emerging role of ISG15 in antiviral immunity. Cell *143*, 187–190.

Spanier, J., Lienenklaus, S., Paijo, J., Kessler, A., Borst, K., Heindorf, S., Baker, D.P., Kröger, A., Weiss, S., Detje, C.N., et al. (2014). Concomitant TLR/RLH Signaling of Radioresistant and Radiosensitive Cells Is Essential for Protection against Vesicular Stomatitis Virus Infection. J. Immunol. *193*.

Steimle, A., Autenrieth, I.B., and Frick, J.-S. (2016). Structure and function: Lipid A modifications in commensals and pathogens. Int. J. Med. Microbiol. *306*, 290–301.

Steinman, R.M., and Cohn, Z.A. (1973). Identification of a novel cell type in peripheral lymphoid organs of mice. I. Morphology, quantitation, tissue distribution. J. Exp. Med. *137*, 1142–1162.

Steinman, R.M., and Cohn, Z.A. (1974). Identification of a novel cell type in peripheral lymphoid organs of mice. II. Functional properties in vitro. J. Exp. Med. *139*, 380–397.

Strober, W., Murray, P.J., Kitani, A., and Watanabe, T. (2006). Signalling pathways and molecular interactions of NOD1 and NOD2. Nat. Rev. Immunol. *6*, 9–20.

Sun, L., Wu, J., Du, F., Chen, X., and Chen, Z.J. (2013). Cyclic GMP-AMP synthase is a cytosolic DNA sensor that activates the type I interferon pathway. Science *339*, 786–791.

Sun, W., Li, Y., Chen, L., Chen, H., You, F., Zhou, X., Zhou, Y., Zhai, Z., Chen, D., and Jiang, Z. (2009). ERIS, an endoplasmic reticulum IFN stimulator, activates innate immune signaling through dimerization. Proc. Natl. Acad. Sci. U. S. A. *106*, 8653–8658.

Szretter, K.J., Brien, J.D., Thackray, L.B., Virgin, H.W., Cresswell, P., and Diamond, M.S. (2011). The interferon-inducible gene viperin restricts West Nile virus pathogenesis. J. Virol. *85*, 11557–11566.

Takahasi, K., Suzuki, N.N., Horiuchi, M., Mori, M., Suhara, W., Okabe, Y., Fukuhara, Y., Terasawa, H., Akira, S., Fujita, T., et al. (2003). X-ray crystal structure of IRF-3 and its functional implications. Nat. Struct. Biol. *10*, 922–927.

Teijaro, J.R., Ng, C., Lee, A.M., Sullivan, B.M., Sheehan, K.C.F., Welch, M., Schreiber, R.D., de la Torre, J.C., and Oldstone, M.B.A. (2013). Persistent LCMV infection is controlled by blockade of type I interferon signaling. Science *340*, 207–211.

Ting, J.P.-Y., Lovering, R.C., Alnemri, E.S., Bertin, J., Boss, J.M., Davis, B.K., Flavell, R.A., Girardin, S.E., Godzik, A., Harton, J.A., et al. (2008). The NLR gene family: a standard nomenclature. Immunity *28*, 285–287.

Trapnell, C., Roberts, A., Goff, L., Pertea, G., Kim, D., Kelley, D.R., Pimentel, H., Salzberg, S.L., Rinn, J.L., and Pachter, L. (2012). Differential gene and transcript expression analysis of RNA-seq experiments with TopHat and Cufflinks. Nat. Protoc. *7*, 562–578.

Trinchieri, G. (2010). Type I interferon: friend or foe? J. Exp. Med. *207*.

Troegeler, A., Mercier, I., Cougoule, C., Pietretti, D., Colom, A., Duval, C., Vu Manh, T.-P., Capilla, F., Poincloux, R., Pingris, K., et al. (2017). C-type lectin receptor DCIR modulates immunity to tuberculosis by sustaining type I interferon signaling in dendritic cells. Proc. Natl. Acad. Sci. U. S. A. *114*, E540–E549.

Varol, C., Mildner, A., and Jung, S. (2015). Macrophages: Development and Tissue Specialization. Annu. Rev. Immunol. *33*, 643–675.

Vogl, T., Eisenblätter, M., Völler, T., Zenker, S., Hermann, S., van Lent, P., Faust, A., Geyer, C., Petersen, B., Roebrock, K., et al. (2014). Alarmin S100A8/S100A9 as a biomarker for molecular imaging of local inflammatory activity. Nat. Commun. *5*, 4593.

Wang, X., Hinson, E.R., and Cresswell, P. (2007). The interferon-inducible protein viperin inhibits influenza virus release by perturbing lipid rafts. Cell Host Microbe *2*, 96–105.

Wang, Y., Swiecki, M., Cella, M., Alber, G., Schreiber, R.D., Gilfillan, S., and Colonna, M. (2012). Timing and magnitude of type I interferon responses by distinct sensors impact CD8 T cell exhaustion and chronic viral infection. Cell Host Microbe *11*, 631–642.

Watanabe, T., Asano, N., Fichtner-Feigl, S., Gorelick, P.L., Tsuji, Y., Matsumoto, Y., Chiba, T., Fuss, I.J., Kitani, A., and Strober, W. (2010). NOD1 contributes to mouse host defense against Helicobacter pylori via induction of type I IFN and activation of the ISGF3 signaling pathway. J. Clin. Invest. *120*, 1645–1662.

Wilson, E.B., Yamada, D.H., Elsaesser, H., Herskovitz, J., Deng, J., Cheng, G., Aronow, B.J., Karp, C.L., and Brooks, D.G. (2013). Blockade of Chronic Type I Interferon Signaling to Control Persistent LCMV Infection. Science (80-.). *340*, 202–207.

Yamamoto, M., Sato, S., Mori, K., Hoshino, K., Takeuchi, O., Takeda, K., and Akira, S. (2002). Cutting edge: a novel Toll/IL-1 receptor domain-containing adapter that preferentially activates the IFN-beta promoter in the Toll-like receptor signaling. J. Immunol. *169*, 6668–6672.

Yamasaki, S. (2014). Clec12a: Quieting the Dead. Immunity *40*, 309–311.

Yamasaki, S., Ishikawa, E., Sakuma, M., Hara, H., Ogata, K., and Saito, T. (2008). Mincle is an ITAM-coupled activating receptor that senses damaged cells. Nat. Immunol. *9*, 1179–1188.

Yarilina, A., Park-Min, K.-H., Antoniv, T., Hu, X., and Ivashkiv, L.B. (2008). TNF activates an IRF1-dependent autocrine loop leading to sustained expression of chemokines and STAT1-dependent type I interferon–response genes. Nat. Immunol. *9*, 378–387.

Yoneyama, M., Kikuchi, M., Natsukawa, T., Shinobu, N., Imaizumi, T., Miyagishi, M., Taira, K., Akira, S., and Fujita, T. (2004). The RNA helicase RIG-I has an essential function in double-stranded RNA-induced innate antiviral responses. Nat. Immunol. *5*, 730–737.

Yoneyama, M., Kikuchi, M., Matsumoto, K., Imaizumi, T., Miyagishi, M., Taira, K., Foy, E., Loo, Y.-M., Gale, M., Akira, S., et al. (2005). Shared and unique functions of the DExD/H-box helicases RIG-I, MDA5, and LGP2 in antiviral innate immunity. J. Immunol. *175*, 2851–2858.

Yu, Y., Wang, S.E., Hayward, G.S., Levy, D.E., Yuan, Y., Fujita, T., Farrell, C.J., Huang, J., Hayward, S.D., Hayward, G.S., et al. (2005). The KSHV immediate-early

transcription factor RTA encodes ubiquitin E3 ligase activity that targets IRF7 for proteosome-mediated degradation. Immunity *22*, 59–70.

Zelensky, A.N., and Gready, J.E. (2005). The C-type lectin-like domain superfamily. FEBS J. *272*, 6179–6217.

Zhao, W. (2013). Negative regulation of TBK1-mediated antiviral immunity. FEBS Lett. *587*, 542–548.

Zhou, S., Cerny, A.M., Zacharia, A., Fitzgerald, K.A., Kurt-Jones, E.A., and Finberg, R.W. (2010). Induction and inhibition of type I interferon responses by distinct components of lymphocytic choriomeningitis virus. J. Virol. *84*, 9452–9462.

Publication

Submitted manuscript:

Li, K., Neumann, K., Duhan, V., Namineni, S., Heikenwälder, M., Lang, K.S., Ruland, J. Damage-sensing C-type lectin receptor Clec12A positively regulates type I interferon response.

Acknowledgements

First and foremost, I would like to thank my Ph.D. supervisor Prof. Dr. Jürgen Ruland for giving me the opportunity to work in his lab. Not only has he guided me and supported me in finishing this Ph.D. project without reservation, but also set an excellent example as a scientist.

Many thanks to Prof. Dr. Mathias Heikenwälder and Prof. Dr. Olaf Groß on my thesis committee for gauging the progress of this thesis and providing important input.

I also want to thank my colleagues in the lab, Dr. Konstanze Pechloff, Dr. Paul Albert-König, Dr. Zsuzsanna Kurgyis, Lara Hartjes, Dr. Oliver Gorka, Dr. Andreas Gewies, Dr. Hanna Bergmann, Tim Wartewig, Svenia Myermann, Begüm Alankus, Dr. Urszula Domanska, Ceren Mutan, Kerstin Burmeister. Special thanks to: Dr. Konstantin Neumann, for introducing me into this project and also contributed a lot; Nicole Prause for being such a nice friend and helpful in many aspects. I am so grateful to have worked together with such a group of people who are so enthusiastic about what they are doing. I learned so much from every one of them.

I also want to acknowledge my collaborators: Prof. Dr. med Karl S. Lang and Vikas Duhan from the University of Duisburg-Essen, Prof. Dr. Mathias Heikenwälder and Sukumar Namineni from Helmholtz Zentrum München, Prof. Dr. Christian Holm and Anne Louise Hansen from Aarhus University, Denmark. They have really been so professional and provided important expertise for this project.

I also want to express my gratitude to my family far away in China, my parents, my sister and my nephew, for everything. Thanks to my wife Ping, for sharing this wonderful journey with me in Munich, for her constant support and love.

Table and figure list

Figure 1: The interferon signaling cascade. 23

Figure 2: IFN-I production signaling downstream of various PRRs converge on TBK1 27

Figure 3: Clec12A controls inflammation upon recognizing MSU crystal and dead cells 30

Figure 3: Clec12A dampens sterile inflammation *in vivo* 44

Figure 4: *Clec12a*$^{-/-}$ mice showed reduced ISG expression in irradiated thymi 46

Figure 6: Clec12A regulates ISG expression at global level 49

Figure 7: Clec12A regulates genes with IFN-I signature 50

Figure 8: Clec12A is required for optimal STAT1 phosphorylation 52

Figure 9: Clec12A does not regulate the signaling triggered by IFNAR engagement 53

Figure 10: Clec12A positively regulates IFN-β production and does not affect MSU-induced cell death 55

Figure 12: Clec12A amplifies the TBK1-IRF3 axis by modulating SFK activity 58

Figure 13: PI3K and actin polymerization mediate the positive effect of Clec12A on IFN-I response 59

Figure 14: Clec12A is required for optimal IFN-I production and protection against acute LCMV infection 62

Figure 15: *Clec12a*$^{-/-}$ mice are more resistant to chronic LCMV infection 64

Figure 16: Clec12A is not required for the IFN-I response induced by influenza virus infection 65

Figure 17: Clec12A controls inflammation induced by MVA infection 67

Figure 18: Clec12A positively regulates RIG-I activated IFN-I response 69

Table 1: Pattern recognition receptors in the innate immune system. 14